12/
2-23-75

SAND 75-0412
Unlimited Release

THE ELECTROMAGNETIC ENVIRONMENTS SIMULATOR (EMES)

G. Bruce Varnado

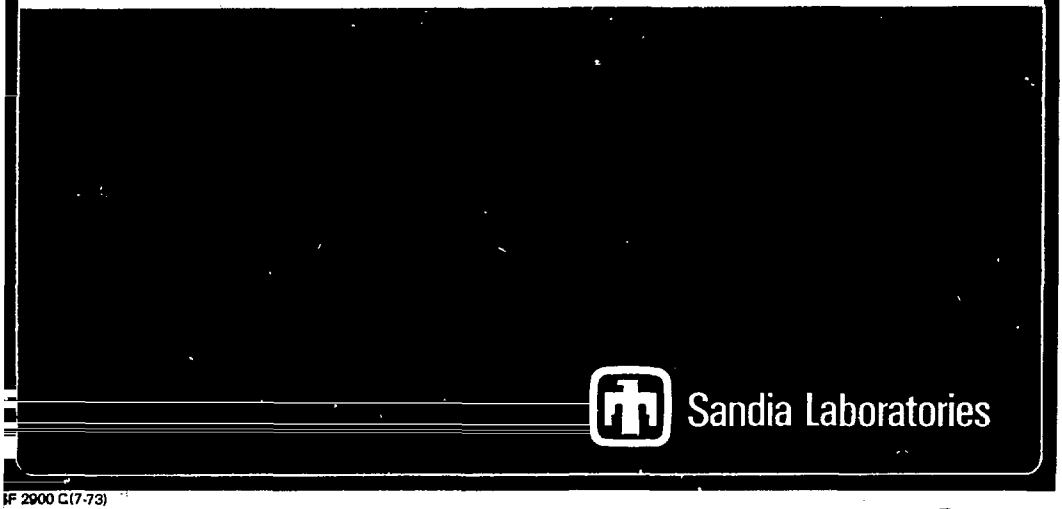

SAND 75-0412

THE ELECTROMAGNETIC ENVIRONMENTS SIMULATOR (EMES)

G. Bruce Varnado

EMR/EMP Instrumentation Division

Sandia Laboratories, Albuquerque, NM 87115

ABSTRACT

A multipurpose electromagnetic environments simulator has been designed to provide a capability for performing EMR, EMP, and lightning near stroke testing of systems, subsystems and components in a single facility. This report describes the final facility design and presents the analytical and experimental verification of the design.

ACKNOWLEDGMENTS

The following individuals are primarily responsible for the successful design of and experimental model verification for the EHES facility. Their contributions to the preparation of this report are gratefully acknowledged.

1. J. O. Reed, Division 9354, who developed the basic design for the simulator, directed a major portion of the experimental program, and provided invaluable comments on the content of this report.

2. N. J. Pollard, Division 9354, who coordinated and participated in the final design work and the experimental program for the facility.

3. R. L. Parker, Division 9353, who was involved in the conceptual design of the facility and made numerous suggestions for improving the analytical and experimental portions of the facility development.

4. H. W. Gilbert, Division 9354, who developed various portions of the instrumentation system for the experimental program and was one of the primary operators of the system.

5. J. C. Bushnell, Division 9352, who developed the computer control software for the experimental program and provided analyses and helpful suggestions in support of the analytical study.

Table of Contents

List of Illustrations

THE ELECTROMAGNETIC ENVIRONMENTS SIMULATOR (EMES)

Introduction

Divisions 9353 and 9354 are responsible for determining the effects of man-made and natural electromagnetic (EM) environments on Sandia systems and components. Experimental and analytical studies are used to evaluate the effects of EM environments on systems; however, the testing capabilities at Sandia Laboratories are limited to relatively narrow frequency ranges and to particular kinds of environments. A new facility, the Electromagnetic Environments Simulator (EMES), has been proposed which will allow broadband testing of large systems to a number of different environments within a single structure.[1] This report addresses the rationale for selection of the facility design, presents the theoretical basis for the design, and discusses the results of experimental studies on scale models of the facility.

The performance requirements for the facility include the following:

(1) The facility should be capable of producing uniform continuous wave (CW) and pulsed fields over the frequency range of 100 kHz to 10 GHz. This capability addresses the electromagnetic radiation (EMR) threat.

(2) The facility should be capable of producing uniform transient fields having the wave shape and magnitude characteristic of a nuclear electromagnetic pulse (EMP).

(3) The facility should be capable of simulating the fields produced by a nearby lightning stroke.

(4) The facility should be large enough to allow testing of weapons systems up to four meters long.

(5) The facility should not radiate appreciable electromagnetic energy into the surrounding area.

In addition to the performance requirements, tight budget constraints have been established for the facility development. Full attention has been given to reducing the size of the facility to the minimum possible for satisfactory operation.

Several techniques are available for producing known, uniform EM fields for system testing. The simplest of these is to set up transmitting antennas out-of-doors and place the item under test in the radiated field. This procedure was used for many years as the basic test approach at Sandia Laboratories.[2] Such an approach has a number of disadvantages: the field levels attainable are low (except at frequencies near or above 1 GHz where high gain horn antennas can be used), automation of the frequency scanning and data acquisition is difficult (because of the lack of broadband radiating structures), and the radiated field may interfere with other radio traffic (resulting in sanctions by regulatory agencies). Because of these disadvantages, the Sandia facilities of this kind have not been used in recent years.

A second approach is to place the radiating system and the item under test inside an anechoic chamber.[3] Absorbing material on the inner walls of the chamber prevents reflections and preserves approximate free space conditions while containing the radiated wave. A major problem with the anechoic chamber approach is the size of the structure required. A high performance chamber

uses absorbing material that is a significant fraction (at least one-quarter) of a wavelength thick at the lowest frequency to be used; therefore, a chamber that would accommodate the frequency range of interest would be prohibitively large.

A third configuration that can be used to generate test fields is the parallel plate transmission line.[4,5] The parallel plate design has been used for a number of EMP simulators and some attention has been given to using such a simulator for CW EMR testing.[6] This kind of facility is a terminated strip transmission line of large dimensions which allows placement of the test item between the strip conductor and the ground plane. Only low frequency environments can be produced in the parallel plate facility because reflections and higher order mode effects create disturbances in the field pattern at high frequencies. Facilities of this type radiate energy into the surrounding area and the radiation increases with increasing frequency. The open parallel plate facility is therefore not suitable for CW or modulated CW operation.

A fourth approach would be to enclose the parallel plate line in a shielded enclosure.[7] The line is then equivalent to a shielded strip (triplate) line or a rectangular coaxial transmission line. A facility of this type should work up to frequencies at which higher order modes begin to propagate and radiation from the center plate begins to occur. At frequencies higher than that, reflections from the walls of the enclosure will cause distortion of the field under the center plate. In addition, the distance from the center plate to the side walls and to the top of the enclosure must be carefully selected to obtain the proper characteristic impedance and field distribution for the line.

The basic elements of the parallel plate and anechoic chamber designs were combined in the EMES facility. The facility is essentially a shielded strip transmission line which has EM absorbing material covering a portion of the inner walls. The premise is that the facility will act as a bounded wave transmission line at low frequencies and (more or less) as an anechoic chamber at high frequencies. Any energy radiating from the center conductor will be contained by the outer walls of the structure and absorbed (thereby preventing the radiated energy from re-entering the test volume and distorting the field distribution). Similarily, reflections from the output end of the facility will be reduced by absorber placed across the output end.

The EMES design is based primarily on the theory of stripline, triplate, and rectangular coaxial transmission lines, parallel plate EMP simulator design and on empirical data from scale models. The purposes of this report are to describe the design of the new facility, to summarize the theoretical analyses which can be used to support the design, and to discuss the procedure and results of scale modeling of the facility.

Summary

To meet the requirements for evaluating the effects of electromagnetic energy on systems, a new multi-purpose electromagnetic environments simulator has been designed. The concept is to combine the desirable properties of the parallel plate simulator and the anechoic chamber in a design that will allow EMR testing over a wide frequency range, EMP testing, and lightning near stroke testing in a single facility.

Several possible facility configurations were evaluated in terms of the characteristics of the electromagnetic fields produced

in the facility, compatibility with existing equipment, and cost. An extensive scale-model experimental program was conducted to determine the feasibility of the designs and to establish some practical bounds on the expected performance of the full-scale facility. The results of the experiments indicate that the basic design philosophy is valid and that satisfactory performance can be achieved with several of the possible configurations.

The design selected for development into a full-scale facility is a truncated version of the tapered rectangular coaxial transmission line. At low frequencies, a resistor in series with the center conductor and equal to the characteristic impedance of the transmission line provides a matched termination for energy propagating on the line. At high frequencies, a wall of electromagnetic absorbing material placed across the output end of the facility provides a non-reflecting termination. By selecting the absorber such that the frequency at which it becomes effective is below the lowest resonant frequency for higher order modes excited on the line, truly broadband performance can be achieved. The variation in field level with frequency is expected to be less than ±6 dB over the frequency range of 100 kHz to 10 GHz. This is an acceptable degree of field uniformity for system response evaluations. The facility will not radiate electromagnetic energy into the surrounding area because it is a closed, shielded transmission line system.

In the experimental program, the broadband performance of the models under low level, continuous wave excitation was stressed. The transient environments (EMP, Lightning) have spectral content only over the low end of the frequency band covered in the experiments and the production of these environments is less sensitive to variations in the physical characteristics of the simulator. Therefore, if the facility can be designed to work properly in the continuous wave mode, satisfactory frequency domain performance

for transient environments will be assured. Although not modeled experimentally, the high voltage breakdown problems associated with production of the transient environments have been addressed in the design through the use of corona suppression tubes at points of high electric stress and the provision for a special high voltage launcher. It is believed that the facility can be built in the configuration suggested to comply with all of the primary requirements for its operation.

Final EMES Design

The final EMES design is illustrated in Figure 1. The simulator consists of (1) a source (CW, pulsed, or transient depending upon the kind of environment being simulated), (2) a launcher (or feed) which provides a transition from the circular coaxial output of the source to the rectangular coaxial geometry of the facility, (3) a pyramidal shaped section of transmission line which gradually increases the cross-sectional dimensions of the facility while maintaining constant electrical properties, (4) a rectangular section in which the test item is placed, and (5) a tapered output section in which the energy used to excite the transmission line is absorbed. A laboratory building to house the sources and work space for the test personnel, and access to the test area via an airlock are also provided in the design. The over-all length of the facility is 28 meters (including a 2.8 meter section that extends into the lab building), the maximum width at the rectangular test section is 20 meters, and the maximum interior height is 8 meters.

The inner walls, the ceiling, and the floor of the facility are lined with a conducting material (two layers of bronze screen) thus forming the shield or outer conductor of a rectangular coaxial transmission line. The center conductor of the line is

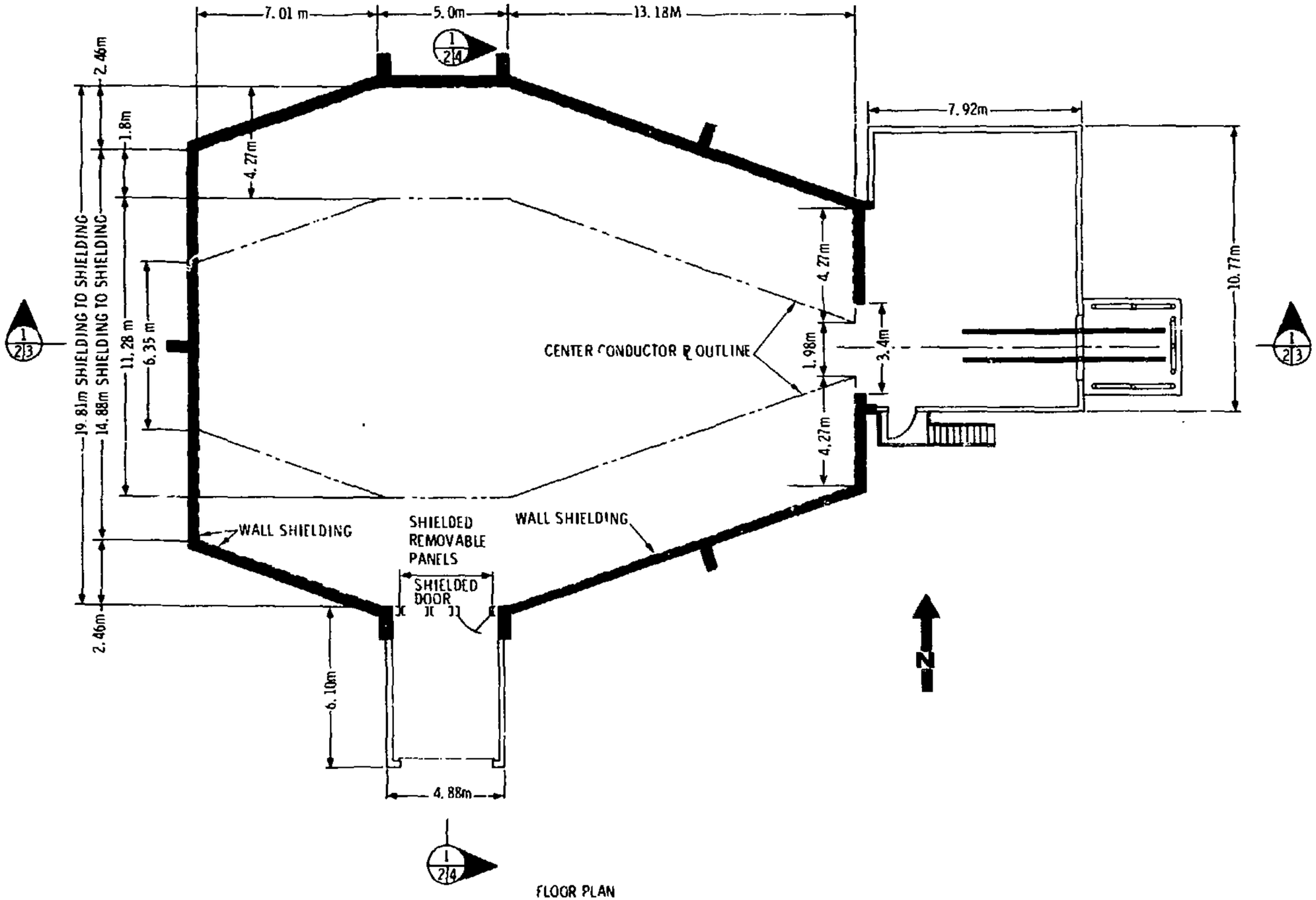

FIGURE 1: SKETCH OF THE EMES FACILITY

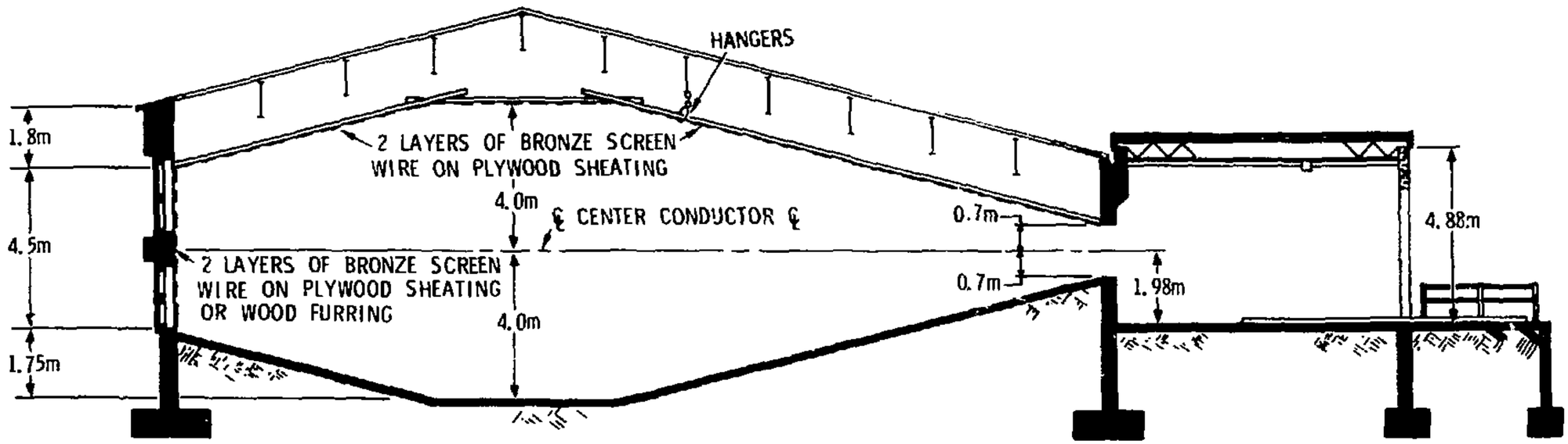

SECTION $\frac{1}{2|3}$

FIGURE 1: (CONT.)

formed by a thin, flat sheet of conducting material mounted on a dielectric support structure. The center conductor, which is suspended from the ceiling on dielectric hangers, runs from the source to the output transition section in a plane half-way between the floor and ceiling. The width of the center plate tapers to a maximum dimension of 11.25 meters in the 5 meter long test area. The item under test will be placed between the center conductor and the floor in the rectangular section of the facility; the test volume is then 5 meters long by 11.25 meters wide by 4 meters high. The edges of the center conductor are rounded to prevent breakdown in high voltage transient operation.

In the input and output transition sections, the width of the center conductor and the separation between the center conductor and the ground planes is changed in such a manner as to maintain a constant ratio between those two dimensions. The distance between the edge of the center plate and each side wall is maintained at approximately 4.25m.

The center conductor is connected to the back wall of the output transition section through a 50 ohm load. Staggered walls of electromagnetic energy absorber extend across the facility above and below the center conductor in the output transition. These two components serve as terminators for the energy propagating in the facility.

EMES is capable of simulating several different environments, EMR (CW and pulsed), EMP, and near stroke lightning fields, by connecting the proper source to its input. For EMR CW environments, sweep generators and broadband amplifiers will be used to produce maximum field levels of approximately 25 v/m over the frequency range of 200 kHz to 10 GHz. For pulsed EMR environments, existing sources are capable of producing peak fields

of 55 V/m or so at frequencies between 1 and 10 GHz. The EMP source is a Van de Graff generator with a maximum charge voltage of 400 KV which is capable of producing a peak field strength in the test volume of approximately 100 KV/m. Details on the lightning environments source have not yet been worked out. The high voltage transient sources will require a special launcher section capable of transmitting large peak voltages without breakdown between the center conductor and the ground plane.

When a voltage from any of the possible sources is applied to the input of the facility, an electromagnetic field is established between the center plate and the ground planes. In the test volume this field is a plane wave with a vertically polarized electric field component.* The orientation of the field components cannot be changed, but the effects on system response of polarization and angle of incidence can be evaluated (for in-flight environments) by changing the orientation of the system under test. The horizontal polarization for a system on the ground cannot be simulated in EMES. This is not a serious limitation for most systems, because at low frequencies (and for the transient environments) the maximum response normally occurs when the electric field is polarized parellel to the axis of the system. At very high frequencies, the ground plane does not significantly affect system response (if multipath reflections are not considered) and the horizontal orientation of the system simulates both in-flight and ground environments reasonably well.

The final design of EMES is specified in Figure 1 and discussed briefly above. The analytical principles and experimental results

---

*The wavefront is not perfectly plane for reasons discussed in a later section, but the primary components of the wave are a vertical electric field vector and a horizontal magnetic field vector.

on which the design is based are presented in the sections which follow.

General Design Concepts

The EMES facility is a rectangular coaxial transmission line with a flat strip center conductor. The dimensions of the facility were selected to produce a transmission line with a characteristic impedance of 50Ω, the same as the impedance of the sources used to drive the line and the load used to terminate the line. Thus a matched transmission system is maintained and reflections due to impedance mismatches are (ideally) eliminated.

The impedance of a rectangular line is controlled primarily by the ratio of the width of the center conductor to the separation between the center conductor and the upper and lower plates. The pyramidal transition sections maintain the width-to-plate separation ratio to provide a constant impedance along the length of the facility while gradually changing the cross-sectional dimensions. The separation between the center conductor and the ground plane is thereby increased from approximately 0.01 meter at the output of the source to 4 meters in the working volume (test volume), a distance large enough to allow the placement of a full sized system inside the transmission line, parallel to the electric field vector.

At low frequencies, the facility behaves as a terminated bounded-wave transmission line. Essentially all the energy supplied to the line by the source is contained between the center conductor and the upper and lower plates and is absorbed in the load. As the frequency is increased, radiation from the line and scattering from imperfections and discontinuities become significant. Absorbing material placed across the output end and perhaps

at other locations in the facility prevent the radiated and scattered energy from being reflected back into the working volume. That portion of the energy that propagates through the absorbing material is contained (and reflected) by the walls of the facility* and must pass back through the absorbing material before re-entering the working volume. After two passes through the absorber, the magnitude of the reflected wave should be low enough to prevent significant perturbation of the field distribution in the working volume.** The low- and high-frequency performance characteristics are discussed separately in the sections which follow.

Low Frequency Design Factors

A number of studies of the quasi-static characteristics of rectangular transmission lines are available in the literature.[8-11] In addition, the theory for stripline or triplate transmission lines[12-14] can be applied if the separation between the edge of the center conductor and the side walls of the line is large enough. Design information for parallel plate EMP simulators is also useful in determining low frequency characteristics.[15-22] From these and other sources, the basic design of the facility can be specified. The primary low frequency considerations in the design of the facility include its characteristic impedance, the field distribution within the test volume, the planarity of the wavefront in the test volume, and the termination of the transmission line in a matched load. The conclusions drawn from low frequency design studies in each of these

---

*The purpose of the side walls is simply to contain the radiated energy; therefore, any conducting material will be suitable. If screen is used, the maximum mesh size should be less than 0.3 cm (0.1 wavelength at 10 GHz).

**As mentioned previously, the thickness of the absorbing material must be a significant fraction of a wavelength to be effective. Selection of the material size is discussed in Appendix A.

areas are presented briefly below and are discussed in greater detail in Appendix A.

The quasi-static solutions are applicable to transmission lines whose dimensions are small enough to support only the TEM propagation mode. For the symmetrical tri-plate line shown in cross section in Figure 2a, higher order modes may propagate when the ground plane spacing, d, exceed one-half wavelength.[12] For the rectangular line (that is, the triplate line with side plates added), the specification of the cutoff wavelengths for higher order modes is complicated by the effects of the side walls; however, for shielded lines with dimensions similar to those of the proposed facility, the cutoff wavelengths in the flat section are essentially the same as for the triplate line.[9] We therefore assume that the upper frequency, f_c, for purely TEM propagation on the line is given approximately by:*

$$f_c = \frac{c}{\lambda_c} = \frac{c}{2d} \qquad (1)$$

where λ_c is the cutoff wavelength for higher order modes and c is the velocity of light in free space. At frequencies higher than f_c, higher order modes will proliferate, radiation from the line will become increasingly significant, and the low frequency concepts of characteristic impedance and field distribution will not be strictly valid. For the EMES design, the ground plane separation in the working volume is 8 meters and f_c is approximately 19 MHz.

Expressions for the approximate characteristic impedance, Z_o, of the coaxial rectangular transmission line shown in Figure 2b,

---

*The prediction of cutoff wavelengths for higher order modes in EMES is further complicated by the varying cross section dimensions of the line in the pyramidal transition sections.

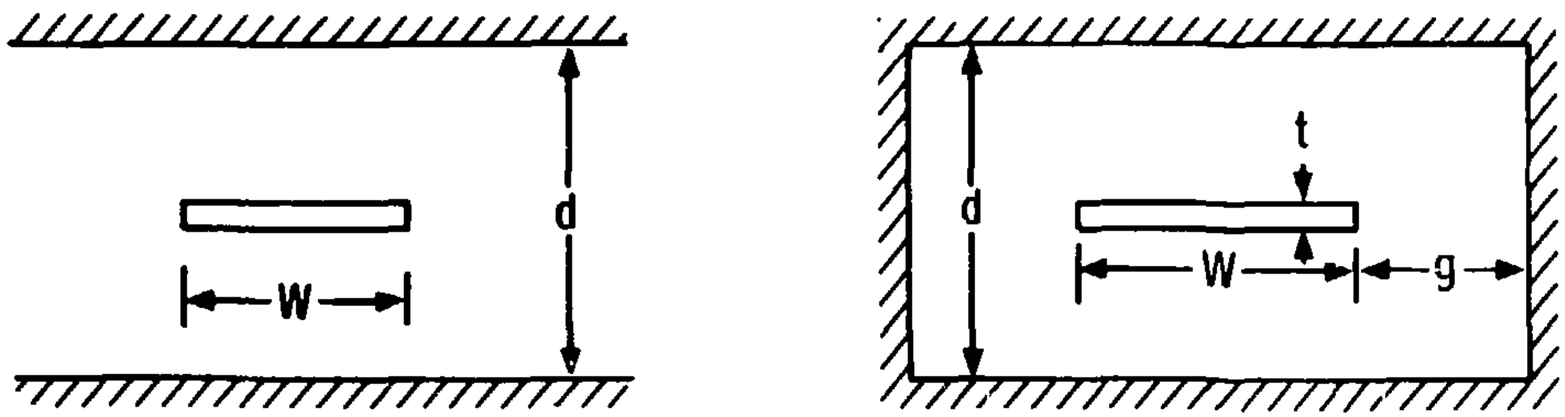

(a) TRI-PLATE LINE (b) RECTANGULAR COAXIAL LINE

FIGURE 2: PARALLEL PLATE TRANSMISSION LINES

are available in the literature.[8,10,11] One such expression for the case of a zero thickness center conductor is given in Equation 2.

$$Z_o = \frac{376.62}{4\left[\frac{W}{d} + \frac{2}{\pi} \ln\left(1 + \coth \frac{\pi g}{d}\right)\right]} \Omega \qquad (2)$$

In Equation 2, g is the separation between the edge of the center conductor and the side wall, W is the width of the center conductor and d is the separation between the ground planes. The width of the center plate in EMES was adjusted to give a characteristic impedance of approximately 50Ω (see Figure 1 for dimensions). Computations based on other approximate expressions for the rectangular line and on the triplate equivalent of the facility gave results within 5 percent of the value given by (2).

The input and output tapered transition sections are used to gradually change the dimensions of the line while maintaining a constant characteristic impedance. This is done by changing the center plate width, W, and the ground plane separation, d, at the same rate so as to maintain a constant ratio of W/d. (See Figure 3.) At any cross-section through the tapered transitions, the conductor configuration and the characteristic impedance are the same as in the rectangular portion of the line.

One objective of the facility design is to obtain a uniform, planar field distribution over the area to be occupied by the test item; that is, the electric field lines and the equipotential lines should be uniformly spaced, with the electric field lines perpendicular to the center plate and the equipotential lines parallel to it. Such a field distribution is very closely approximated in the region between the center plate and the upper and lower ground planes of a rectangular coaxial transmission line, provided certain conditions

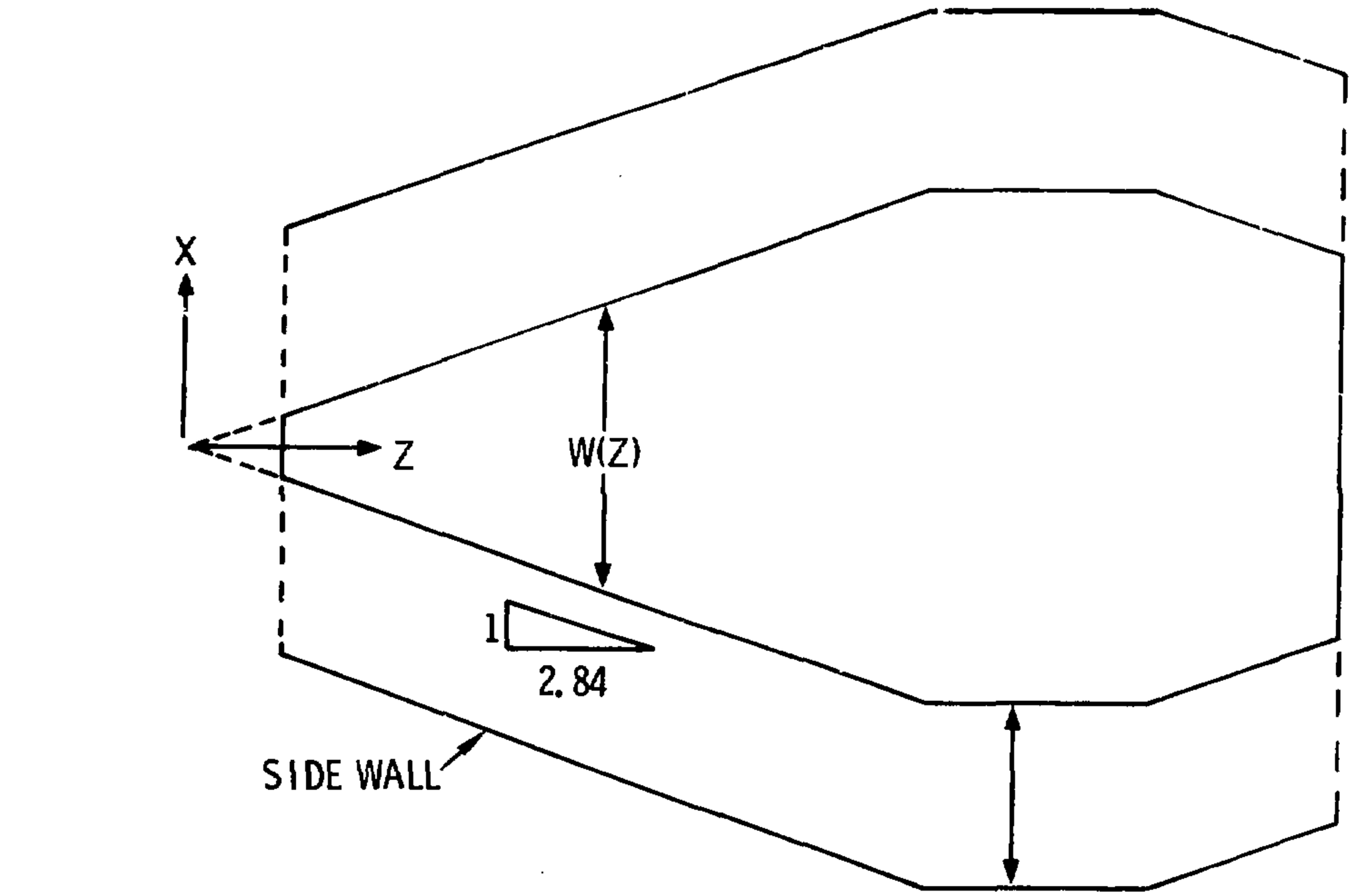

(a) TOP VIEW

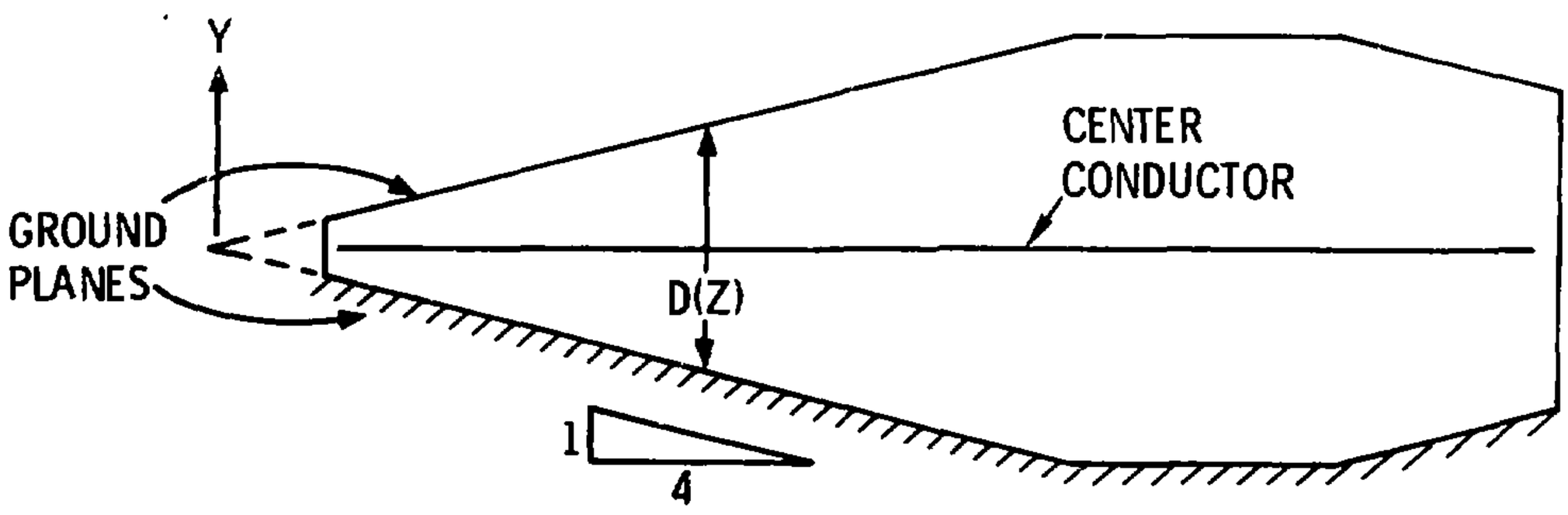

(b) SIDE VIEW

FIGURE 3: SKETCH OF EMES CENTER CONDUCTOR AND GROUND PLANE ARRANGEMENT

on the physical characteristics of the line are satisfied. These conditions are summarized below.

1. The field under the center plate is essentially uniform at distances from the edge greater than approximately 0.25d (one-quarter of the distance between ground planes).

2. The distance from the edges of the center conductor to the side walls of the transmission line should be at least one-half the ground plane spacing (0.5d) to assure that the side walls do not cause disturbances in the field distribution in the working volume.

3. The electric field increases precipitously near the edge of the center conductor. Some form of high voltage breakdown suppression should be provided to assure that arcing does not occur in the tapered input transition section.

Distortion of the wavefront in the working volume is the consequence of several factors: (1) time dispersion across the wavefront which results from launching the spherical wave from the pyramidal transition section onto the flat section; (2) reflection and diffraction of the wave at discontinuities (such as the bends in the ground planes) in the transmission line;[23] and (3) reflection at the side walls of energy radiated from the center plate. These factors are illustrated in Figure 4. As discussed more fully in Appendix A, the effects of these disturbing factors are reduced by making the angle between the tapered and flat sections as small as is practical, using the front portion of the working volume for the test item location, and placing electromagnetic absorber across the output end of the facility.

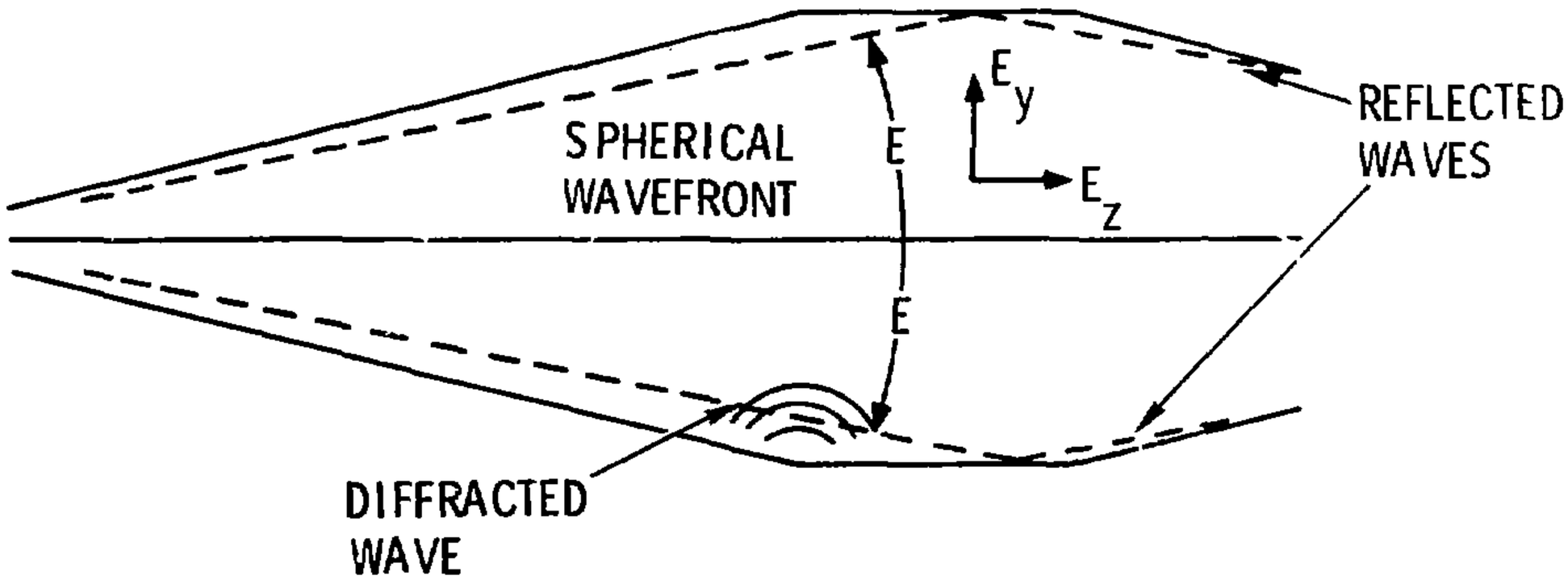

FIGURE 4: ILLUSTRATION OF WAVE CHARACTERISTICS IN EMES

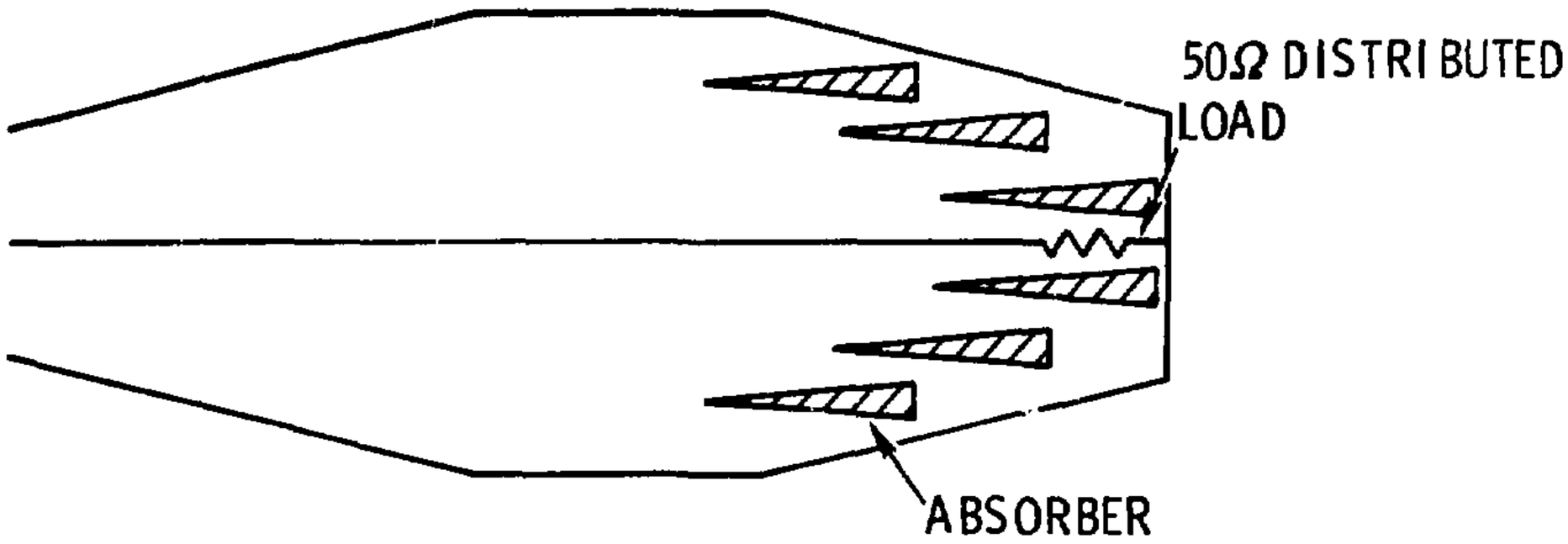

FIGURE 5: OUTPUT TERMINATION ARRANGEMENT

The final critical factor in the low frequency design of the facility is the output load arrangement. For the frequency range in which the facility behaves as a TEM mode transmission line, it is necessary to terminate the line in its characteristic impedance to avoid reflections back into the working volume. In EMES this termination is provided by a distributed fifty ohm resistive load mounted in the center plate near the output end. The load is located at approximately the same axial position in the output transition section as is the staggered wall of absorber. The load tends to gradually dissipate the low frequency energy as the volume occupied by the absorber increases. Thus, the distributed resistor helps to compensate for the increased low frequency capacitance caused by the presence of the absorber. It is also possible to compensate for the increased capacitance by narrowing the center conductor and thereby increasing the inductance of the transmission line. Additional scale model experiments are planned to determine how much the plate must be narrowed to achieve optimum low frequency performance. A sketch of the output termination arrangement is shown in Figure 5.

High Frequency Design Factors

At frequencies for which the dimensions of the facility are comparable to or larger than the wavelength, modes other than the TEM mode can propagate on the line.[24] These higher order modes are not properly terminated by the series load impedance and energy coupled into these modes is reflected at the output end of the line, causing disturbances in the field distribution in the working volume. Several features of the facility design tend to suppress the higher order modes and thereby extend the frequency range of the facility.

Discontinuities on the transmission line allow the higher order modes to be excited. Presumably, if there were no abrupt changes

in the physical characteristics of the facility, the TEM mode would be the only one propagating on the line. Severe discontinuities (such as significant changes in the characteristic impedance of the transmission line) will result in reflection of a portion of the TEM wave and create standing waves along the line. Therefore, it is necessary that the conductor surfaces be reasonably smooth and planar.

Particular care must be used in making the feed, or launcher, for the input end of the facility. The feed matches the circular coaxial cable from the source to the rectangular geometry of the facility. Because the spacing between conductors is small, their positions must be carefully controlled to maintain a constant impedance and avoid discontinuities that might excite higher order modes. The current design employs a coax-to-strip line launcher in which the high-dielectric substrate is gradually tapered to provide a smooth transition to the air dielectric facility as shown in Figure 6. Other designs which provide better mechanical stability are being considered.

A wave launched into the facility must be absorbed in the load impedance or at the boundaries to avoid disturbance of the field in the working volume. Previous attempts to use parallel plate facilities for high frequency CW test work have shown that a major contributor to field non-uniformities in the working volume is the reflection that occurs at the output tapered section of the line. Several approaches have been proposed for terminating a parallel plate line in a generalized admittance sheet instead of the lumped characteristic impedance of the line.[20,25-29] Such a sheet might be composed of a grid of inductors, capacitors, resistors, or even active networks. This approach to the high frequency termination problem does not appear to be practical over the broad frequency range necessary for EMES.

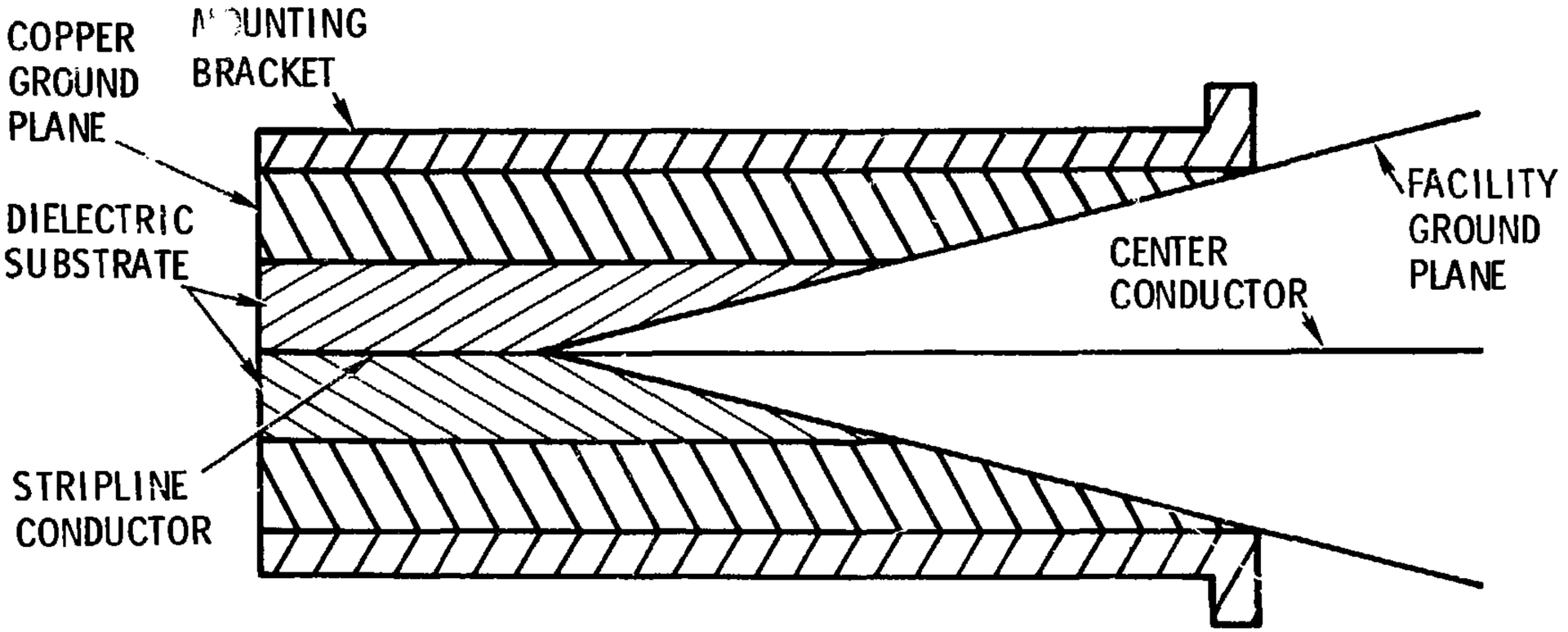

FIGURE 6: STRIPLINE LAUNCHER

The EMES design provides a termination for the non-TEM components by placing a wall of absorbing material across the output end of the facility. This high frequency termination is roughly equivalent to the sheet admittance mentioned above. The absorber is placed so as to intercept all reflected waves emanating from the bends at the intersections of the input tapered section with the flat section of the facility.

Absorber can also be placed on the side walls and the floor of the facility to prevent reflection into the working volume of energy scattered from the bends in the ground plane or from a metal test item. The goal is to absorb all the energy that leaves the working volume and thereby preserve essentially free-space conditions in the vicinity of the test item. In many respects the high frequency performance of the facility is more like an anechoic chamber than a transmission line.

The requirement for non-interference with nearby users of the EM spectrum places additional constraints on the high frequency performance of the system. It has been estimated that the facility walls will need to provide approximately 55dB of shielding effectiveness in order for the facility to meet Federal radiation limits when driven by a 200 watt CW source (see Appendix A). This level of shielding effectiveness is attainable over the frequency range required through the use of inexpensive screen-wire construction for the ground planes and side walls.[30]

High Voltage Transient Design Factors

To produce EMP and lightning environments, high voltage pulses must be applied to the facility. The same considerations for impedance matching, load termination, reflection and diffraction at discontinuities, and field uniformity apply to the transient mode of operation as to CW operation. A design which meets the

requirements for CW operation at all frequencies specified should be entirely satisfactory for transient operation.*

The unique problems associated with the transient operation of the facility involve high voltage breakdown phenomena. The primary concern is that the maximum voltage applied to the center conductor does not cause arcing from the center conductor to the ground surfaces. In addition, it is desirable to suppress corona discharge from the center conductor. The maximum source voltage anticipated at the present time is 400 KV.

The mechanisms of high voltage breakdown are briefly summarized in Appendix A.[31] High voltage stand-off is accomplished in FMES in two ways. (1) In the main part of the facility, the edges of the center plate are rounded to reduce the electric stress. A center plate radius of 0.1 meter gives a reasonable compromise between voltage stand-off capability and effects on the characteristic impedance of the increased thickness of the center plate. (2) In the first 2.8 meters of the input transition section, where the separation between the center plate and the ground planes is small, the volume surrounding the center plate is filled with high dielectric strength material capable of withstanding the high stress. This portion of the input transition is gas- or oil-tight and is removable to allow connection of the high frequency CW feed. At the point where the center conductor passes out of the "gas box", the sparkover voltage in the facility (air dielectric) is greater than 800 KV. This value is considered adequate for high voltage breakdown protection.

---

*The transient signals of interest, in general, do not have significant spectral content at frequencies above 500 MHz.

Scale Modeling of the Facility

Electromagnetic scale modeling is an effective method of obtaining solutions in analog form to the field equations with complicated boundary conditions.[32-34] The modeling is accomplished by appropriately scaling the physical dimensions, the electrical characteristics, and the frequency of operation of the system. The requirements for the scale factors are determined by comparing the forms of the Maxwell equations in the full scale and the model spaces.[32] The ability to construct valid models rests on the linearity of the differential equations which describe the fields in the system. This implies that it is necessary to exclude any nonlinear media.

Requirements for Electromagnetic Scale Modeling

The most common approach is to require that the fields in the model be proportional to the fields in the full-scale system and to make the model space simply a space of different size than the full-scale space. That is:

$$\bar{E}\ (x,y,z) = \alpha\bar{E}'(x',y',z') \tag{3}$$

$$\bar{H}\ (x,y,z) = \beta\bar{H}'\ (x',y',z')$$

$$\ell = \rho\ell'$$

where $\bar{E}$ is the electric field vector, $\bar{H}$ the magnetic field vector, ℓ an element of length in the full-scale system with spatial coordinates x, y, z, the primed quantities are the equivalent variables in the model space, and α, β and ρ are arbitrary constants of proportionality. The exclusion of nonlinear materials makes it practically impossible to scale the permittivity, ε, and permeability, μ, of insulators (such as air). The accepted practice,

therefore, is to simulate air (and other dielectrics) in the full-scale system with air (and the same dielectrics) in the model. Thus:

$$\epsilon = \epsilon' \qquad (4)$$

$$\mu = \mu' . \qquad (5)$$

This also leads to the condition that the wave impedance $(\bar{E}/\bar{H})$ must be the same in both spaces and

$$\frac{\alpha}{\beta} = 1 . \qquad (6)$$

Frequency (time) must be scaled so that

$$f = f'/\rho . \qquad (6)$$

To properly model conductors, the conductivity must be scaled as

$$\sigma = \sigma'/\rho . \qquad (7)$$

It is the restriction of Equation 7 that leads to the greatest difficulty in constructing valid scale models. This condition is not strictly satisfied by using air in the model to represent air in the full-scale system because air actually has a small, frequency varying conductivity. The error involved in treating air as a perfect insulator is generally dismissed as being negligible at practical frequencies.[34] Modeling good conductors can also be a problem; for example, a 1/10 scale model of a copper conductor should be made from a material with 10 times the conductivity of copper. Good conductors are generally treated as perfect conductors (infinite conductivity) and are used in the full-scale system and the model alike with negligible error.

A model which satisfies the conditions expressed in Equations 3 through 7 is a geometrical model of the full-scale system it is designed to represent. The structure of the fields within and near the model will be the same as that of the fields in the full-scale system. Thus, qualitative information on the field distribution in a system can be obtained from measurements on a model of convenient size.

Experimental Procedure and Results

Several scale models of possible EMES designs were examined in an extensive experimental program. Details of the experimental approach and the results are reported elsewhere.[35] In this report the experimental results that impact the final design decisions are summarized.

The same dielectric materials used in the design of the full-scale facility were used in the models (air, dielectric substrates, dielectric supporting material). Copper sheet and bronze screen were used to model conducting surfaces. The model size for which the largest amount of data was obtained was a 1/5 scale ($\rho = 5$). Data were taken over the frequency range of 10 MHz to 10 GHz, corresponding to frequencies in the full-scale facility of 2 MHz t. 2 GHz. In addition, a 1/20 scale model of the truncated design was used for a series of experimental studies over the same frequency range.

It was not possible to properly scale the conductivity of the absorbing material used as the termination for several of the model configurations because the material is obtained commercially and is available only in standard compositions. The results obtained in the experiments, therefore, do not necessarily represent the precise performance to be expected in the full-scale facility. However, because of the nature of the broadband response of the scale models

(as will be discussed later) good qualitative results were obtained. In spite of this violation of one requirement for precise scale modeling, the information required to answer several critical design questions was generated.

The scale models were designated FEMES (Fifth-Scale Electromagnetic Environments Simulator) and TWEMES (Twentieth-Scale Electromagnetic Environments Simulator). Several configurations of FEMES as described in Appendix B were examined in detail in the experimental program. The model for the truncated configuration, the final design model, is shown in Figure 7.

The magnitude of the relative electric field strength was measured at several points in a plane at the front edge of the working volume as shown in Figure 7. Data were obtained for the vertical, horizontal, and axial components by measuring the output of correspondingly polarized field probes,[36] dividing by a reference field level and expressing the result in dB. Measurements were also made of the voltage standing wave ratio (VSWR) and (where appropriate) the normalized output power; that is, the power dissipated in the load termination divided by the power coupled to the input of the facility. Control and data logging operations were performed by a mini-computer controlled instrumentation system. The results of measurements on each of the models are discussed in Appendix B and are presented in detail in Reference 35.

The primary results of the model studies are summarized below with particular emphasis on the results for the truncated model.

1. The highest frequency at which the facility performs satisfactorily without absorbing material in the output transition is approximately that predicted by Equation 1.

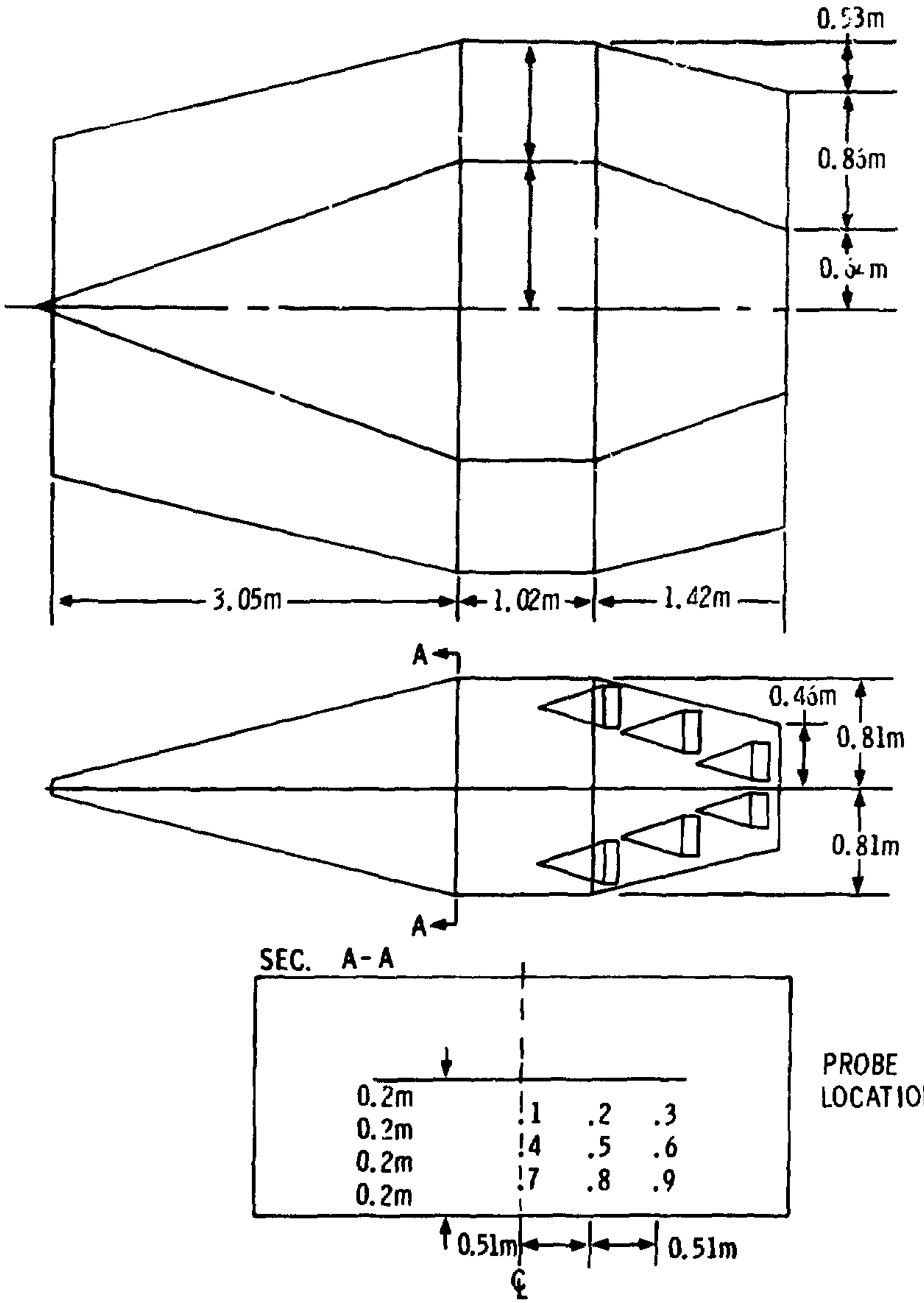

FIGURE 7: TRUNCATED CONFIGURATION

2. Addition of the absorber to the output transition improves greatly the high frequency performance of the facility by suppressing resonances associated with the higher order modes. It also degrades slightly the low frequency performance by increasing the capacitance at the load end.

3. Mechanical alignment of the launcher is critical to proper operation at frequencies above 1 GHz.

4. Changing the position of the side walls does not significantly affect the performance of the facility as long as the separation between center plate and side walls is at least as great as the separation between center plate and ground planes. This implies that the width of the facility can be reduced as the width of the center conductor is reduced in the input and output transitions, thereby reducing construction costs.

5. The truncated design with a distributed load impedance and proper absorber placement gives satisfactory performance over the required frequency range.

6. The load impedance should be distributed laterally and axially in the center plate.

7. The absorber should be staggered along the output transition section and should be separated from the back wall of the facility to minimize the effect of the absorber on the low frequency impedance of the transmission line.

The normalized vertical electric field at the center front edge of the working volume of the truncated model is shown in Figure 8. The field level is within a range of approximately ±6dB at all frequencies examined. Attaining this degree of field uniformity over three frequency decades in a facility the size of FEMES provides an impressive verification of the basic design. The VSWR for the truncated model is shown in Figure 9. The maximum values of 2.5 or so are acceptable for operation with high power CW amplifiers. The experimental results indicate that EMES can meet its design goals in the truncated version specified in Figure 1.

Absorber Effects

To interpret the results of experiments involving the use of EM absorbing material, it is necessary to understand some of the basic characteristics of the absorber. These characteristics are summarized briefly in Appendix C and will be applied to the discussion of the experimental results which follows.

Because the conductivity of the absorber could not be scaled properly, the models used in the experimental studies were not precise geometric models of EMES. The data, however, emphasize the broadband characteristics of the absorber and indicate that valid qualitative decisions can be based on the experimental results. The field levels at frequencies above 200 MHz were essentially the same for all model configurations examined (Appendix B). This indicates that the absorber is more like a distributed termination than a lumped element at frequencies for which the absorption (reflection attenuation) is significant (20 to 25 dB or greater). Therefore, if the absorber is thick enough relative to the wavelength and if the facility dimensions are such that the wave can propagate into the absorber without being reflected, the conductivity of the absorber will have essentially no effect upon the field level in the working volume.

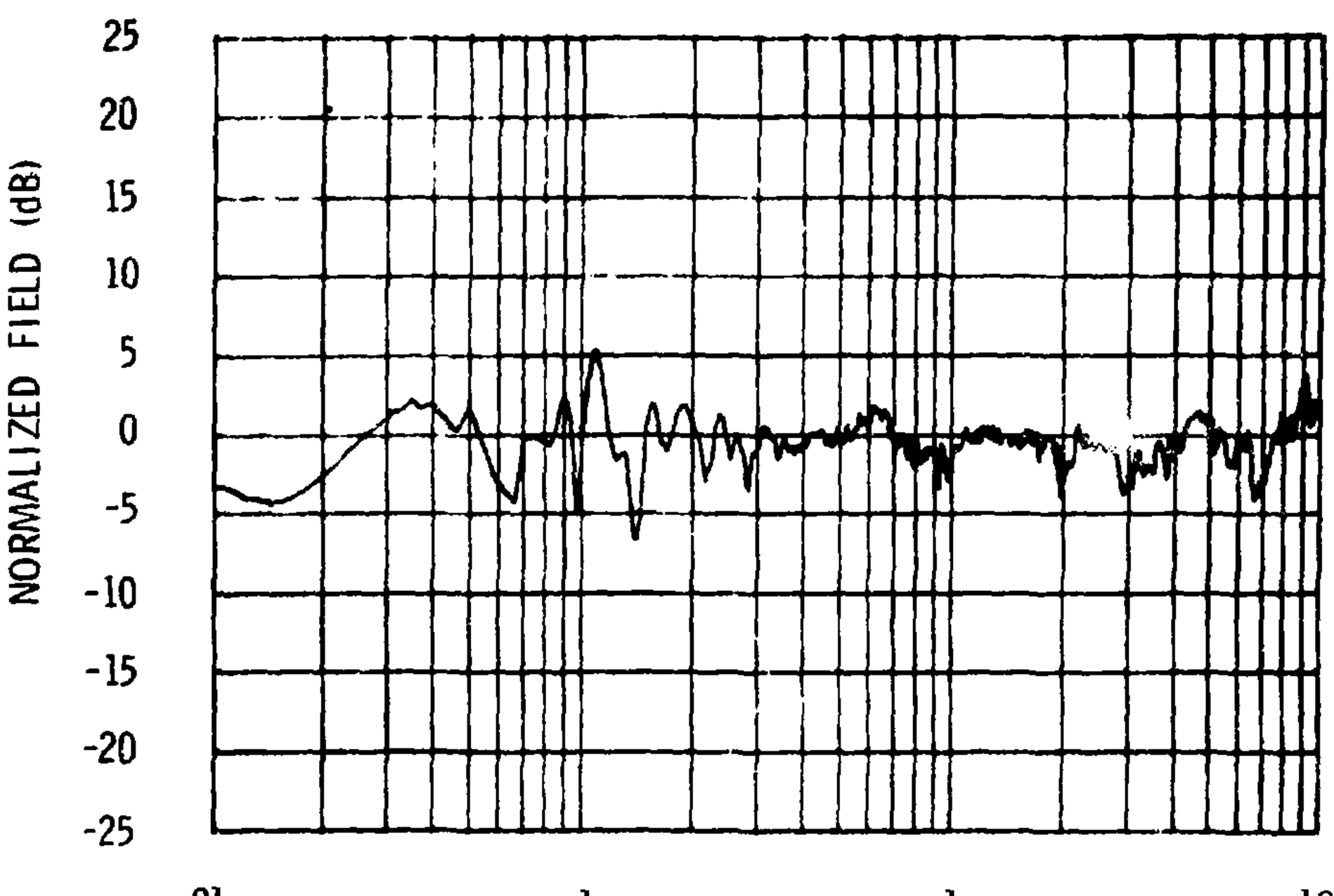

FIGURE 8: NORMALIZED ELECTRIC FIELD STRENGTH FOR THE TRUNCATED MODEL WITH ABSORBER

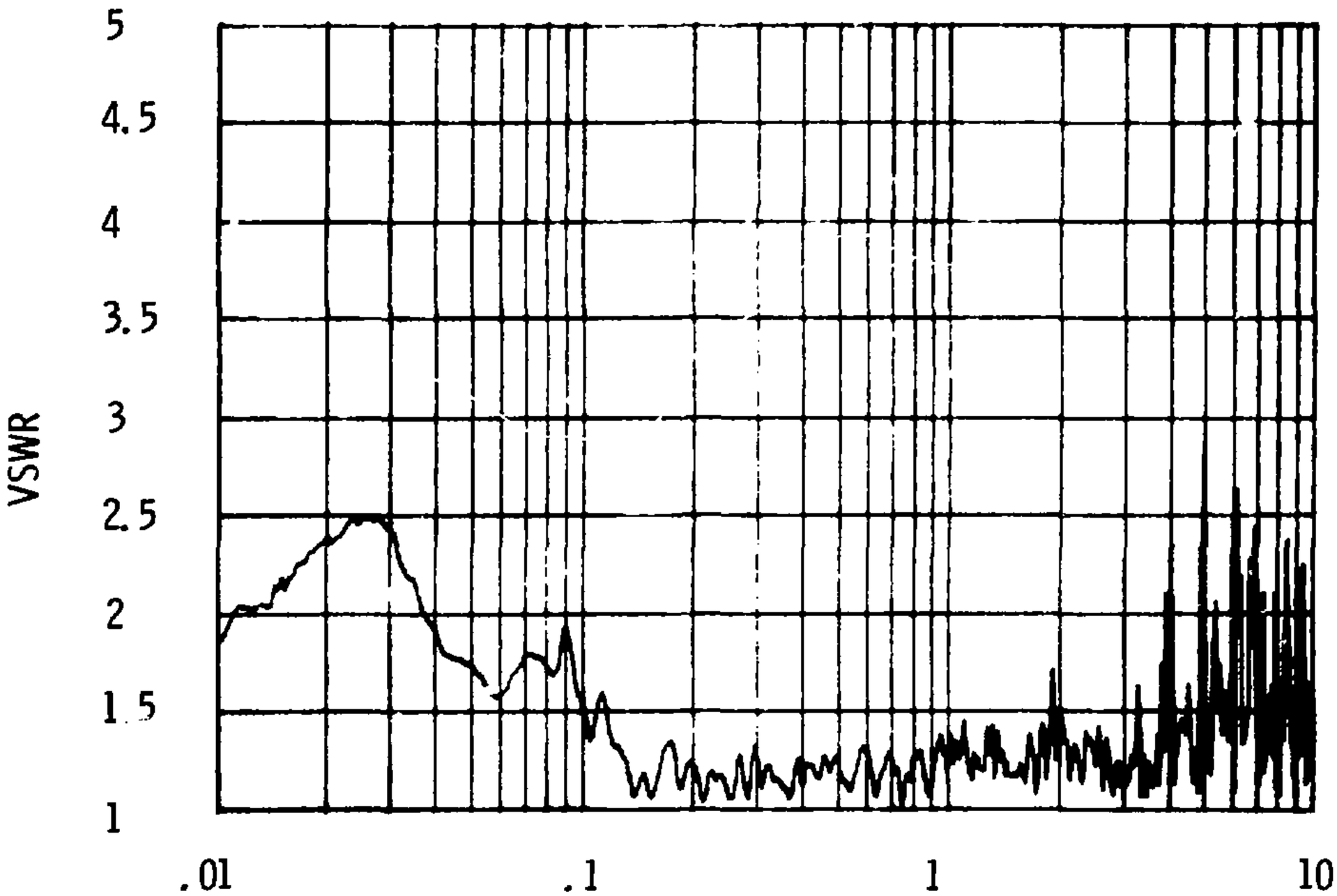

FIGURE 9: VSWR FOR THE TRUNCATED MODEL WITH ABSORBER

The broadband characteristics of the absorber also give confidence that the performance of EMES will be satisfactory to 10 GHz even though the maximum scaled frequency in the models was equivalent to only 2 GHz. The field level variations are essentially the same over almost two decades in the models; therefore, there is no reason to suppose that the performance would not have continued if it had been possible to increase the test frequencies. The absorber characteristics improve with increasing frequency and reflections from the termination should continue to decrease. As mentioned earlier, the feed arrangement has a much greater effect on the high frequency performance of the system than do other variables in the construction of the facility. The feed used in the models is essentially the same as that to be used in the full-scale facility and its performance to 10 GHz has been demonstrated. Although it was impossible to scale the frequency to the maximum value required in the design, the data from the model experiments indicate that the design will meet its requirements to 10 GHz.

At low frequencies, of course, the reflection attenuation is small and the absorber has the effect of increasing the capacitance between the center conductor and the ground planes. The models may underestimate the disturbance caused by the absorber at these frequencies by providing a lower conductivity than necessary to satisfy the requirements for geometric modeling. If the low frequency performance of EMES should be significantly worse than predicted by the models, it would at worst mean that the absorber would have to be removed from the output transition section for testing at low frequencies. However, by properly dispersing the absorber within the output transition, it should be possible to achieve the required high frequency absorption without destroying the low frequency characteristics of the transmission line.

From the data in Appendix C, it is possible to predict that the reflection attenuation for the absorber will be 20 dB at the

frequency for which the absorber is approximately 0.25 λ thick. For the 4-meter-long absorber to be used in EMES this means that the absorber will provide a highly effective termination for frequencies of 19 MHz and above. From Equation 6 and the experimental results, the lowest resonant frequency is expected to be 19 MHz. In the models, the 20 dB reflection attenuation frequency (114 MHz) was somewhat higher than the first resonant frequency (95 MHz). It is therefore expected that the performance near the first resonance in the full-scale facility will be better than that of the models.

Conclusions

The analytical and experimental studies completed thus far indicate that the basic design requirements for a new electromagnetic environments test facility can be satisfied by a properly terminated rectangular coaxial transmission line. Such a facility would be capable of producing EMR, EMP, and lightning near-stroke environments and would not radiate appreciable energy. In the designs considered in these studies, the maximum length of systems which could be exposed to the environments with the electric field parallel to the system axis is 4 meters.

Experimental scale model studies were conducted to determine the optimum configuration for the facility based on uniformity of the field levels within the test area, input characteristics, and size (cost). The design selected (the truncated configuration) consists of an adapter from coaxial to rectangular geometry, an input transition section of gradually increasing cross-sectional dimensions, a test area (working volume) of constant cross section, and a foreshortened output transition section. The center conductor is a flat plate of tapered width in the input and output transition sections with a series distributed load impedance equal to the characteristic impedance of the transmission line at the output end. EM absorber

is installed in the output transition section to prevent high frequency reflections from the back wall of the facility.

The truncated model is expected to provide field levels in the working volume with variations of not more than ±6 dB at frequencies of interest. With a properly constructed launcher, the VSWR at the input to the facility should be less than 2.5. Construction tolerances do not have to be extremely tight to achieve this kind of performance except in the first part of the input transition section where cross-sectional dimensions are small.

References

1. J. O. Reed and R. L. Parker, "EMR/EMP Parallel Plate Transmission Line Facility," Sandia Laboratories, Division 9353 Report, July 26, 1974.

2. R. J. Sons, "Sandia Low-Power RF Testing Facility," SC-TM-69-461, November 1970.

3. "Measurement at the B. F. Goodrich Tapered Chamber for the Naval Weapons Station, Seal Beach, California," B. F. Goodrich Report No. MR-112, August 14, 1970.

4. B. E. Roseberry and R. B. Schulz, "A Parallel-Stripline for Testing RF Susceptibility," IEEE Transactions on EMC, Vol. EMC-7, pp 142-150, June 1965.

5. R. L. Hutchins, ARES Facility Description Volume II Electromagnetic Environment, Braddock, Dunn, and McDonald, Inc., Report No. BDM/A-86-72-TR, 6 May, 1972.

6. J. C. Giles, et al, Evaluation and Improvement of the CW Performance of the ALECS Facility, EG&G Report No. AL-1085, 29 July, 1974.

7. M. L. Crawford, "Generation of Standard EM Fields Using TEM Transmission Cells," National Bureau of Standards.

8. H. Guckel, "Characteristic Impedances of Generalized Rectangular Transmission Lines," IEEE Transactions on Microwave Theory and Techniques, May 1965.

9. R. H. T. Bates, "The Characteristics Impedance of the Shielded Slab Line," IRE Transactions on Microwave Theory and Techniques, January 1956.

10. Tsung-Shan Chen, "Determination of the Capacitance, Inductance, and Characteristic Impedance of Rectangular Lines," IRE Transactions on Microwave Theory and Techniques, September 1960.

11. M. A. R. Gunston, Microwave Transmission-Line Impedance Data, Van Nostrand Reinhold Company, 1972.

12. R. W. Peters, Ed., Handbook of Tri-Plate Microwave Components, Sanders and Associates, Inc., 1956.

13. H. A. Wheeler, "Transmission Line Properties of Parallel Strips Separated by a Dielectric Sheet," IEEE Transactions on Microwave Theory and Techniques, March 1965.

14. Reference Data for Radio Engineers, Fifth Edition, Howard W. Sams & Co., Inc., 1968.

15. R. E. Partridge, "EMP Testing Facility," Electromagnetic Pulse Sensor and Simulation Notes (EMPSSN), AFWL EMP 1-1, Note 1, February 1964.

16. C. E. Baum, "Impedances and Field Distributions for Parallel Plate Transmission Line Simulators," EMPSSN, AFWL EMP 1-1, Note 21, June 1966.

17. C. E. Baum, "The Conical Transmission Line as a Wave Launcher and Terminator for a Cylindrical Transmission Line," EMPSSN, AFWL EMP 1-2, January 1967.

18. C. E. Baum, "The Single-Conductor, Planar, Uniform Surface Transmission Line, Driven From One End," EMPSSN, AFWL EMP 1-3, Note 46, July 1967.

19. G. W. Carlisle, "Impedance and Fields of Two Parallel Plates of Unequal Breadths," EMPSSN, AFWL EMP 1-6, Note 90, July 1969.

20. C. E. Baum, "Admittance Sheets for Terminating High-Frequency Transmission Lines," EMPSSN, AFWL EMP 1-3, Note 53, April 1968.

21. S. K. Cho, C. Chu, and C. Tai, "Proximity Effect of Semi-Infinite Parallel Plate Transmission Line in the Presence of a Perfectly Conducting Ground," EMPSSN, AFWL EMP 1-12, Note 137, August 1971.

22. C. Chu and S. K. Cho, "Field Distribution for Parallel Plate Transmission Line of Finite Width in Proximity to a Conducting Plane," EMPSSN, Note 161, November 1972.

23. C. E. Baum, "The Diffraction of an Electromagnetic Plane Wave at a Bend in a Perfectly Conducting Planar Sheet," EMPSSN, AFWL EMP 1-3, Note 47, August 1967.

24. J. C. Bushnell, "Analysis of the Tri-Plate Line (TPL)-I," Division 9353 Memo to Distribution, January 31, 1975.

25. C. E. Baum, "A Distributed Inductor for use with a Two-Dimensional Simulator Structure," EMPSSN, AFWL EMP 1-4, Note 57, June 1968.

26. R. W. Latham and K. S. H. Lee, "Inductance of Periodic Distributed Inductors," EMPSSN, AFWL EMP 1-4, Note 67, January 1969.

27. R. W. Latham and K. S. H. Lee, "Termination of Two Parallel Semi-Infinite Plates by a Matched Admittance Sheet," EMPSSN, AFWL EMP 1-5, Note 68, January 1969.

28. C. E. Baum, "A Sloped Admittance Sheet Plus Coplanar Conducting Flanges as a Matched Termination of a Two-Dimensional Parallel-Plate Transmission Line," EMPSSN, AFWL EMP 1-7, Note 95, December 1969.

29. D. L. Wright, "Sloped Parallel Resistive Rod Terminations for Two-Dimensional Parallel-Plate Transmission Lines," EMPSSN, AFWL EMP 1-8, Note 103, May 1970.

30. E. A. Lindgren, Contemporary RF Enclosures, Erik A. Lindgren & Associates, Inc., 1967.

31. F. W. Peek, Jr., Dielectric Phenomena in High Voltage Engineering, McGraw Hill Book Co., 1929.

32. R. W. P. King, Electromagnetic Engineering, McGraw-Hill Book Co., 1945, pp 316-320.

33. W. L. Weeks, Electromagnetic Theory for Engineering Applications, John Wiley & Sons, Inc., 1964, pp 46-50.

34. G. Sinclair, "Theory of Models of Electromagnetic Systems," Proceedings of the I.R.E., Vol 36, Nov. 1948, pp 1364-1370.

35. J. O. Reed, N. J. Pollard, G. B. Varnado, FEMES Data Summary, April 1975.

36. J. C. Barnes, "Radio-Frequency E-Field Sensor," Sandia Laboratories, SC-DR-71 0219, July 1971.

37. S. Galagan, "Understanding Microwave Absorbing Materials and Anechoic Chambers," Part 3, Microwaves, April 1970, pp. 47-50.

38. S. Galagan, "Understanding Microwave Absorbing Materials and Anechoic Chambers - Part 1," Microwaves, December 1969.

39. R. D. Moyer, "Microwave Absorber, Emerson and Cumming Type HPY-12," Sandia Laboratories Evaluation Report, December 15, 1975.

APPENDIX A

EMES DESIGN DETAILS

APPENDIX A

EMES DESIGN DETAILS

In this Appendix, the basic design considerations for EMES are presented in some detail. As discussed in the text, the dividing line between low and high frequency operation is the cutoff frequency for higher order mode propagation on the transmission line. Below that cutoff frequency, f_c, the TEM mode is the only one propagating on the line and quasi-static solutions for characteristic impedance and field distribution hold. Above f_c, special precautions must be taken to assure that the TEM mode remains the predominate propagating mode.

Characteristic Impedance

Expressions for the characteristic impedance of triplate or rectangular lines are available from a number of sources.[8,10,12] A general equation for the impedance, Z_o, of lines like those shown in Figure A-1 is:[12]

$$Z_o = \frac{94.15}{\sqrt{\varepsilon_r}\left(\frac{W/d}{1-t/d} + \frac{C_f}{8.85\ \varepsilon_r}\right)}\ \Omega\ ;\ \frac{W}{d} \geq 0.35 \qquad \text{(A-1)}$$

Where ε_r is the relative dielectric constant of the medium surrounding the center plate ($\approx$1 for air), W is the width of the center conductor, d is the separation between the ground planes, t is the thickness of the center conductor, and C_f is the fringing capacitance in pf/m from the center conductor to the ground planes.

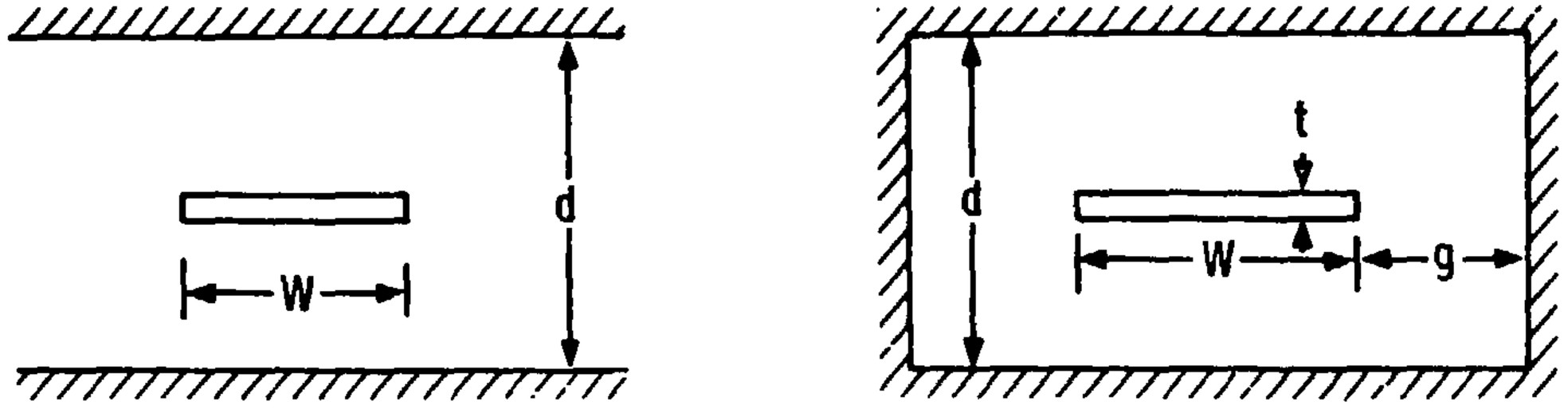

(a) TRI-PLATE LINE

(b) RECTANGULAR COAXIAL LINE

FIGURE A-1: PARALLEL PLATE TRANSMISSION LINES

C_f can be specified in simple form for the tri-plate line as:[12]

$$C_f = \frac{8.85}{\pi} \varepsilon_r \left\{ \frac{2}{1-t/d} \ln\left(\frac{1}{1-t/d} + 1 \right) - \left[\frac{1}{(1-t/d)} - 1 \right] \left[\ln\left(\frac{1}{(1-t/d)^2} - 1 \right) \right\} \text{pf/m} \qquad (A-2)$$

For the rectangular line, determination of C_f is more complicated, requiring numerical solution or measurement on scale models.[8,6] Fortunately, closed form expressions for the approximate characteristic impedance of the coaxial rectangular line have also been derived.[8,10,11] One such expression for the case of a zero thickness center conductor is given in Equation A-3.

$$Z = \frac{94.15}{\frac{W}{d} + \frac{2}{\pi} \ln\left(1 + \coth \frac{\pi g}{d}\right)} \ \Omega \qquad (A-3)$$

From (A-3) it can be seen that the characteristic impedance varies inversely with the sum of W/d and $\left|(2/\pi) \ln (1 + \coth \pi g/d)\right|$. The EMES design maintains the distance, g, between the edges of the center plate and the side walls at a constant value in the transition section. This means that g/d increases as the line tapers down toward a point. However, the hyperbolic cotangent function slowly approaches a limiting value of unity with increasing values of the argument. The variation in Z_o with changing g/d is further moderated by the logarithmic dependence on g. The net effect is that holding g constant in the transition region does not significantly change the characteristic impedance. For the dimensions of EMES, the impedance in the rectangular section is within about 1.5 percent of the value that would obtain if the side walls were infinitely removed ($g/d \rightarrow \infty$); therefore, the largest change in the impedance in the transition sections due to the fixed center plate-to-side wall spacing is less than 1.5 percent.

Field Distribution

One objective of the facility design is to obtain a uniform, planar field distribution over the area to be occupied by the test item; that is, the electric field lines and the equipotential lines should be uniformly spaced, with the electric field lines perpendicular to the center plate and the equipotential lines parallel to it. The field distribution in the symmetrical tri-plate transmission line with infinite ground plans is given in References 15 and 16. The electric and magnetic field lines near one edge of the center conductor in a tri-plate line is shown in Figure A-2. For large W/d, the distance, ΔX, from the edge of the center conductor to the point at which the field is essentially uniform is given by:

$$\Delta X = \frac{d}{\pi} \ln (2) = .22d \qquad (A-4)$$

Therefore, we expect the field to be uniform under the line at points farther from the edge than about one-fourth the ground plane spacing (one-half the center conductor to ground plane spacing). The normalized electric field*, Ey, is plotted as a function of distance along the plane of the center conductor (y=0) and along the ground planes (y=±d/2) in Figure A-3. Note that the field intensity becomes very large at the edge of the center plate (y=0, x=0), a fact which leads to high-voltage breakdown problems for thin plates.

The ground planes of EMES of course, are not infinite. One way to judge the effects of the finite width outer plates on the field distribution is to determine the magnitude of the fringing field at the edge of the outer plates. In Figure A-3, the normalized

*The field is normalized to the magnitude of the electric field in the uniform field region. The normalized magnetic field is equal to the normalized electric field and is perpendicular to it.

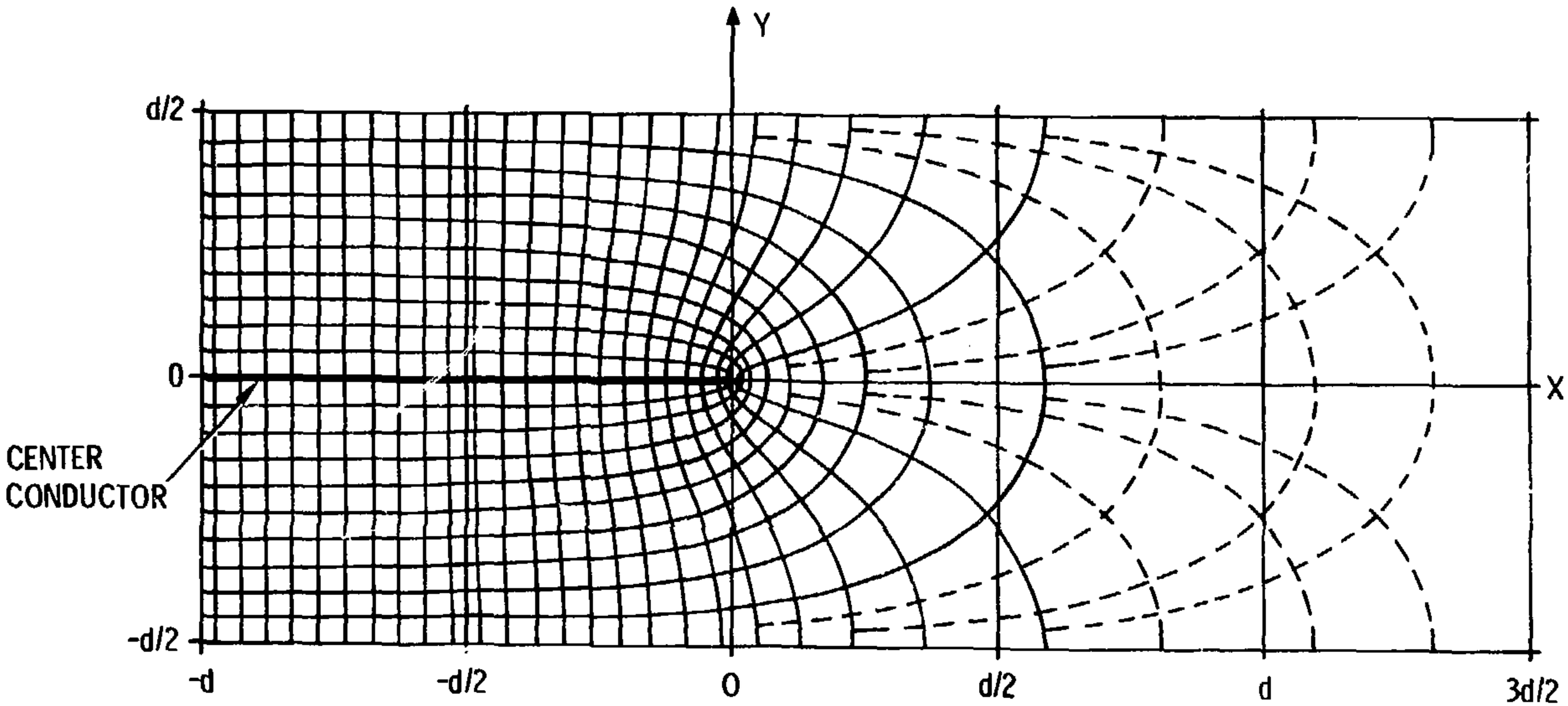

FIGURE A-2. FIELD AND POTENTIAL DISTRIBUTION WITH SEMI-INFINITE CENTER CONDUCTOR IN INFINITE THREE CONDUCTOR PARALLEL-PLATE TRANSMISSION LINF

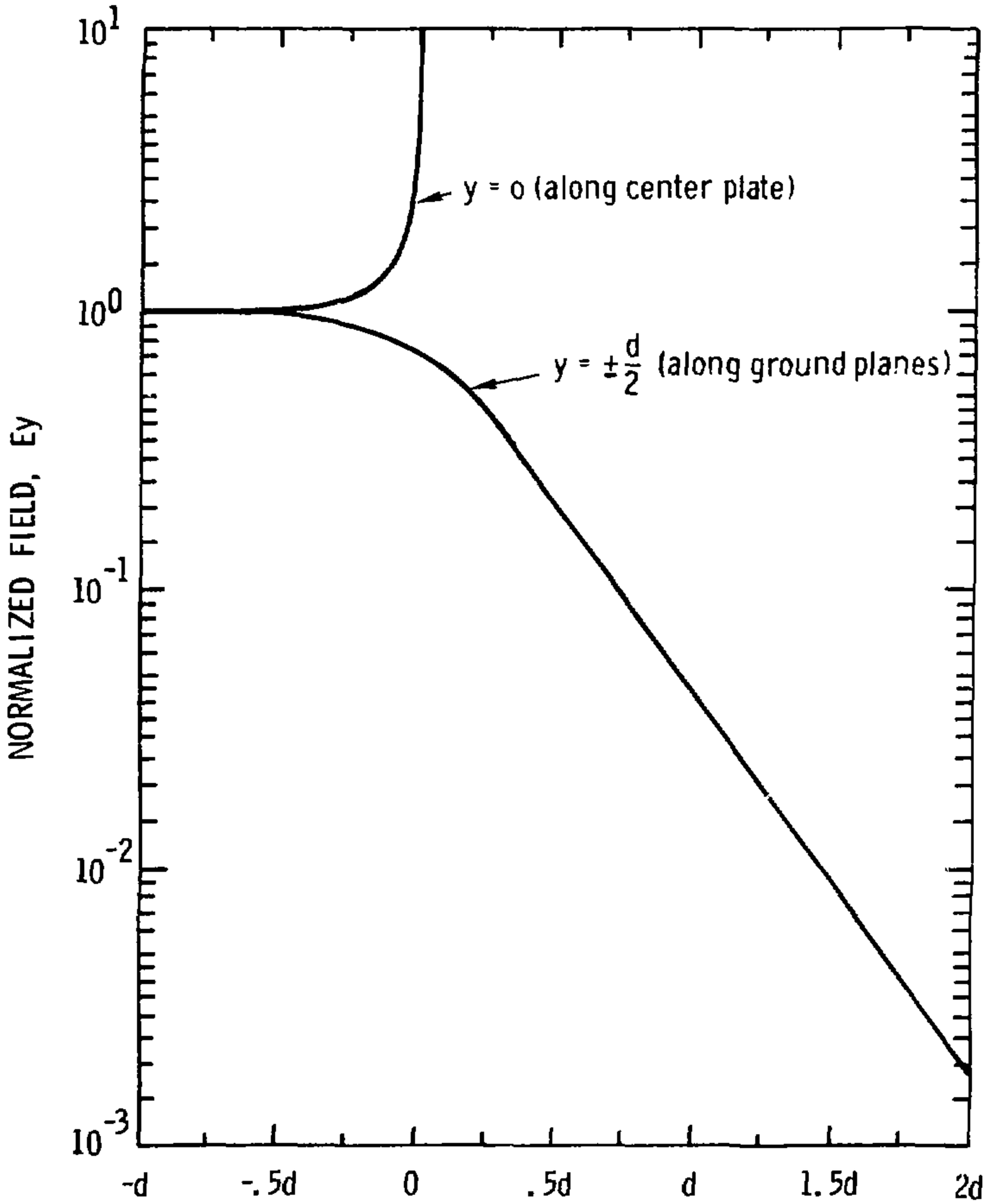

FIGURE A-3. NORMALIZED FIELD DISTRIBUTION WITH SEMI-INFINITE CENTER CONDUCTOR IN INFINITE THREE CONDUCTOR PARALLEL PLATE TRANSMISSION LINE. d IS THE SEPARATION BETWEEN THE GROUND PLANES

electric field along the outer conductors (y=±d/2) is plotted vs. distance.[16] From this plot, one can estimate how far beyond the edge of the center conductor the outer plates must be extended until the fringing field is below a specified level. For example, the 0.1 fringing field level is at approximately x=0.75d; therefore, the width W′, of the outer plates required to assure that the fringing field at the edge of the outer plates is no more than one-tenth of the field under the center of the line is approximately:

$$W' = W + 2(.75d) = W + 1.5d \qquad (A-5)$$

The magnitude of the field at the edges of the outer plates provides an indication of how strongly the side walls will interact with the wave traveling down the transmission line. Additional insight into this problem is available in a study of the effects of the proximity of a ground plane to a semi-infinite parallel plate transmission line.[21,22] The geometry of the problem is illustrated in Figure A-4. Although the plate arrangement is not the same as that for the facility, the general results should provide guidance for determining the effects of the facility side walls on the field distribution under the line.

In Reference 21, the difference between the magnitudes of the normalized fields under the line with and without the ground plane present are computed for the case of semi-infinite parallel plates (that is, the plates extend away from the ground plane to infinity). Figures A-5 and A-6 show the results of these computations for two values of ground plane proximity distance (g = 0.05d and g = 0.5d)*. The conclusion drawn is that the ground plane has no significant effect on the field between the plates if the separation

---

*Only the upper half of the line (y/d>0) is shown because the distribution in the lower half is the mirror image of that shown.

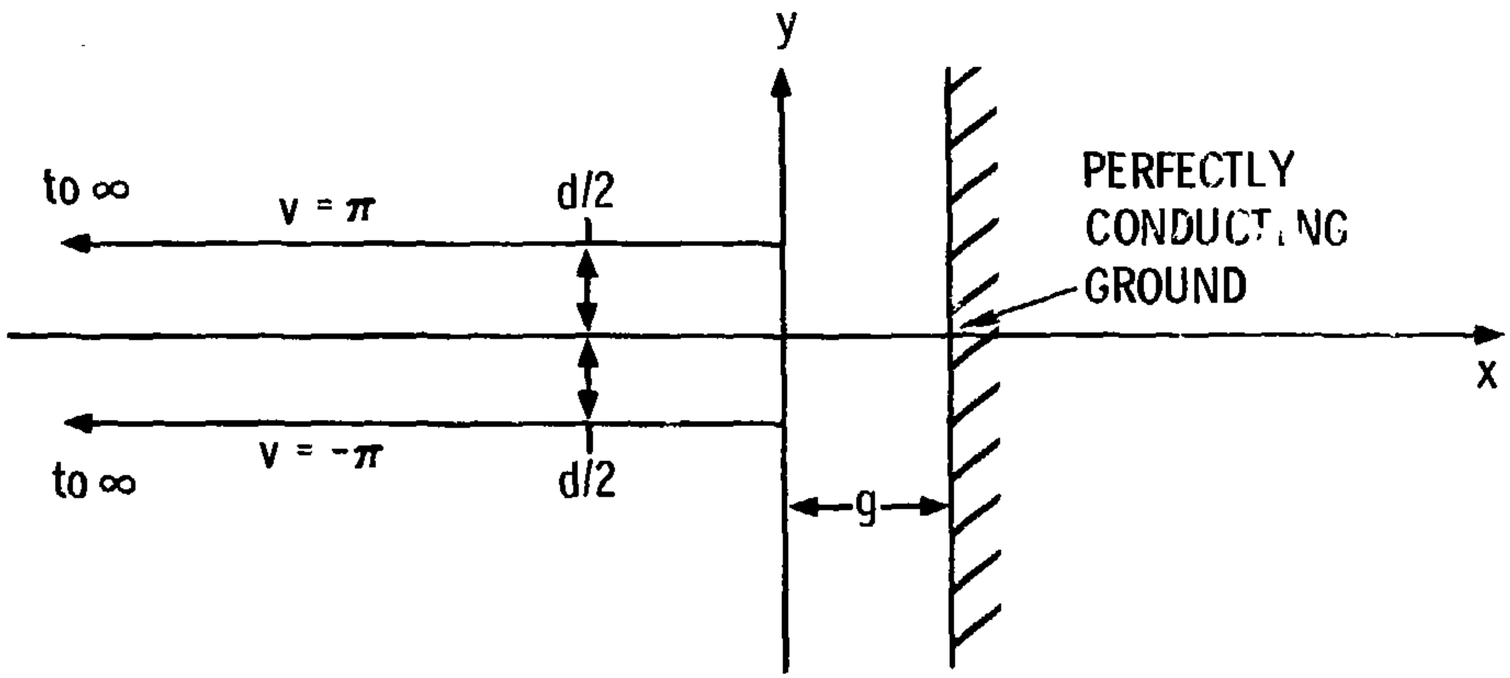

FIG. A-4. GEOMETRY OF SEMI-INFINITE PARALLEL PLATE TRANSMISSION LINE NEAR PERFECTLY CONDUCTING PLANE GROUND.

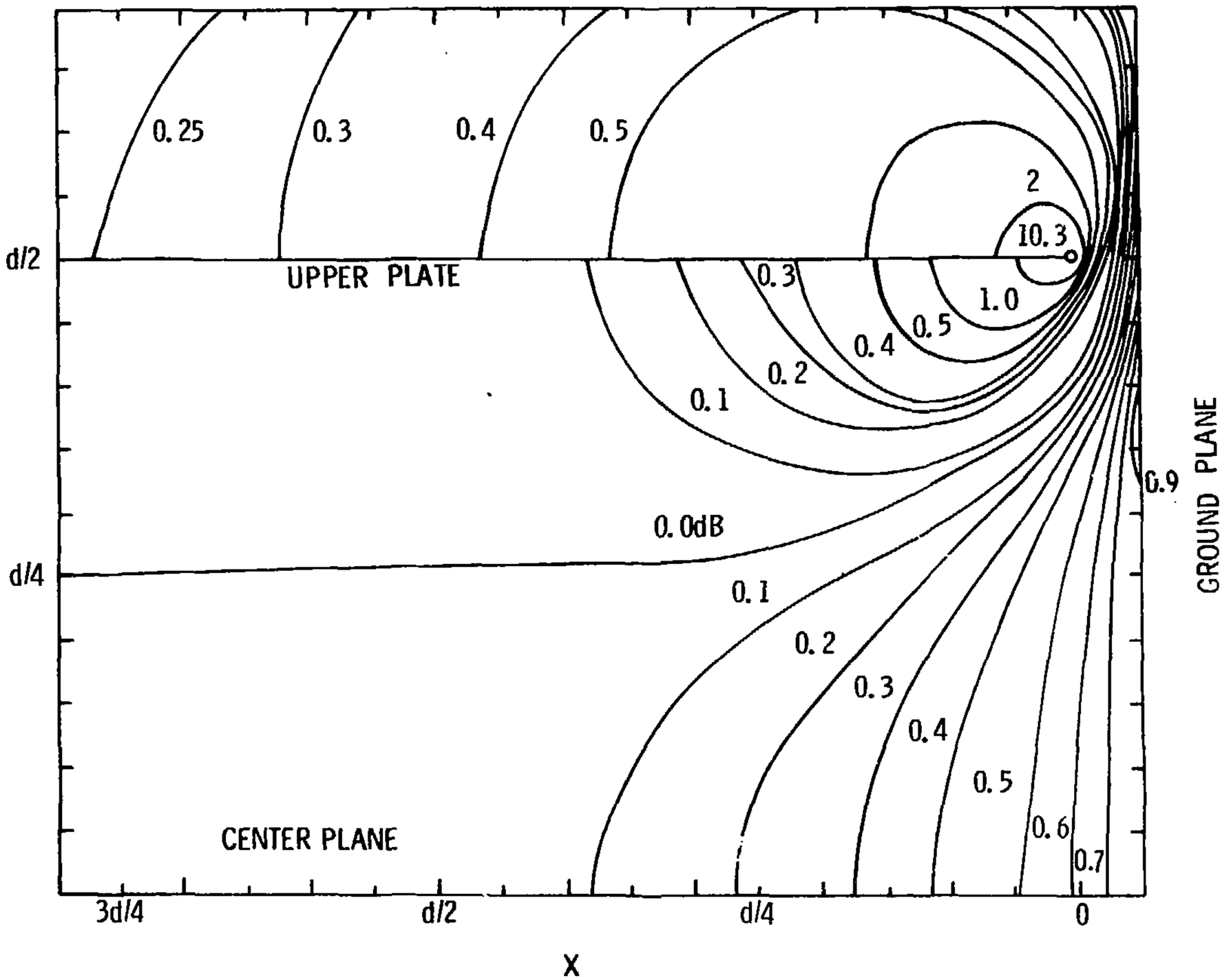

FIGURE A-5 RATIO IN dB OF THE NORMALIZED FIELD BETWEEN TWO SEMI-INFINITE PARALLEL PLANES NEAR A GROUND PLANE TO THE NORMALIZED FIELD BETWEEN THE PLANES IN THE ABSENCE OF THE GROUND PLANE. g = 0.05d

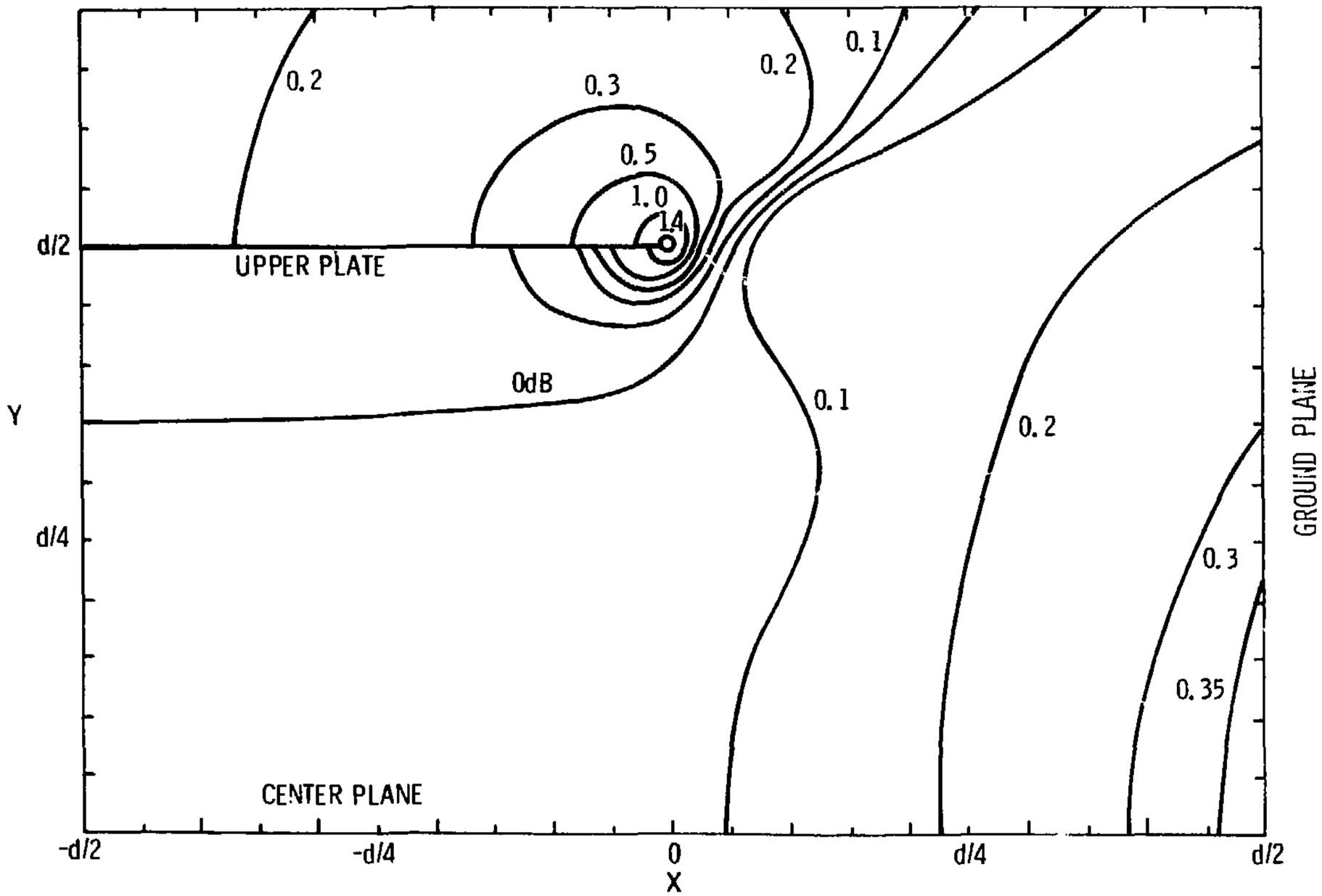

FIGURE A-6: RATIO IN dB OF THE NORMALIZED FIELD BETWEEN TWO SEMI-INFINITE PARALLEL PLANES NEAR A GROUND PLANE TO THE NORMALIZED FIELD BETWEEN THE PLANES IN THE ABSENCE OF THE GROUND PLANE. g=0.5d

between the edge of the plates and the ground plane is greater than one half the plate separation ($g>d/_2$).[21] Figure A-6 illustrates this in that the field between the plates with the ground plane present is within 0.1dB of the field without the ground plane at all points between the plates (except very near the edges of the plates). Differences between the field distribution with the ground plane present and the uniform field distribution are shown in Figure A-7. Note that the field between the plates is within 0.1dB of the uniform field distribution at points further from the edge than approximately 0.25d (see equation A-4).

The finite plate width problem is treated in Reference 22 and is illustrated in Figure A-8. The primary conclusions reached from the study of this problem are that the field between the plates is not significantly affected by the ground plane for g>0.5d (as before) and that the field distribution between the plates becomes increasingly uniform with increasing plate width. The relative field intensity as a function of distance (x) across a line whose width and separation from the ground plane are d and 0.5d respectively is shown in Figure A-9 for several positions (y) between the plates. The variation of field with vertical position is apparently unavoidable.[5,6] The uniformity with horizontal position can be improved by making the plates wider. The field magnitude increases sharply near the edges of the plate (at x=0 and x=-d in Figure A-9), and it will be desirable to round the edges of the center conductor in the facility to reduce the field concentrations along those surfaces. In EMES, the side walls have been placed at a distance of at least d/2 from the edges of the center plate to reduce their effect on the field in the test volume to a negligible level.

Wavefront Characteristics

As illustrated in Figure A-10, the wavefront in the tapered section is spherical rather than planar as is desired in the working

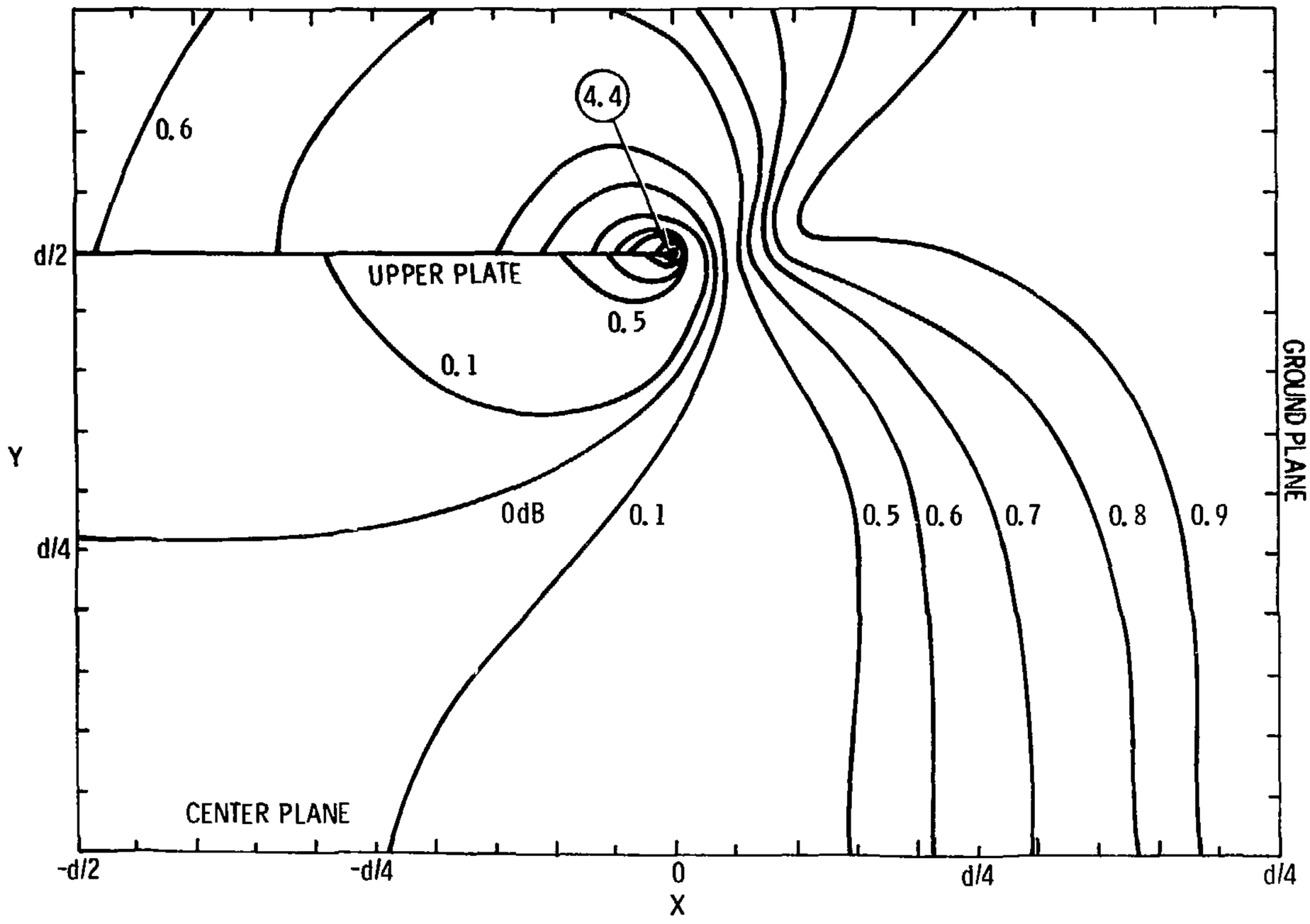

FIGURE A-7: RATIO IN dB OF THE NORMALIZED FIELD BETWEEN TWO SEMI-INFINITE PARALLEL PLATES NEAR A GROUND PLANE TO THE UNIFORM DISTRIBUTION LEVELS. g=0.5d

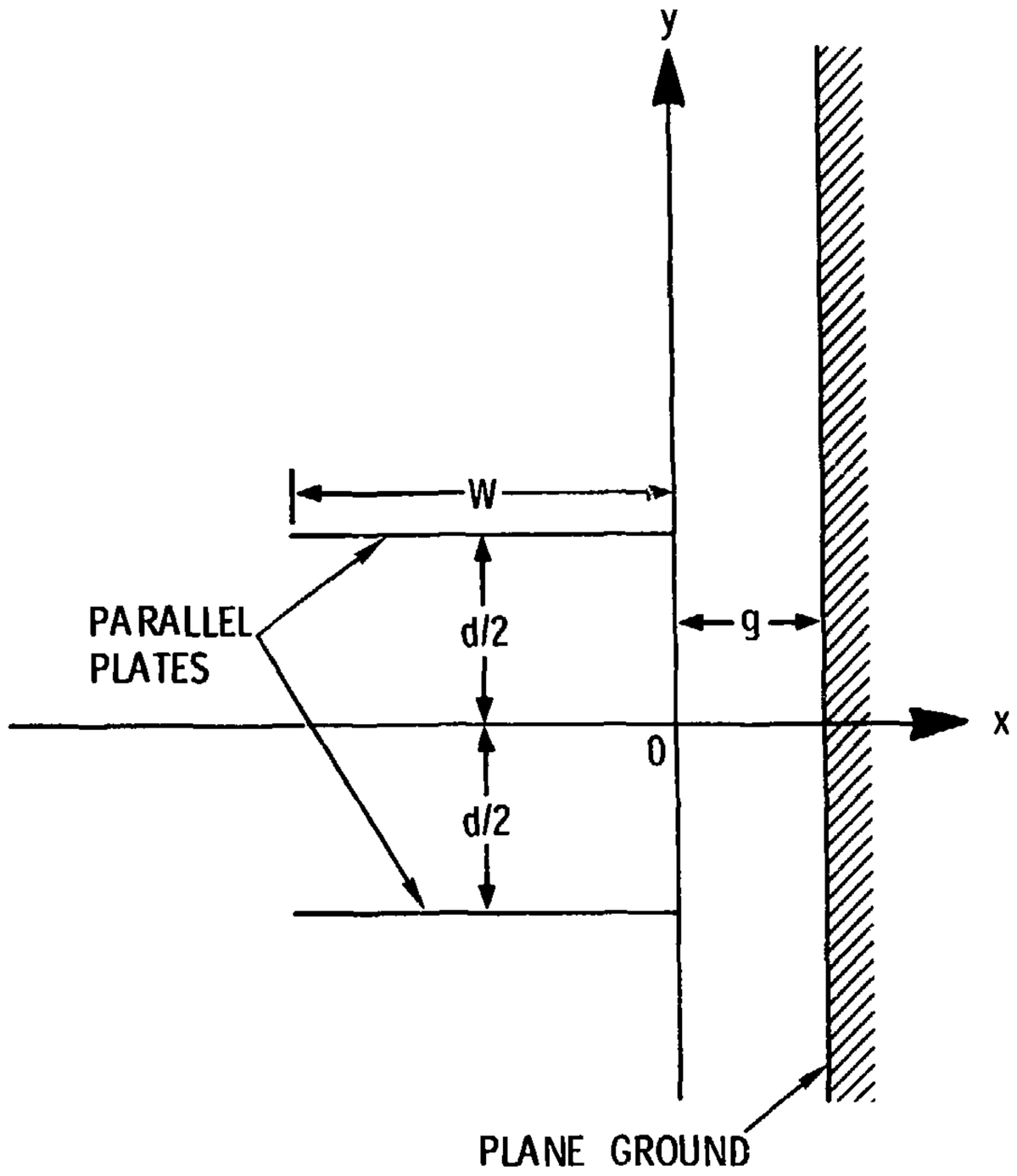

FIGURE A-8: GEOMETRY OF A PARALLEL PLATE TRANSMISSION LINE OF FINITE WIDTH NEAR A PLANE GROUND IN (x, y) COORDINATE SYSTEM FOR THE RELATIVE FIELDS.

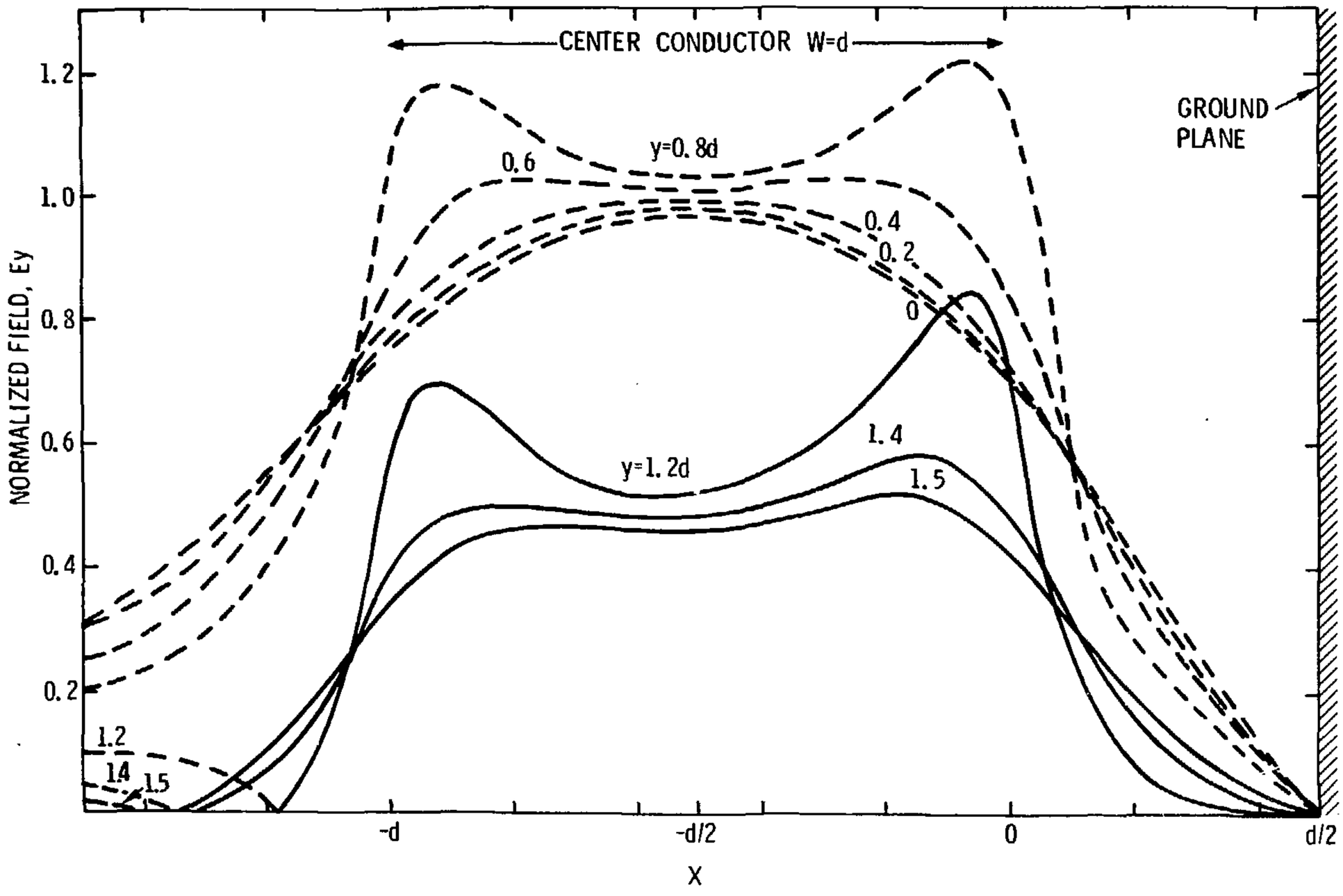

FIGURE A-9: NORMALIZED FIELD AT SEVERAL VERTICAL POSITIONS ABOVE AND BELOW ONE PLATE OF A FINITE WIDTH PARALLEL PLATE TRANSMISSION LINE NEAR A GROUND PLANE. g=0.5d

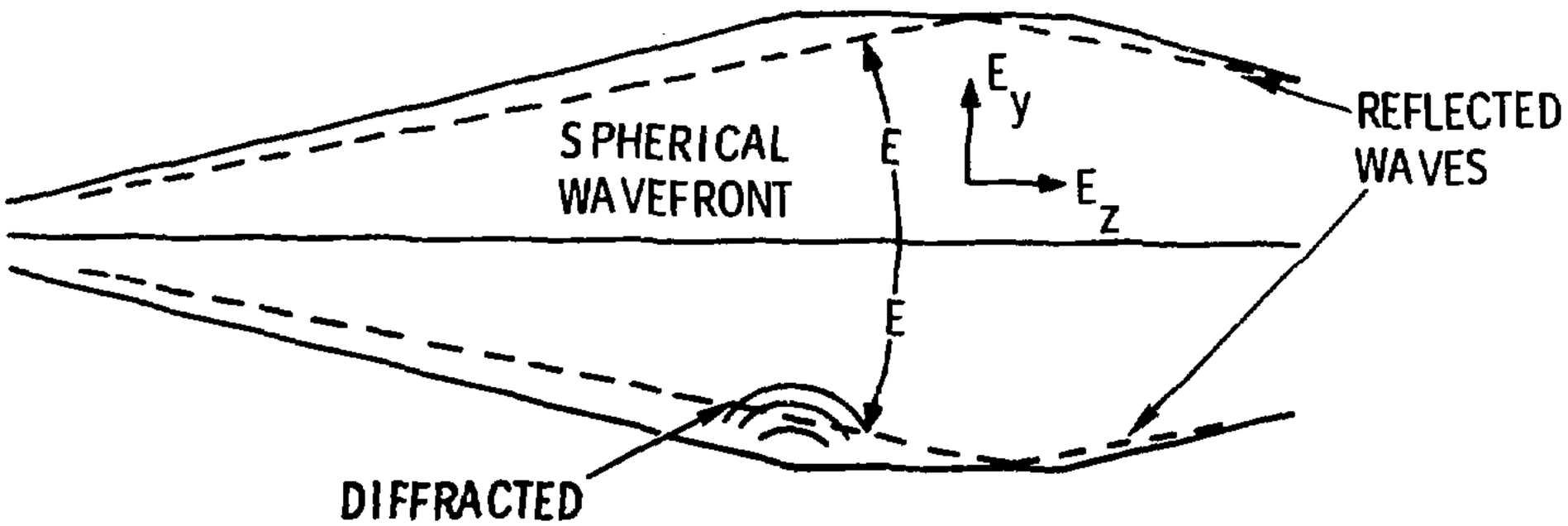

FIGURE A-10: ILLUSTRATION OF WAVE CHARACTERISTICS IN EMES

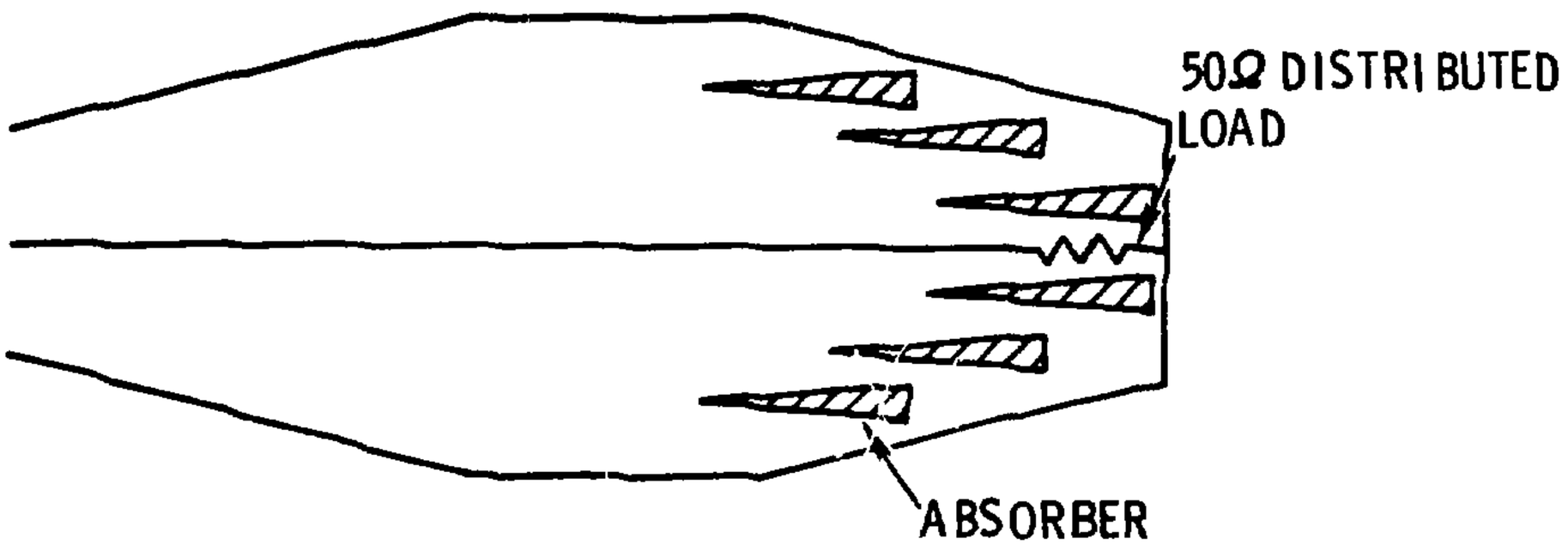

FIGURE A-11: OUTPUT TERMINATION ARRANGEMENT

volume. When the wave is launched onto the flat section of the transmission line from the tapered section there is some time dispersion across the wavefront.[17] A cross-section of the line is therefore not a plane of constant phase. This dispersion of the wave gives rise to an axial component of the electric field (in the direction of propagation) on the flat section of the line in addition to the desired vertical component. Obviously, reducing the slope of the tapered section reduces the dispersion on the flat section. For a fixed working volume size, the length of the tapered input section should be made as great as is practical.

Reflection and diffraction of the wave at discontinuities in the transmission line can also cause non-uniformity of the field in the working volume. Figure A-10 illustrates the problem of reflection and diffraction at the point at which the tapered and flat sections intersect. Considering only first reflections, one can see that the maximum reflection angle from the upper or lower ground planes is equal to the angle of the input taper. This fact suggests that the forward portion of the flat section should be used for the test item location and that some measures should be taken to assure that the reflected waves are not allowed to re-enter the working volume after subsequent reflections. Multiple reflections are suppressed in EMES by placing EM absorber at critical locations.

Reflections can also occur from the side walls of the facility with a much larger set of possible reflection paths to the working volume. At low frequencies, however, the wave is well contained (as discussed in the preceding section) and very little energy reaches the side walls. Again, the proper placing of absorber can help eliminate the high frequency problem.

Diffraction at the bends in the upper and lower ground planes and at the edges of the center plate is a more complicated problem.[23]

The diffracted wave has components which radiate in all directions from the discontinuity and which cannot be prevented from entering the working volume. However, the magnitude of the diffracted wave is small. An analysis of a similar facility indicated that the diffracted component in the working volume was no greater than 5 to 10 percent of the incident wave.[5] It is not anticipated that diffraction will cause significant disturbances to the fields in the working volume.*

Output Termination

For proper operation of the facility, the energy coupled to the input must be absorbed in a matched load at the output end. This termination is provided at low frequencies by a resistive load and at high frequencies by absorbing material. One method of providing the proper low frequency load is to taper the output of the line down to the dimensions of a conveniently sized coaxial line and use a broadband 50Ω termination. This was the initial design approach used.

In the interest of reducing the size of the facility, a second configuration was examined and was subsequently selected as the optimum design (see Figure 1 in the main body of the report). Instead of tapering the output section down to small dimensions, the facility was truncated at some point past the working volume.** A

*Making the connection between the tapered and flat sections a smooth curve instead of a sharp bend is one way of reducing diffraction from the joints if it should prove to be significant. Diffraction from the edges of the center plate will be reduced by the rounding of the edges which must be done anyway for corona suppression.

**The distance from the back edge of the working volume to the rear wall of the facility is determined primarily by the space needed to install EM absorbing material in the output transition.

50Ω distributed load impedance connected between the center plate and the rear wall of the facility provides the proper termination for the low frequency bounded wave (see Figure A-11). The EM absorbing material should absorb the higher frequency components and prevent their reflection from the rear wall.

The EM absorbing material is a carbon loaded polyurethane foam covered with a fire retardant paint. The material to be used in EMES is shaped into 4m long pyramids with 0.61m square bases. The absorptive properties of the material depend upon a number of factors such as the frequency and angle of incidence of the wave, the thickness and density of the absorber, and the amount of carbon dispersed in the foam. For typical absorbers with normal wave incidence, the reflected component* decreases with frequency at approximately 20 dB/decade and is equal to approximately -30 dB at the frequency for which the material is one wavelength thick.[37]

At low frequencies, the absorber increases significantly the capacitance between the center plate and the ground plane. This, of course, changes the impedance of the line and causes a reflection from the impedance discontinuity. To reduce the effect of the absorber, it is spread out along the length of the output section as shown in Figure A-11 instead of being placed in a vertical plane. At approximately the same axial location the distributed load impedance is installed in the center plate. The co-location of the absorber and the distributed load tends to gradually dissipate the low frequency wave as the volume occupied by the absorber increases.

Shielding Requirements

The requirement for non-interference with nearby users of the EM spectrum places additional constraints on the performance of the

*The reflected wave is measured with the absorber mounted on a conducting plane.

system. The FCC requires that the field strength at a distance of 1000 ft. (305m) from a test facility must not be greater than 1.5×10^{-5} v/m. If the far field radiation condition* is assumed to hold and the maximum power to be used is known, the minimum shielding which the facility walls must provide can be computed. The maximum allowable field level just outside the facility (0.1m is used as the minimum practical distance at which measurements can be made) would be approximately:

$$E_1 = \left(1.5 \times 10^{-5}_{\text{v/m}}\right) \left(\frac{305\text{m}}{0.1\text{m}}\right) = 4.6 \times 10^{-2} \text{ v/m}$$

The field strength in the working volume is approximately equal to the line voltage divided by the distance between center conductor and ground plane. For a 200 w source the field is:

$$E_2 = \left[\left(200 \text{ w}\right)\left(50\Omega\right)\right]^{1/2}/_{4\text{m}} = 25 \text{ v/m}$$

The required shielding effectiveness, SE, in db is then:

$$SE = 20 \log \left(^{E2}/_{E_1}\right) \approx 55 \text{ db}$$

<u>High Voltage Breakdown</u>

To produce EMP and lightning environments, high voltage pulses must be applied to the facility. The design must assure that under high voltage excitation arcing does not occur between the center conductor and the ground surfaces. The maximum voltage which will be applied to the facility is anticipated to be 400 KV.

---

*At points far from the source, field intensity varies inversely with distance.

As the voltage between two conductors is gradually increased, corona discharge will develop. The first evidence of this discharge is a hissing noise accompanied by localized streamers. As the voltage is increased the visual critical corona point is reached; corona streamers cover the surface of the conductors, but do not bridge the gap separating them. If the voltage is further increased, sparkover will occur.* Transient voltages have been shown to produce essentially the same discharge characteristics at approximately the same levels as do continuously applied voltages.[31] The voltage levels at which corona and sparkover occur depend primarily upon the size and shape of the conductors, the distance by which they are separated, and the characteristics of the dielectric material surrounding them. It is generally desirable to eliminate areas of high electric stress by avoiding sharp points and bends. In EMES this implies that the edges of the center conductor should be rounded. Cross-section views of two possible center plate designs are shown in Figure A-12, a and b.

For a gap such as the one illustrated in Figure A-12a, if we assume that the stress is concentrated at the edge of the plate and that the nearest ground plane can be replaced by an equivalent image conductor, data on the breakdown characteristics for parallel wires can be used to approximate the performance of the EMES design. Such an approximation should yield conservative results because the large size of the center conductor will tend to increase the actual breakdown voltage. A sketch of the parallel wire model is shown in Figure A-12c. Plots of the visual critical voltage and the sparkover voltage for the parallel wire model are shown in Figures A-13 and A-14 for several values of conductor radius (r). For the larger

---

*For small ratios of conductor radius to separation distance, sparkover occurs before (or at the same time) the visual critical corona point is reached.

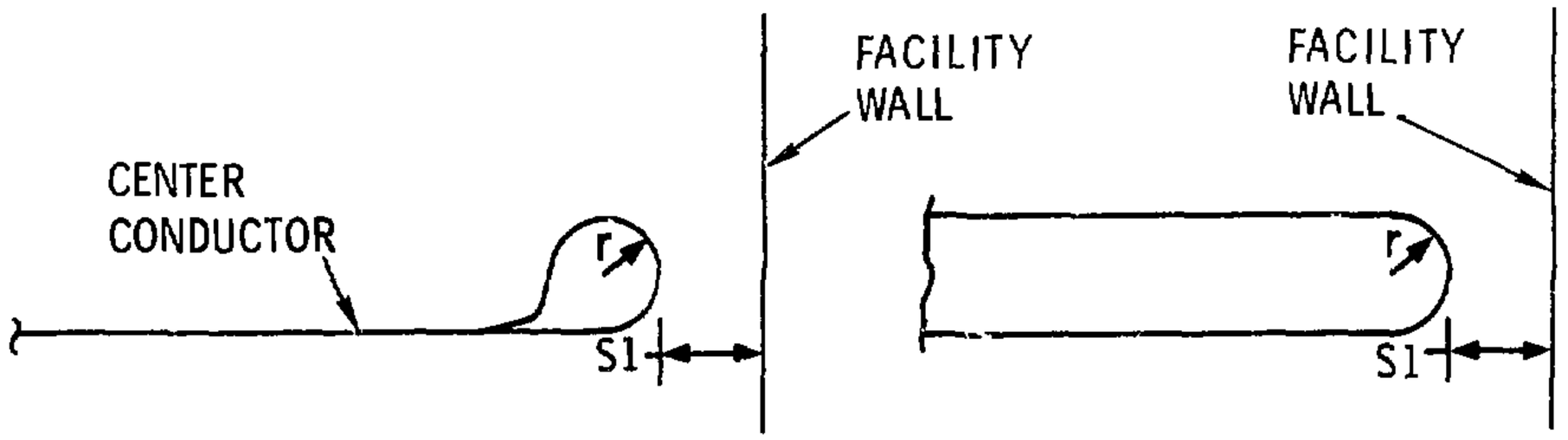

(a) THIN CENTER CONDUCTOR WITH ROUNDED EDGE

(b) THICK CENTER CONDUCTOR WITH ROUNDED EDGE

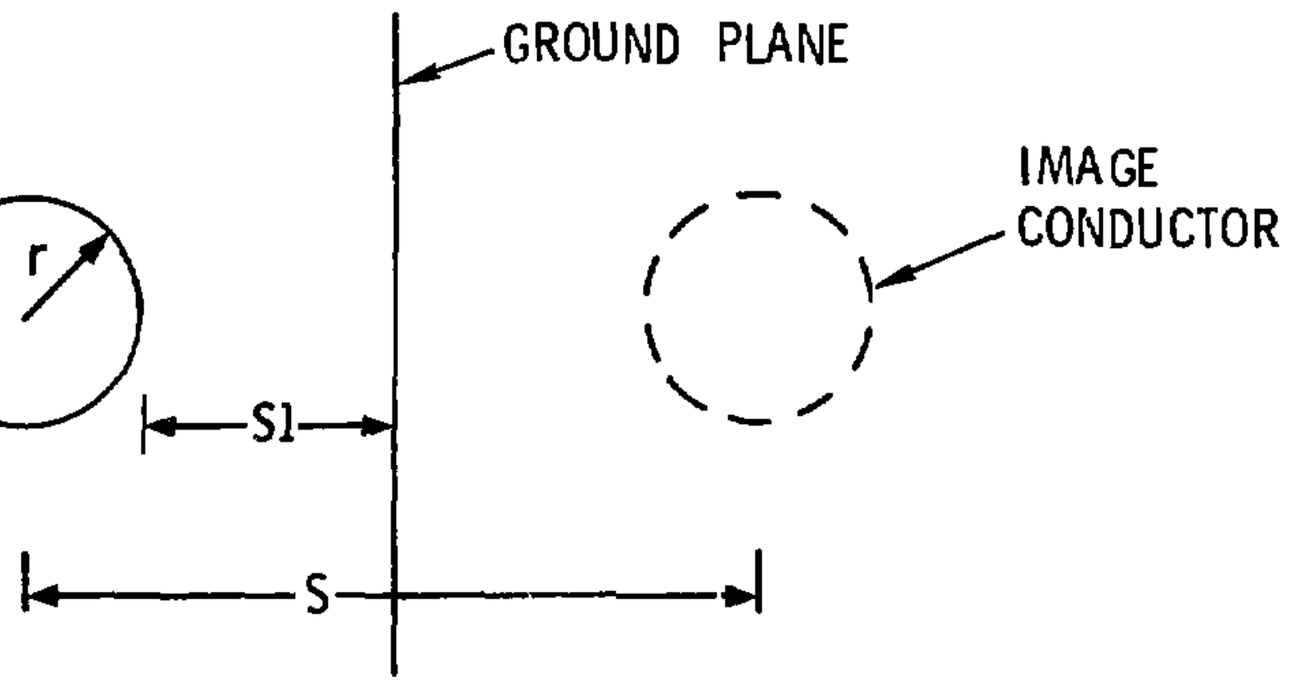

(c) APPROXIMATE PARALLEL WIRE MODEL FOR THE CENTER CONDUCTOR - TO - GROUND PLANE GAP.

FIGURE A-12: POSSIBLE CENTER CONDUCTOR DESIGNS AND HIGH VOLTAGE BREAKDOWN MODEL

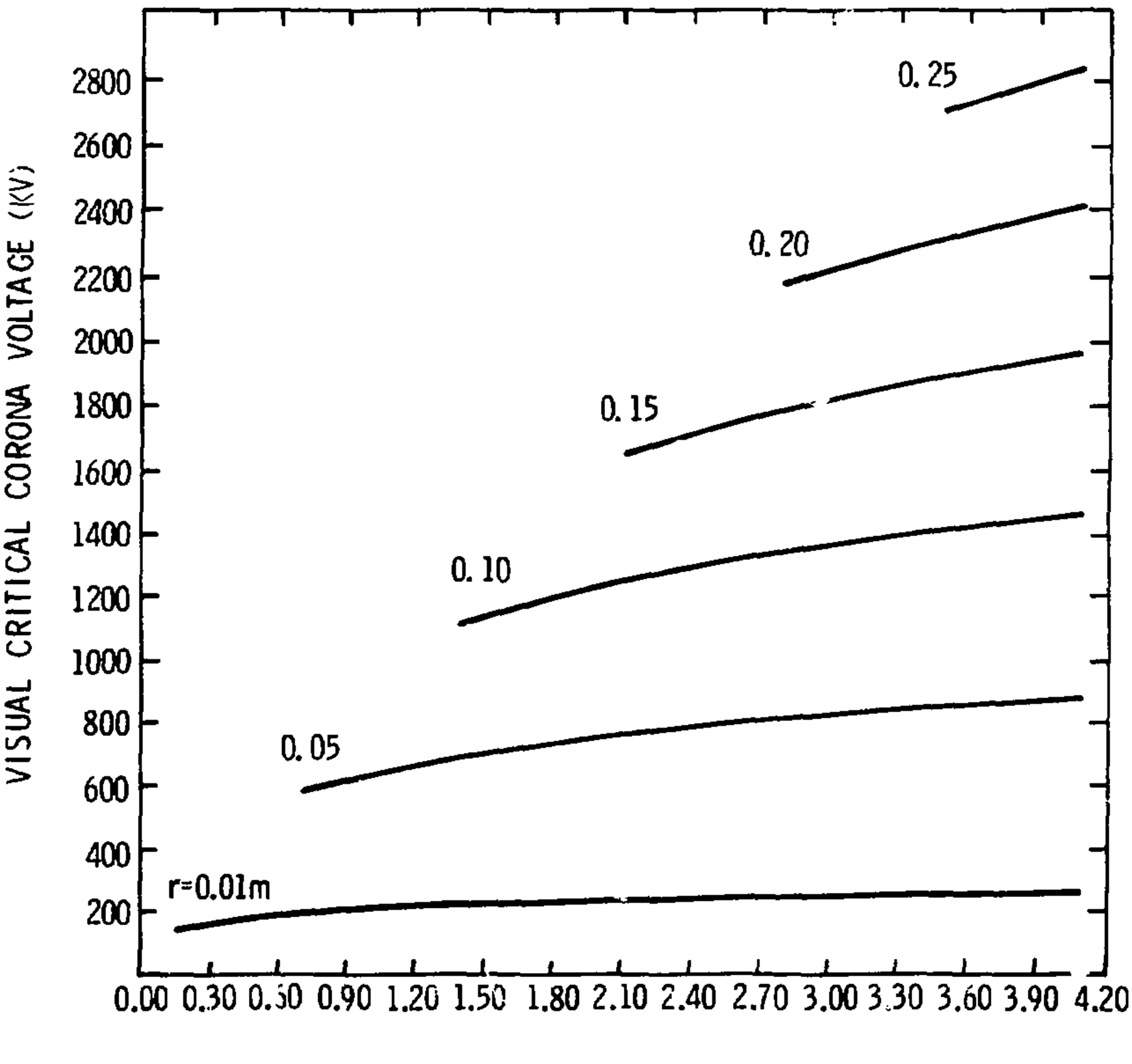

FIGURE A-13: VISUAL CRITICAL CORONA VOLTAGE FOR A ROUND WIRE OF RADIUS R SEPARATED FROM A GROUND PLANE BY A DISTANCE S1.

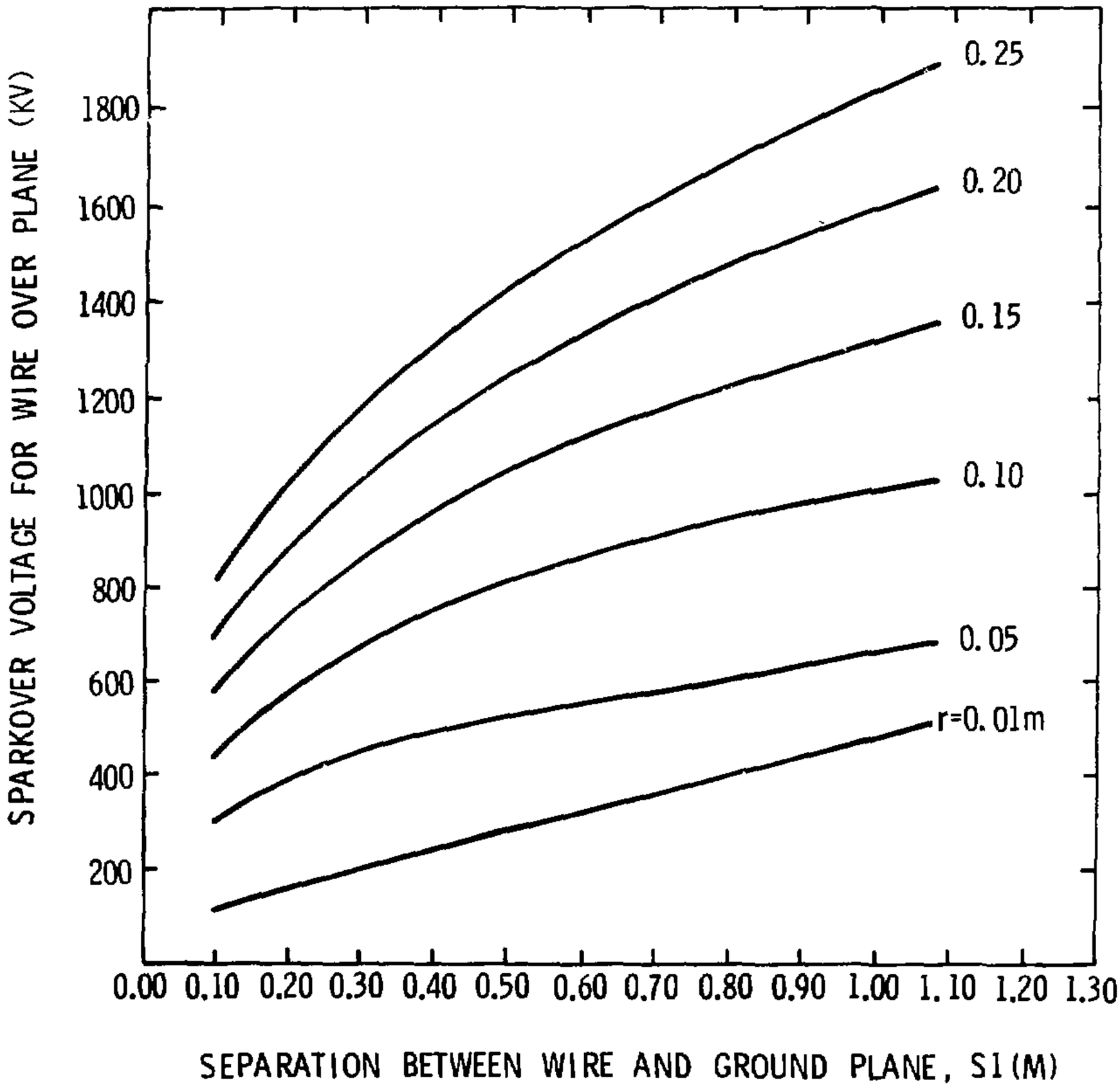

FIGURE A-14: SPARKOVER VOLTAGE FOR A ROUND WIRE OF RADIUS r SEPARATED FROM A GROUND PLANE BY A DISTANCE S1.

conductor sizes, sparkover occurs before the visual corona point is reached; therefore, the curves in Figure A-13 do not extend to the minimum separation considered.

It is apparent that the radius of the edge of the center conductor should be made as large as possible to suppress breakdown. However, the thickness of the center conductor affects the impedance of the transmission line, particularly in the input transition section where the center conductor to ground plane spacing becomes relatively small. It is, therefore, necessary to compromise between high-voltage breakdown and impedance characteristics of the facility. The effect of the center plate thickness is illustrated in Figure A-15 where the impedance of the EMES transmission line is plotted as a function of distance between the upper and lower ground planes for several values of plate thickness. Obviously, a thick center plate cannot be extended all the way to the source connection without causing a significant impedance discontinuity.

To gain the voltage stand-off capability required in the throat of the facility, it is necessary to enclose the center conductor in a dielectric that has better breakdown characteristics than does air. The input transition for high voltage pulse work therefore consists in part of some type of gas- or oil-tight container through which the center conductor will run. This "gas box" section is removable and extends into the facility far enough that the air dielectric can withstand the maximum voltage (at least 400 KV) at the point where the center conductor exits. To prevent large impedance discontinuities, the maximum radius of the center plate corona tube was set at 0.1m. The gas box extends to a point where the ground plate spacing is 1.4 meter (plate to ground spacing is 0.7m). Together with the specified value (0.1m) for the radius of the plate edge, this gives an impedance within about 10% of the desired value (Figure A-15). From Figure A-14, with S1 = 0.7 and r = 0.1, the

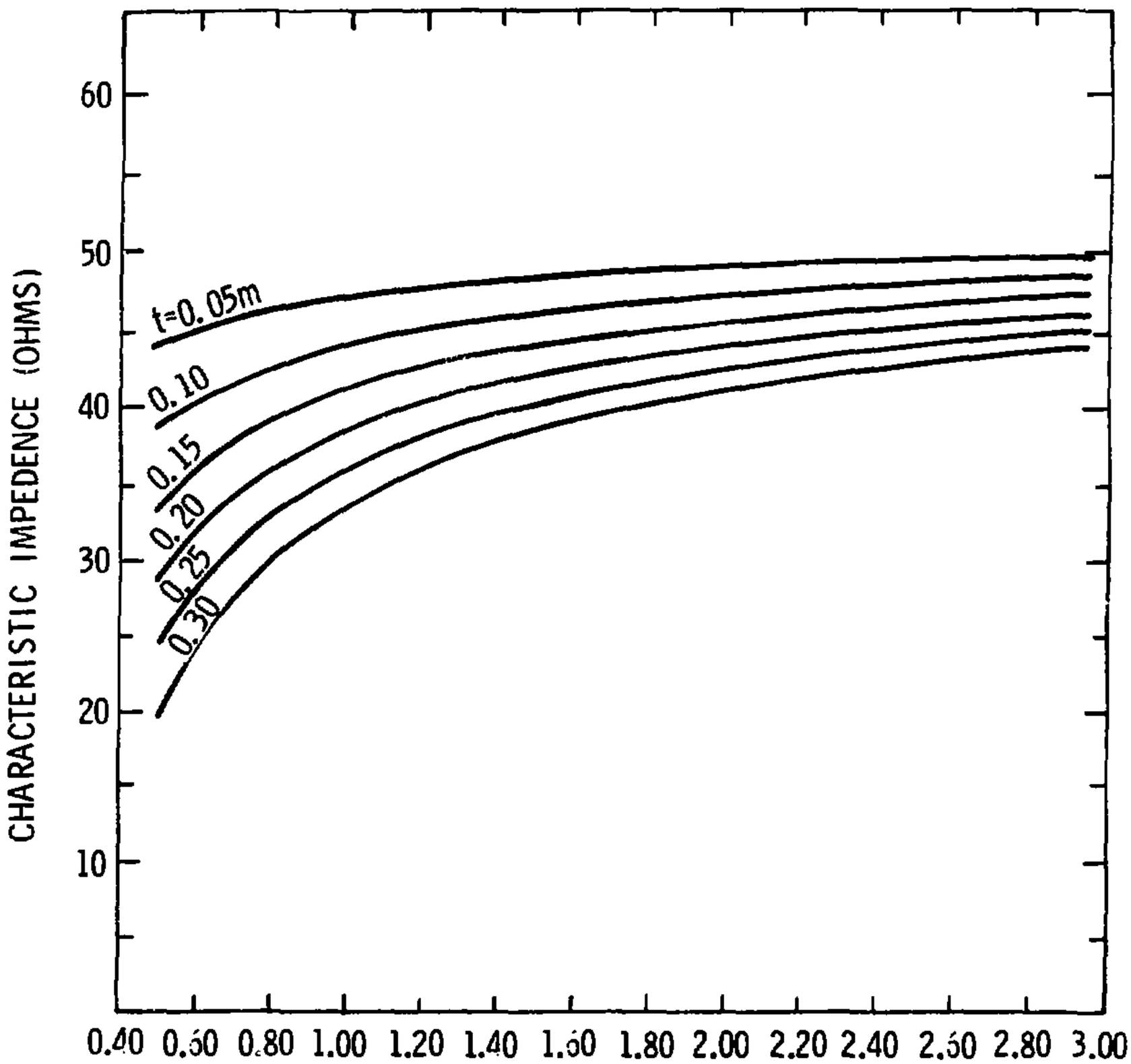

FIGURE A-15: VARIATION OF IMPEDENCE WITH GROUND PLANE SPACING d, FOR SEVERAL VALUES OF CENTER CONDUCTOR THICKNESS, t.

sparkover voltage is approximately 800 KV. This value is considered adequate for high voltage breakdown protection. The gas box section will extend into the facility approximately 2.8m from the input end.

APPENDIX B

SCALE MODEL EXPERIMENTAL RESULTS

APPENDIX B

SCALE MODEL EXPERIMENTAL RESULTS

Several scale models of possible facility designs were examined in an extensive experimental program. Four different physical configurations were modeled on a 1/5th scale and one was modeled on a 1/20th scale. Data were taken over a frequency range of from 10 MHz to 10 GHz using a computer controlled data acquisition system.

Experimental Configurations

The 1/5 scale model was designated FEMES (Fifth-Scale Electromagnetic Environments Simulator). Three FEMES configurations as described below were examined in detail in the experimental program.

1. Constant Width Configuration (straight side walls). In this configuration (Figure B-1) the side walls of the model were plane parallel surfaces. This is the largest of the designs considered. The upper and lower ground plane separation was gradually reduced in both the input and output transition sections to allow termination in a rectangular-to-circular coaxial feed. The load was a lumped 50-ohm coaxial termination. Measurements were made with and without the absorbing material in the output transition.

2. Tapered Width Configuration. In the interest of reducing the size of the facility (and therefore the construction costs) the side walls were made to slope inward from the edges of the working volume to the input and output feed attachment points (Figure B-2). The same ground plane arrangement

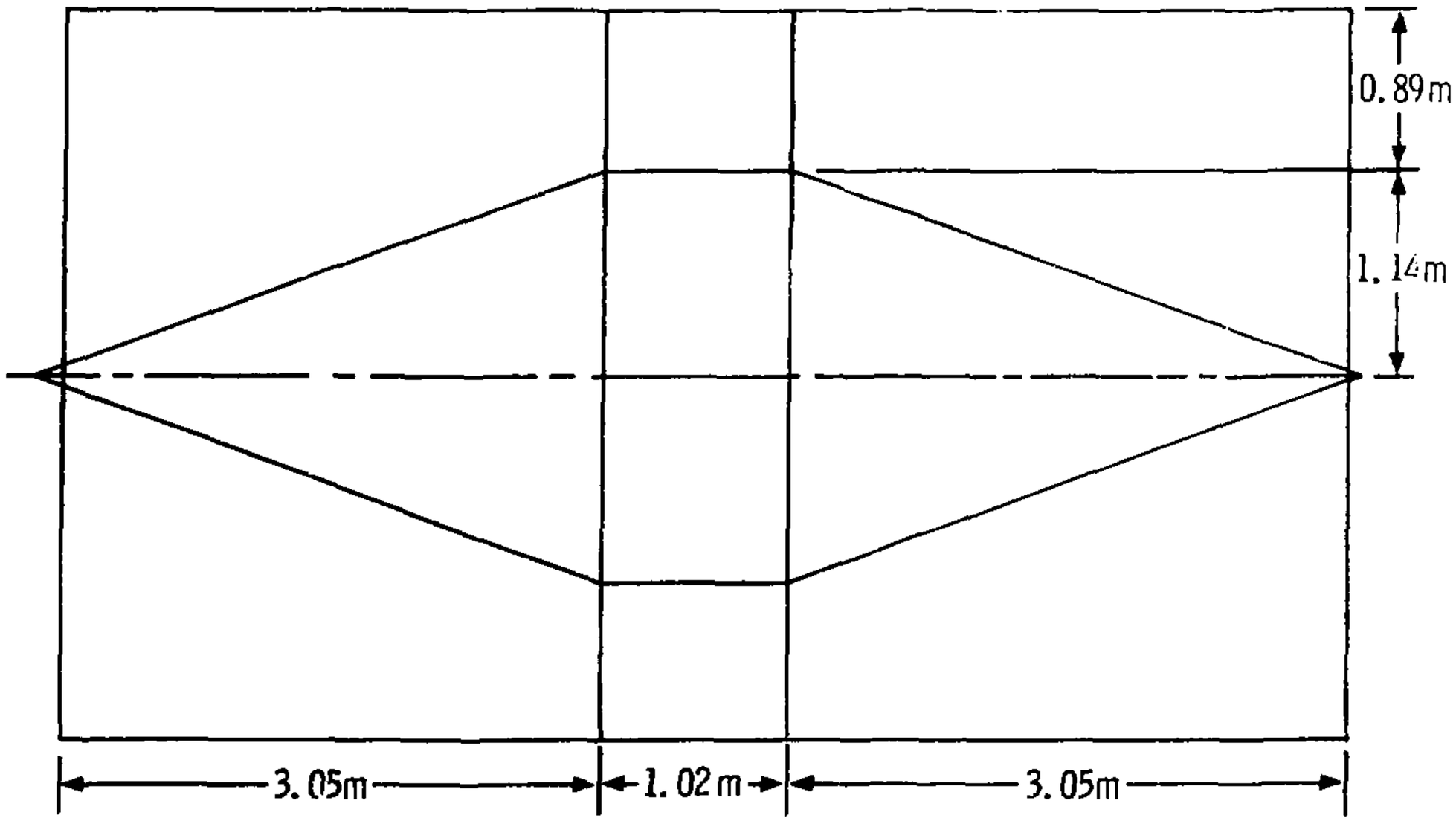

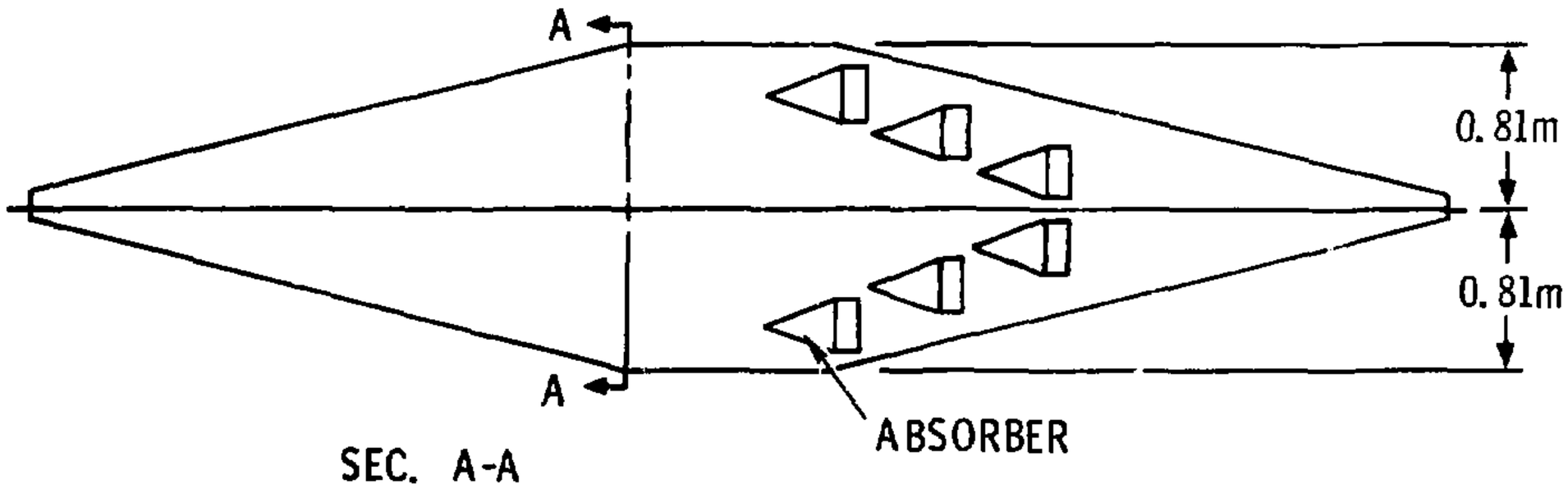

SEC. A-A

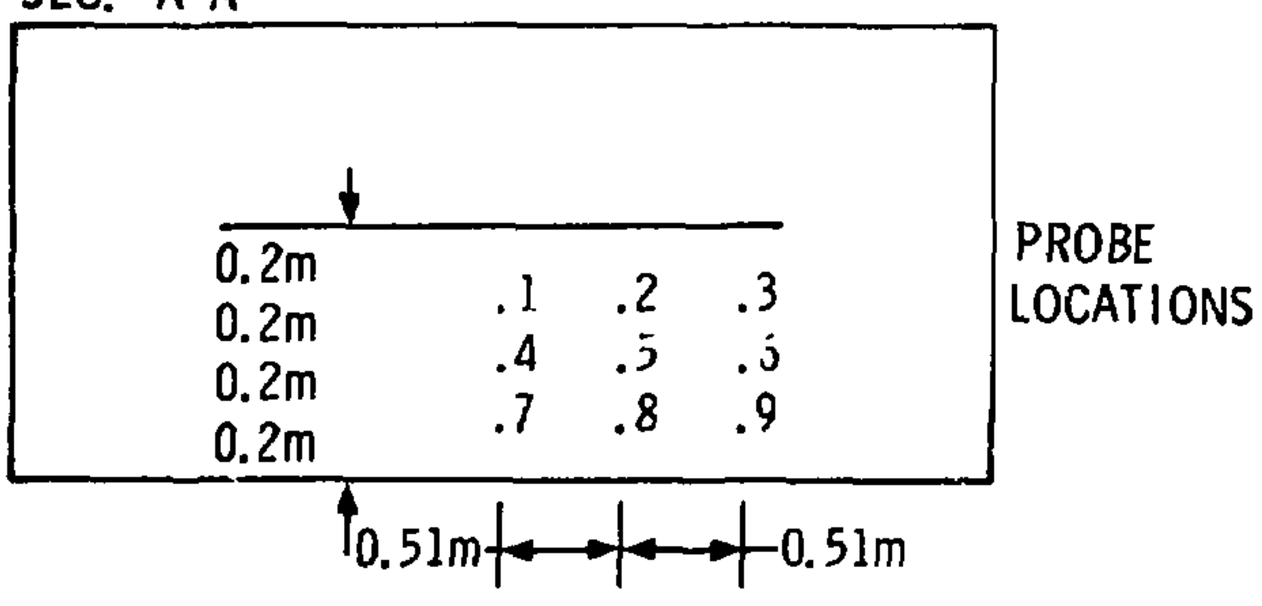

FIGURE B-1: CONSTANT WIDTH CONFIGURATION

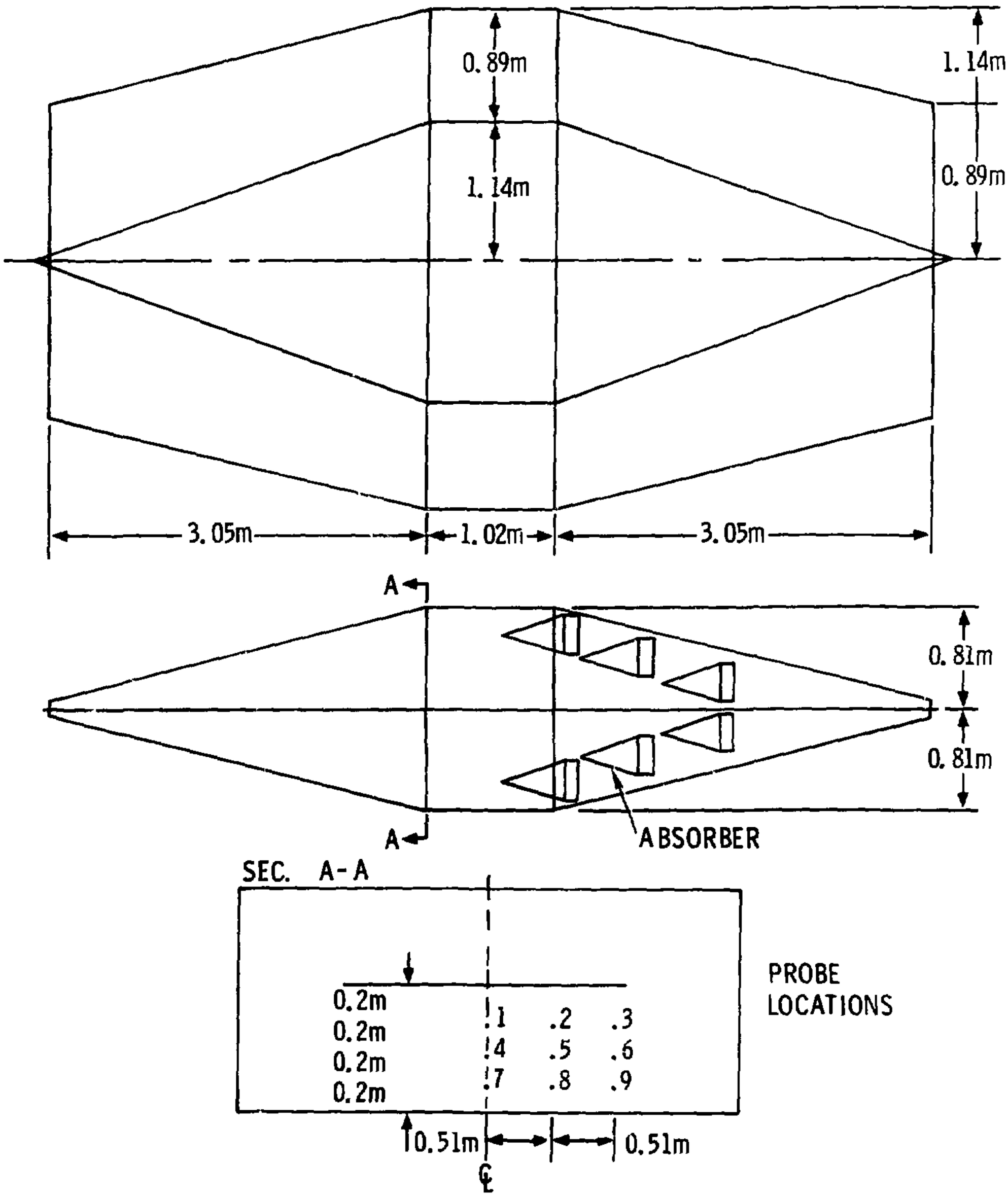

FIGURE B-2: TAPERED WIDTH CONFIGURATION

and output load were used as in the constant width configuration. Data were obtained only with the absorbing material in the output transition.

3. Truncated Configuration. To further reduce the size and cost of the facility, a truncated version was examined (Figure B-3). The tapered width model was altered by placing a conducting wall at a convenient place across the output transition section. The load impedance was installed as a distributed resistor in the center conductor. Data were taken with the absorbing material in the model.

A fourth configuration, described below, was examined in less detail.

4. Eccentric Configuration. In this configuration, the spacing between the upper ground plane and the center conductor was reduced to one-half the spacing between the lower ground plane and the center conductor (Figure B-4). The center plate width and the ground plane width were reduced to maintain a 50-ohm line impedance.[8,10] The distributed resistor load and the truncation point were the same as for the truncated configuration. Data were obtained with the absorbing material in the output transition.

The 1/20th scale model (TWEMES) was constructed primarily to provide some preliminary information on the feasibility of truncation.

5. TWEMES Configuration. In this configuration (Figure B-5) the side walls and ground planes of the input transition section were tapered from the small dimensions at the input to the working volume dimensions. At the output of

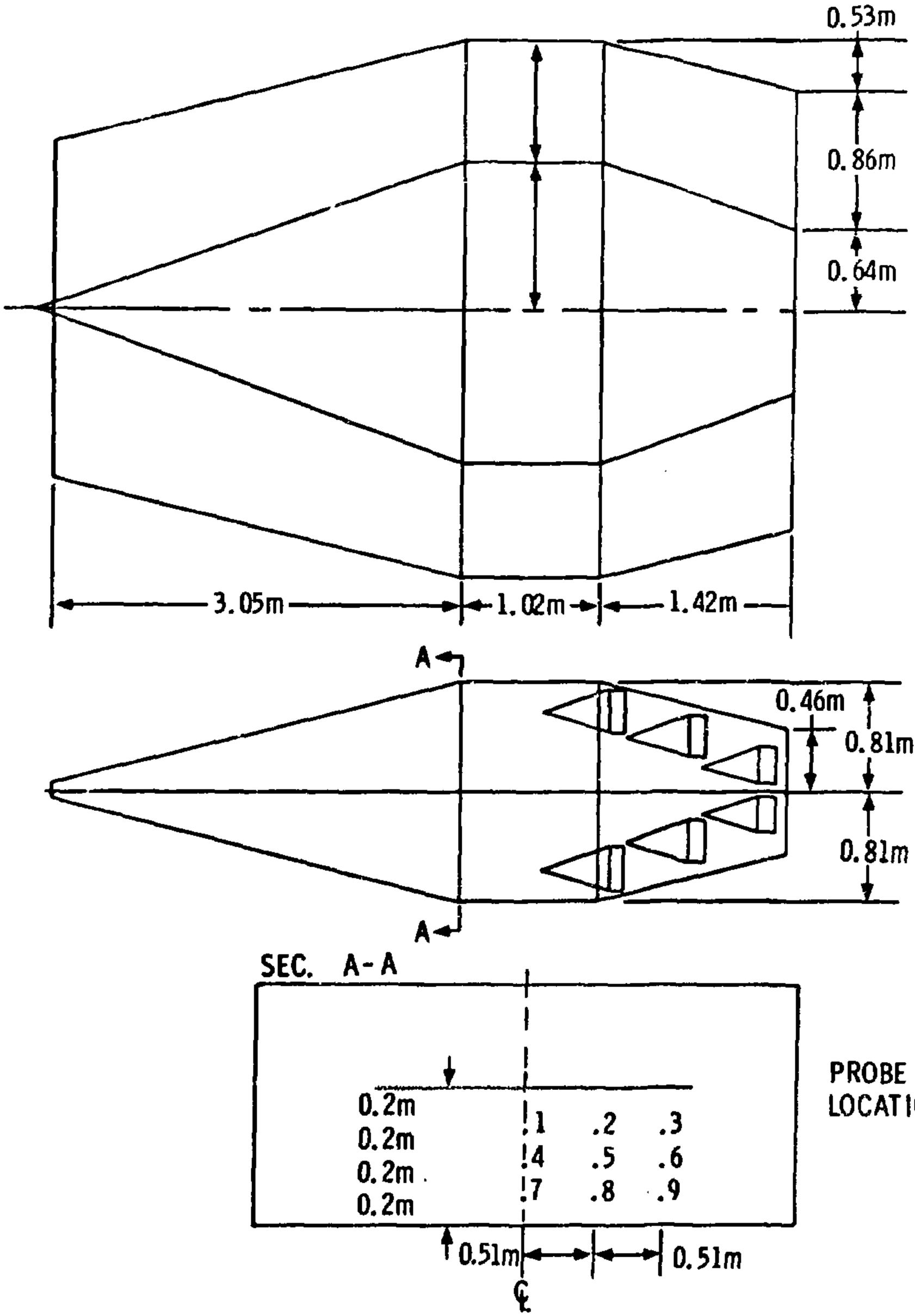

FIGURE B-3: TRUNCATED CONFIGURATION

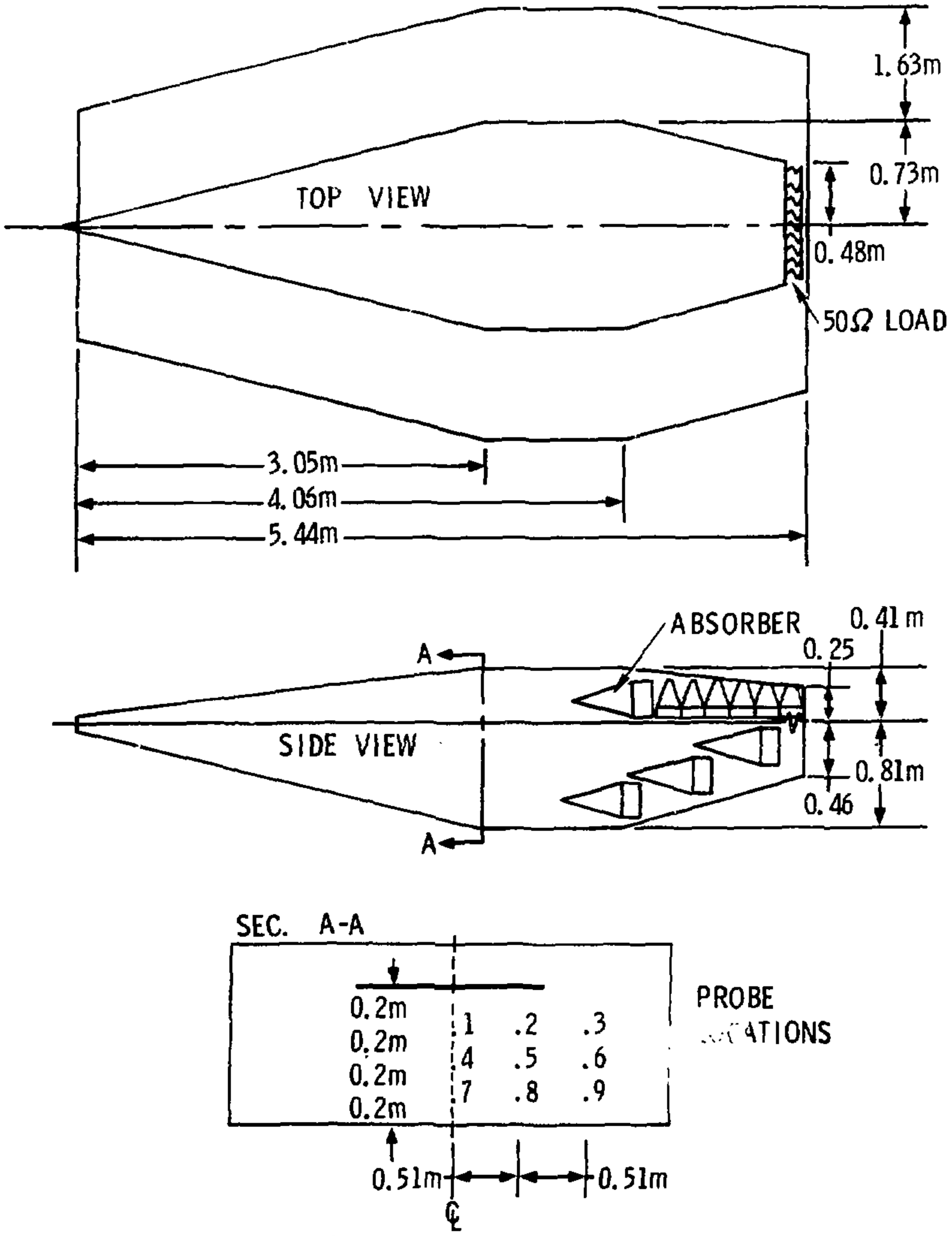

FIGURE B-4: ECCENTRIC CONFIGURATION

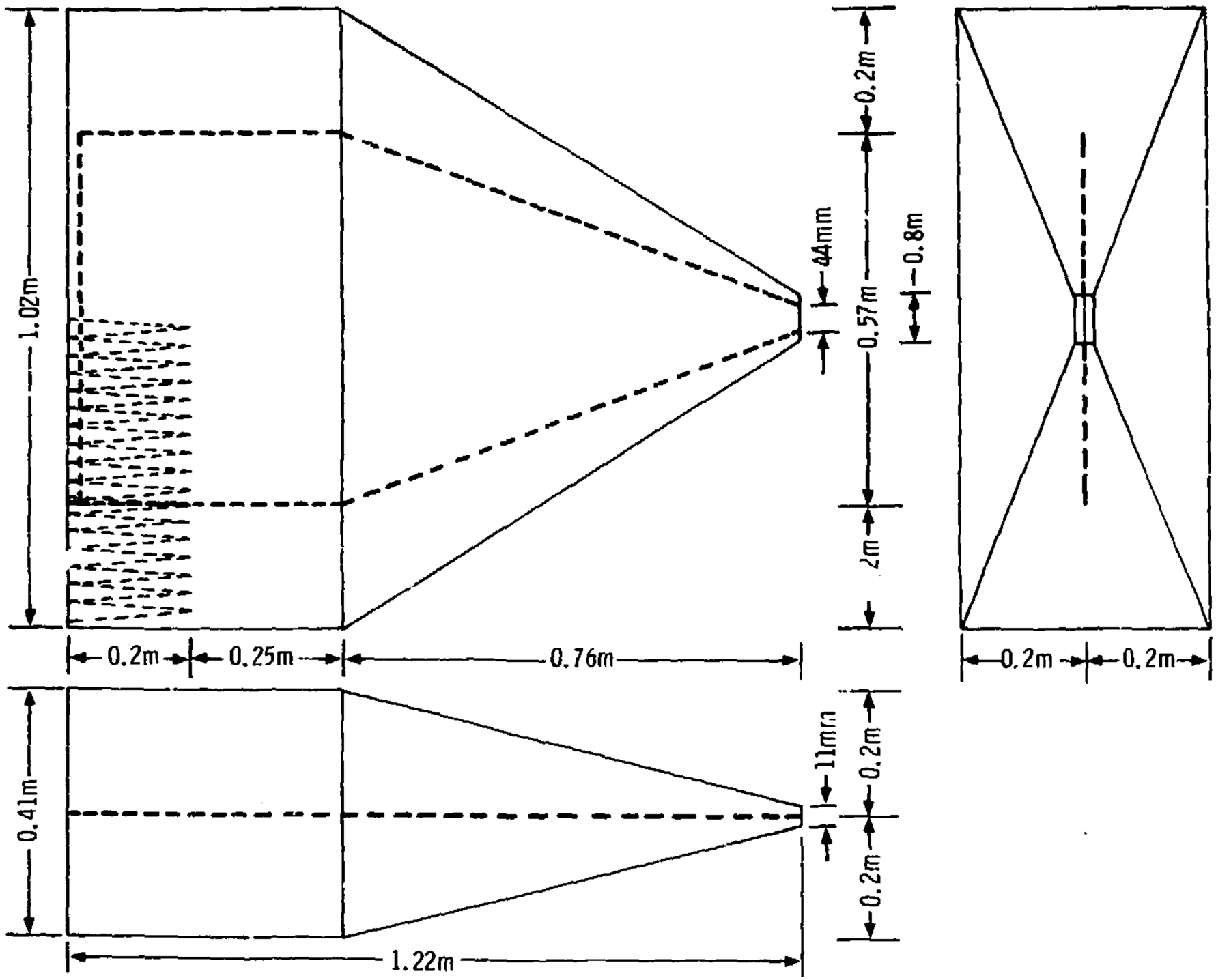

FIGURE B-5: TWEMES CONFIGURATION

the working volume, the height and width of the model were maintained out to the point where the back wall was located. The center conductor was also maintained at a constant width at the output of the working volume and was connected to the back wall through a 50 ohm distributed load. Absorber was placed in various configurations across the output end of the model.

The magnitude of the electric field strength was measured at several points in a plane at the front edge of the working volume as shown in the configuration sketches. Data were obtained for the vertical, horizontal and axial components of the electric field by measuring the output of correspondingly polarized field probes.[36] These data were then normalized to the net input field and expressed in dB. The net input field was determined by computing the field strength that would exist in the working volume if the net input power (incident power minus reflected power) were propagating on the line as a TEM wave. The voltage, V_N, and field strength, E_N, under these conditions would be:

$$V_N = \sqrt{P_N/Z_o}$$

$$E_N = V_N/(d/2) \qquad \text{(B-1)}$$

where Z_o is the characteristic impedance of the transmission line and d/2 is the spacing between the center conductor and the ground plane. Measurements were also made of the voltage standing wave ratio (VSWR) and (for configurations 1 and 2) the normalized output power; that is, the power dissipated in the load termination divided by the net input power.

A diagram of the measurement system is shown in Figure B-6. Measurements were made at a density of approximately 50 points per octave at frequencies above 500 MHz and at a somewhat lower density at frequencies below 500 MHz.

Experimental Results

The data from only one probe location, the center front edge of the working volume (Probe 4 in the configuration sketches), will be discussed in detail in this report. A complete set of data taken in the experimental studies is available in the data summary.[35]

Constant Width Model Without Absorber: The normalized field at the center front edge of the working volume for facility geometry 1 (constant width configuration) without absorbing material in the output transition is plotted versus frequency in Figure B-7. The field is essentially constant and within 1 dB or less of the desired level (0 dB) at frequencies up to approximately 80 MHz. The first large resonance occurs at approximately 95 MHz which is very close to the cutoff frequency (93.5 MHz) for higher order modes predicted by Equation 1 in the body of the report for the FEMES dimensions (d = 1.6m). At frequencies above 100 MHz, the field level varies wildly (± 15 dB or more). A modal analysis of the facility performance was successful in identifying the eleven resonances that occur between 95 MHz and 200 MHz as four different higher order modes and their harmonics.[24] Because of the rapid proliferation of modes (and observed resonances) with increasing frequency and the problem of sorting out the harmonics of and the interference between these modes, the approach was not extended to higher frequencies. It is clear that the initial configuration does not produce anything like uniform fields across the required frequency range and that it would not be suitable for system testing.

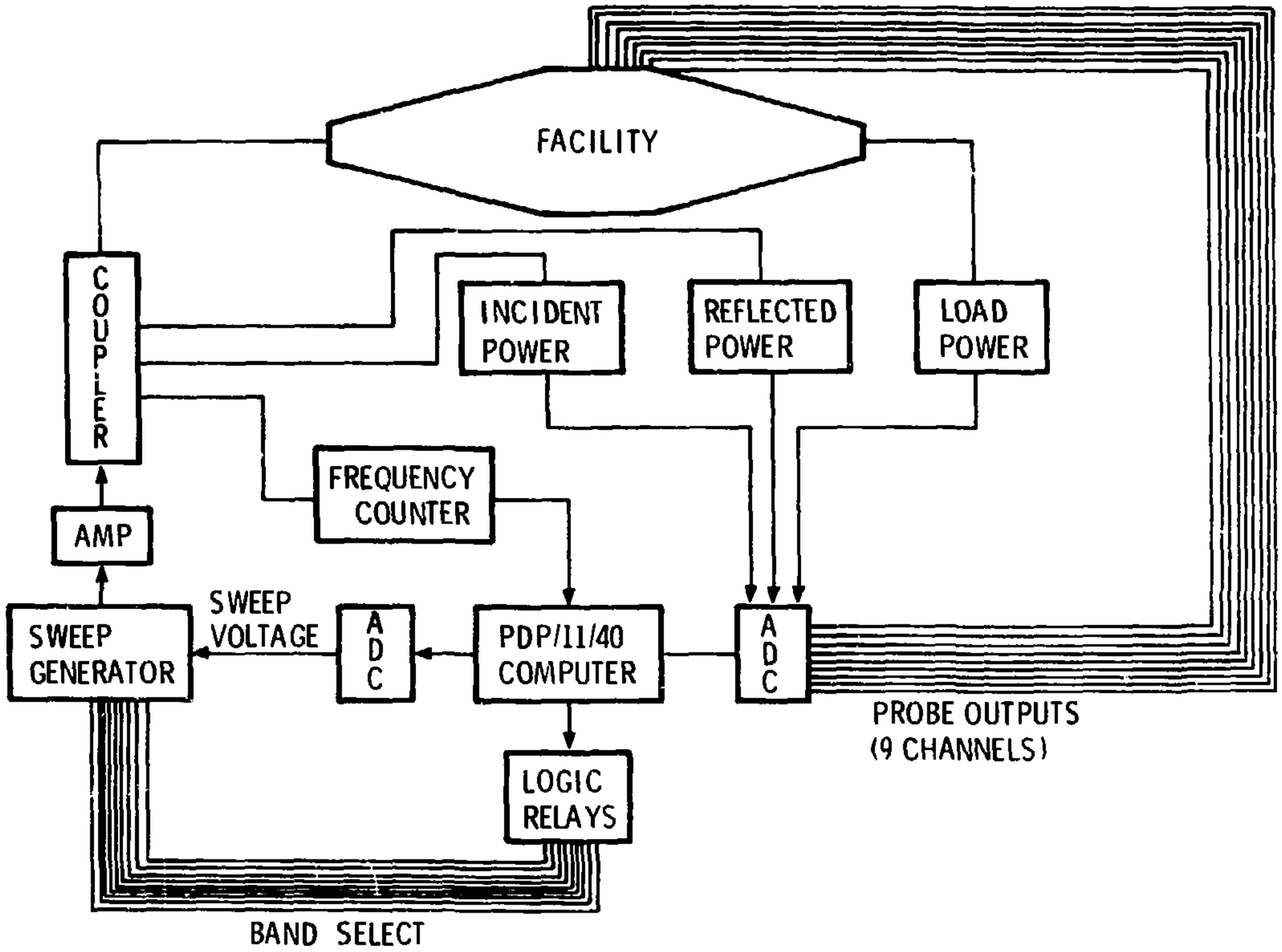

FIGURE B-6: MEASUREMENT SYSTEM FOR MODEL STUDIES

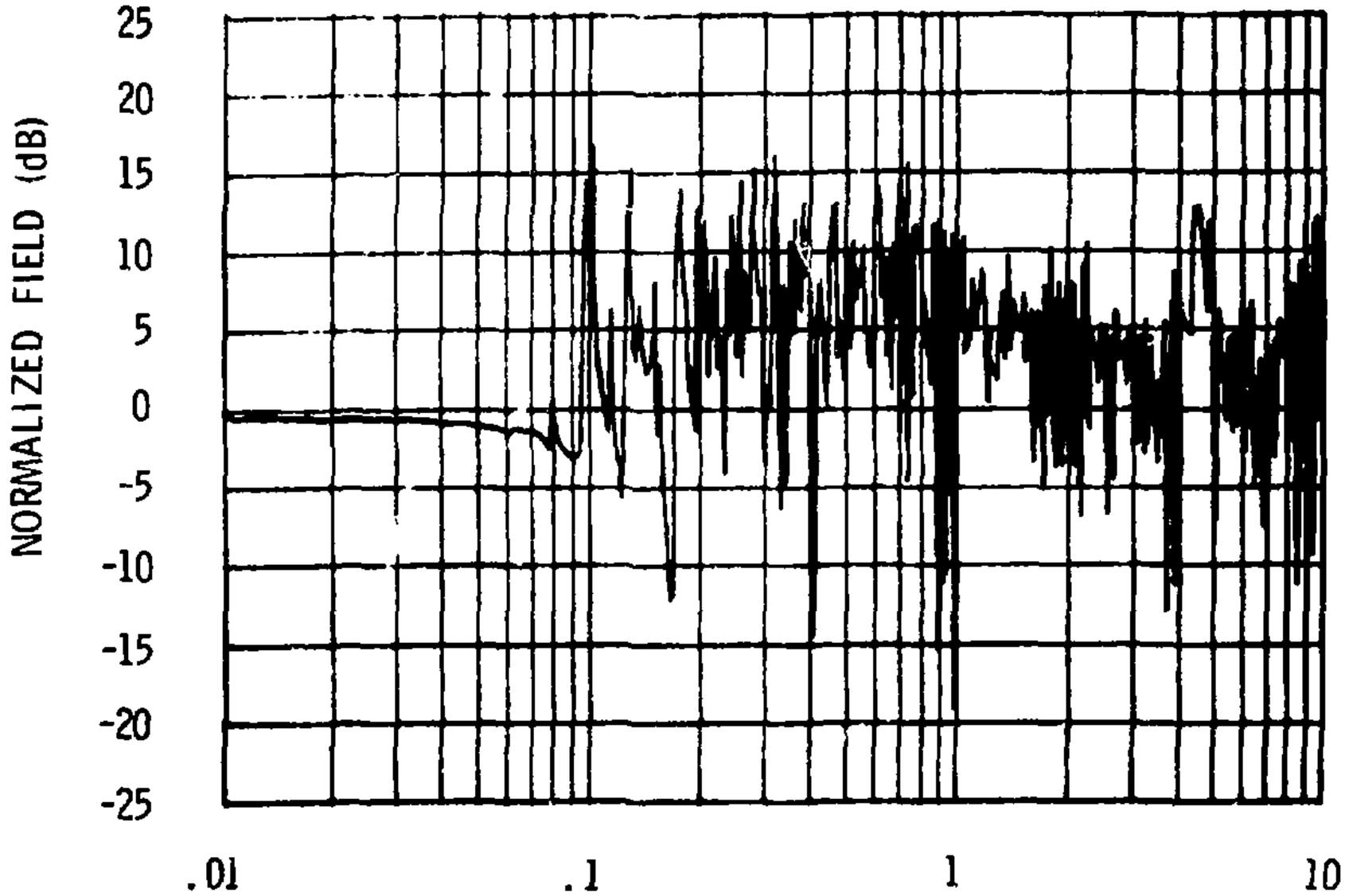

FIGURE B-7: NORMALIZED ELECTRIC FIELD STRENGTH AT THE CENTER FRONT EDGE OF THE WORKING VOLUME FOR THE CONSTANT WIDTH FACILITY GEOMETRY WITHOUT ABSORBER

Plots of the VSWR and the normalized load power for facility geometry 1 without absorbing material are shown in Figures B-8 and B-9. The VSWR is less than 1.1 at frequencies below 90 MHz. Peaks in the VSWR curve are numerous above 100 MHz and correspond (at least for the first octave or so) with resonances in the probe response data (Figure B-7). Apparently the higher order modes which can be excited at frequencies above approximately 95 MHz are not properly terminated by the tapered output transition section and lumped load. Reflections from the output end and from the bends in the ground planes cause large variations both in the field in the working volume and in the input characteristics of the line. The maximum VSWR is approximately 11 which indicates that the input impedance of the facility is not very close to 50Ω. The maximum permissible VSWR for a load connected to a high power amplifier is typically 2.5 to assure that the amplifier is not damaged by power reflected from the load. This configuration of the facility would not present a satisfactory load for the amplifiers.

It is not clear why the VSWR is small (less than 2) between 900 MHz and 4.5 GHz and is considerably larger at frequencies both below and above this range. Perhaps the higher order modes and their harmonics (which can interfere destructively) fortuitously cancel at the input for frequencies in this range. Such near-perfect cancellation over several octaves of frequency does not seem highly likely; the apparent decrease in VSWR in this frequency range is probably the result of some characteristic of the transmission line which is not presently understood.

The normalized output power (Figure B-9) for the constant width model without absorber is essentially constant at zero dB up to the cutoff frequency for higher order modes; that is, essentially all the power delivered to the line is transferred to the output load at low frequencies. The value of the load power at points

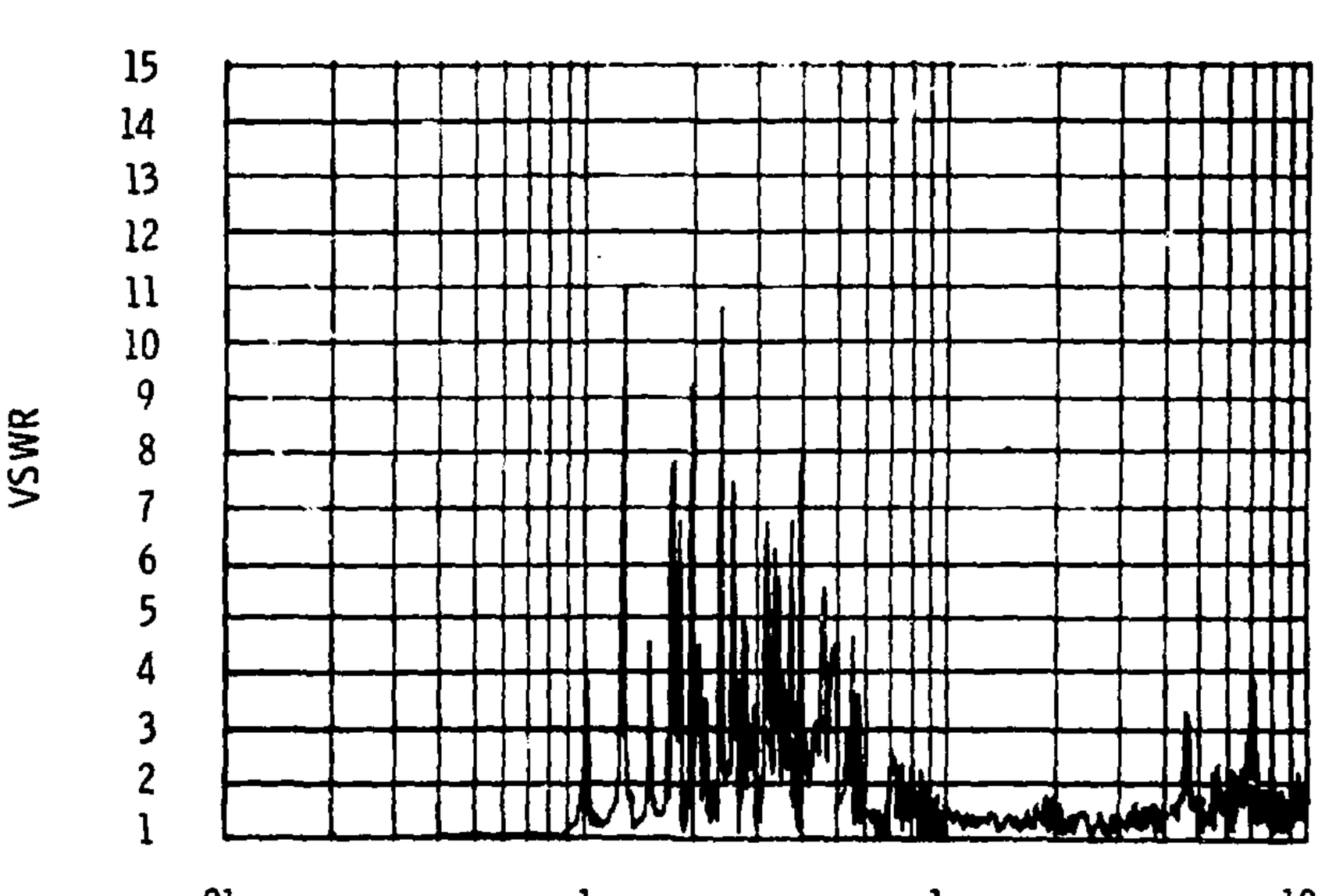

FIGURE B-8: VSWR FOR THE CONSTANT WIDTH GEOMETRY WITHOUT ABSORBER

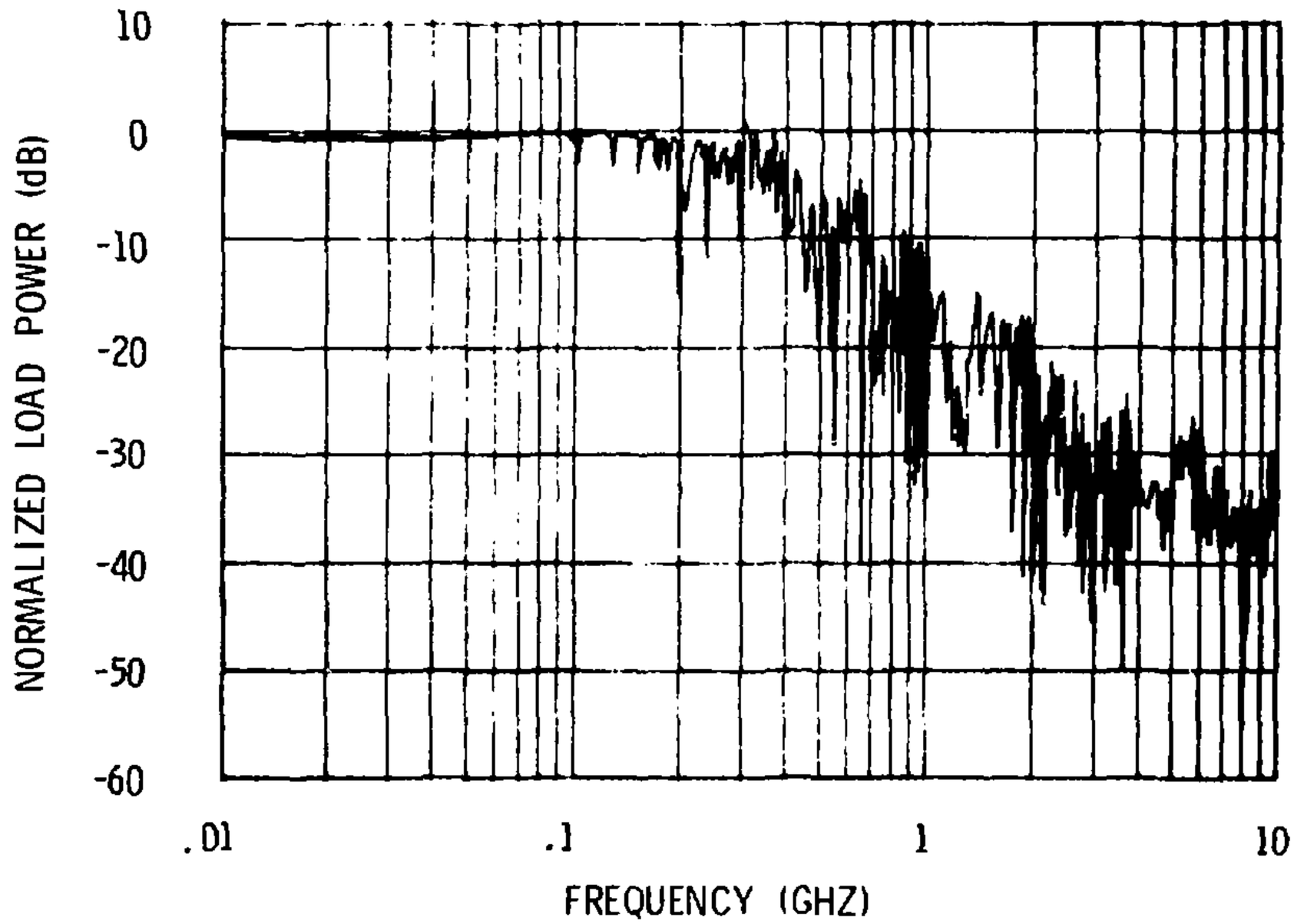

FIGURE B-9: NORMALIZED LOAD POWER FOR THE CONSTANT WIDTH GEOMETRY WITHOUT ABSORBER

between resonances remains near 0 dB at frequencies up to roughly 200 MHz. At higher frequencies the load power decreases on the average at approximately 20 dB/decade. Above 1 GHz, less than 1/100 of the power coupled to the input of the line reaches the output load. The VSWR curve indicates that very little of the input power is reflected to the input port at frequencies between 900 MHz and 4.5 GHz; therefore, the major portion of the power is apparently dissipated in the center conductor and ground planes. The wave must suffer multiple reflections at the conductor surfaces and thereby be gradually absorbed.

Constant Width Model with Absorber: The normalized field at the center front edge of the working volume for the constant width configuration with absorbing material in the output transition section is shown in Figure B-10. The notable characteristics of these data when compared with the results for the same facility geometry without absorbing material installed (Figure B-7) include a marked improvement in field uniformity at frequencies above 200 MHz, some degradation in performance below 90 MHz, a large disturbance in the field magnitude between 100 MHz and 200 MHz, and somewhat smaller ones near 6 and 7 GHz. The absorbing material across the output section of the facility obviously provides a reasonably good termination for any higher order modes propagating on the line and absorbs the high frequency energy reflected and diffracted at the bends and discontinuities and prevents its re-reflection into the working volume.

The degradation in the performance of the line at low frequencies (below 90 MHz) results from the effect of the absorber on the line impedance. The absorbing material increases the capacitance in the output transition section and therefore decreases the impedance of the line, resulting in reflections of the TEM wave which alter the field configuration.

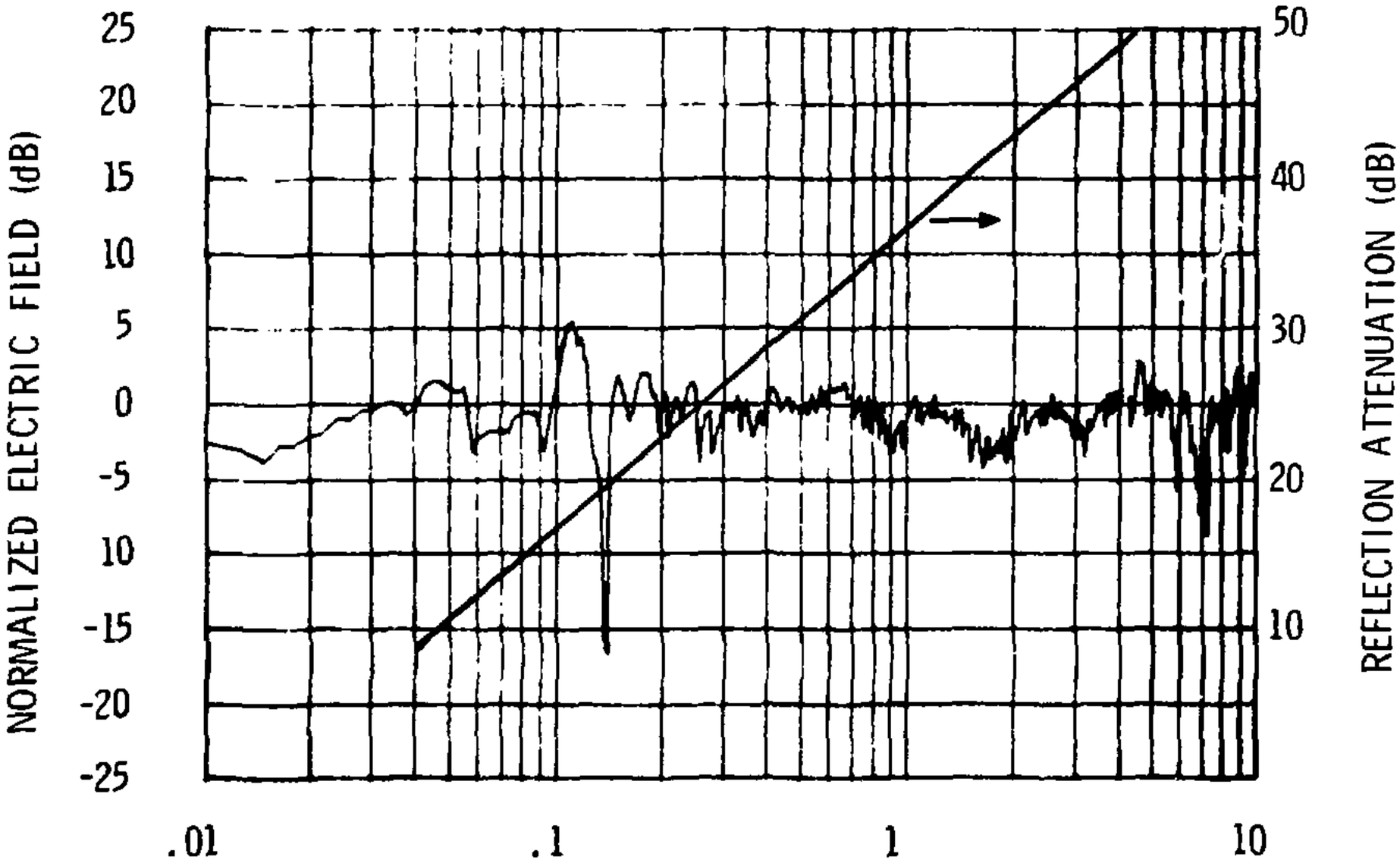

FIGURE B-10: NORMALIZED ELECTRIC FIELD STRENGTH AT THE CENTER FRONT EDGE OF THE WORKING VOLUME FOR THE CONSTANT WIDTH FACILITY GEOMETRY WITH ABSORBING MATERIAL IN THE OUT-PUT TRANSITION SECTION. REFLECTION ATTENUATION FOR THE ABSORBER IS SHOWN ON THE RIGHT HAND ORDINATE

The large swing in field level at approximately 140 MHz appears to be caused by a higher order mode which is not absorbed by the EM absorbing material. The reflection attenuation* for the absorber used in EMES, which is also plotted in Figure B-10, increases with frequency and provides an increasingly more effective termination for the higher order modes as the frequency is raised. The cutoff wavelength for a given mode varies with position along the line as the separation between the ground planes and the distance to the termination change (see Equation 1 in the body of the report and Reference 24). A higher order mode traveling into the output transition section will propagate to the point at which the line dimensions become too small to support the mode and will, for practical purposes, be reflected from that point back toward the working volume. If the facility dimensions become too small to support the mode before the wave reaches the absorber, the absorber will have little effect on the disturbances in field pattern produced by that mode.** This is apparently what causes the resonance at approximately 140 MHz. At higher frequencies, the higher order modes propagate further into the transition section, intercept more of the absorber (which is staggered along the transition) and have less effect on the fields in the working volume.

Another possible explanation for the resonance at 140 MHz is that it is the result of reflection of the TEM wave at the impedance discontinuity created by the absorber. The distance from the probe location (front edge of the working volume) to the first row of absorber is approximately one-quarter wavelength at 140 MHz. A later experiment (eccentric model), in which the facility dimensions

---

*See Appendix C.

**The absorber may cause a shift in the resonant frequency associated with the mode.[24]

were reduced but the positions of the probes and the absorber remained unchanged, gave a resonance at approximately 68 MHz but none at 140 MHz. This would seem to indicate that different modes are responsible for the two resonances and that the existence of those modes depends on the facility geometry and dimensions.

The relatively large dips in the field level near 6 and 7 GHz were identified with mechanical misalignment in the input feed. These disturbances in field level were reduced in later experiments by carefully re-working the launcher, but were never completely eliminated.

The VSWR for the constant width facility geometry with absorber is shown in Figure B-11. These data show a marked improvement in the input characteristics of the facility over those exhibited by the same configuration without absorbing material (Figure B-8). The normalized load power is shown in Figure B-12 and the reflection attenuation for the absorber used in FEMES is plotted on the same graph. The load power data have the same general form as those for the constant width model without absorber (Figure B-9); that is, most of the power reaches the load at low frequencies and the transmission loss gradually increases at frequencies above 100 MHz. The large excursions in power level have been reduced significantly because the resonances within the facility are suppressed by the absorber. The decrease in load power with increasing frequency is more rapid with the absorber present. The difference in normalized output power with and without absorber is approximately equal to one-half the reflection attenuation for the absorber, as one would expect.

Tapered Width Model: Data for the tapered width model were obtained only with absorber in the line. The normalized field at the center front edge of the working volume is shown in Figure B-13. These

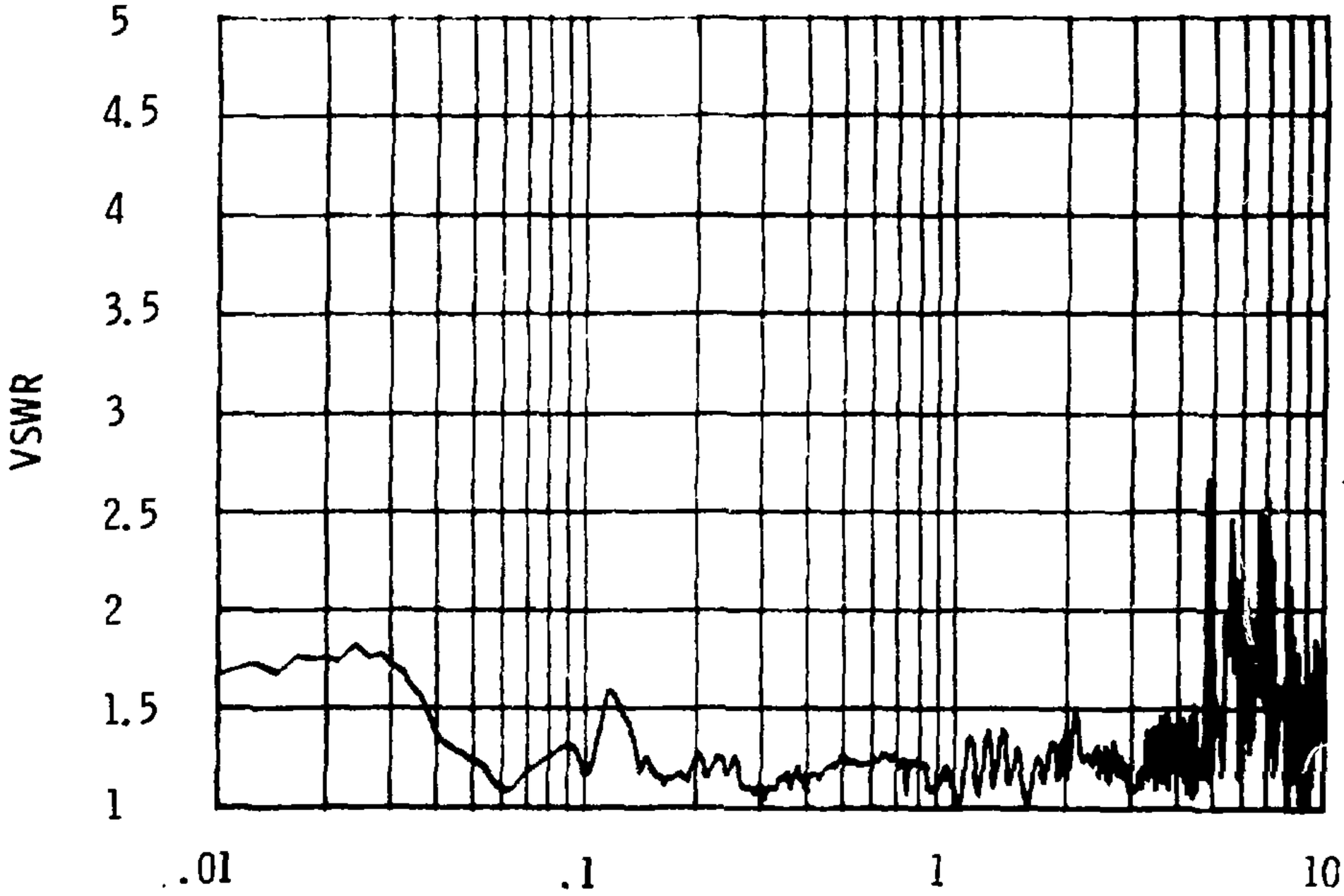

FIGURE B-11: VSWR FOR THE CONSTANT WIDTH MODEL WITH ABSORBER.

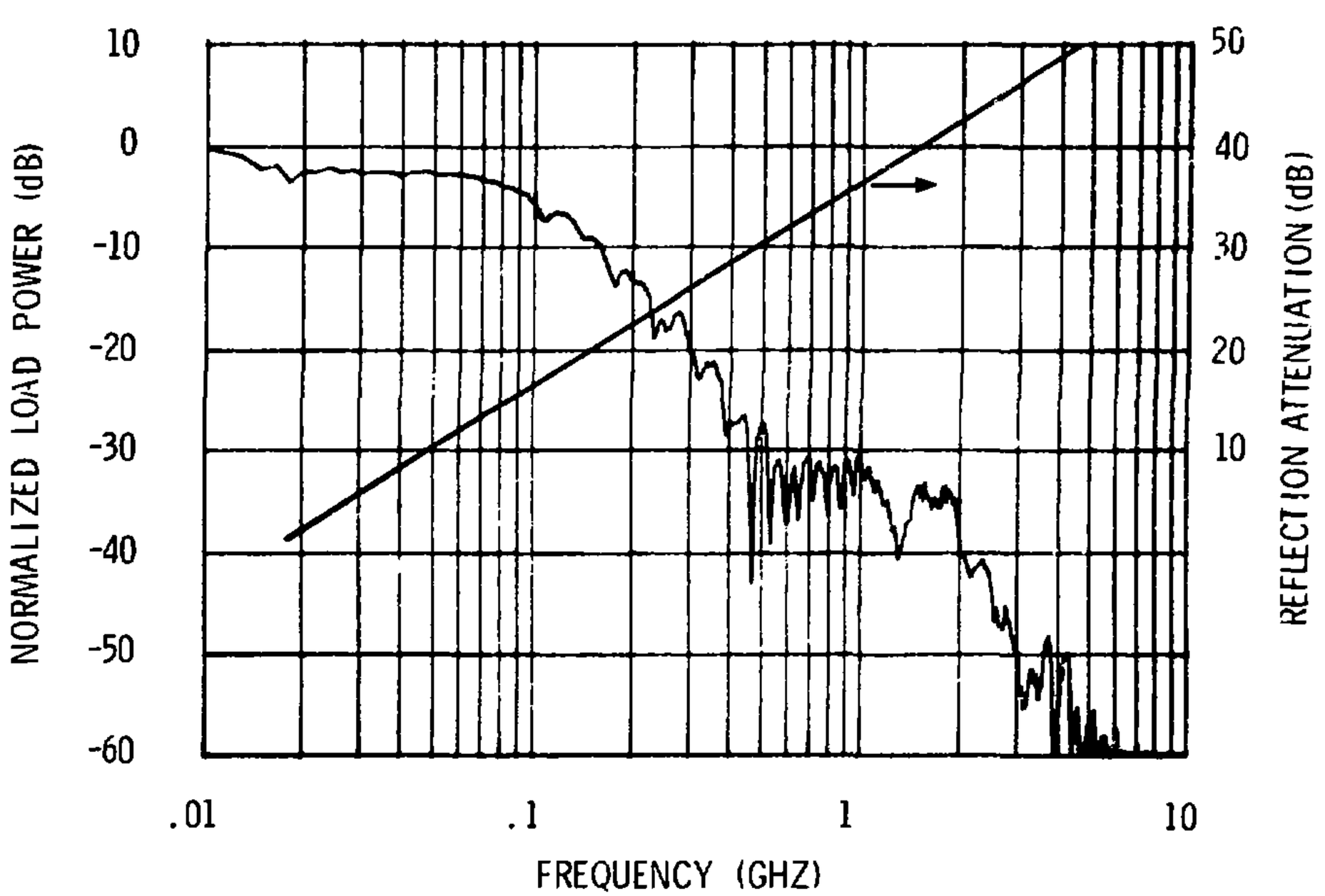

FIGURE B-12: NORMALIZED LOAD POWER FOR THE CONSTANT WIDTH MODEL WITH ABSORBER. REFLECTION ATTENUATION FOR THE ABSORBER IS PLOTTED ON THE RIGHT HAND SCALE

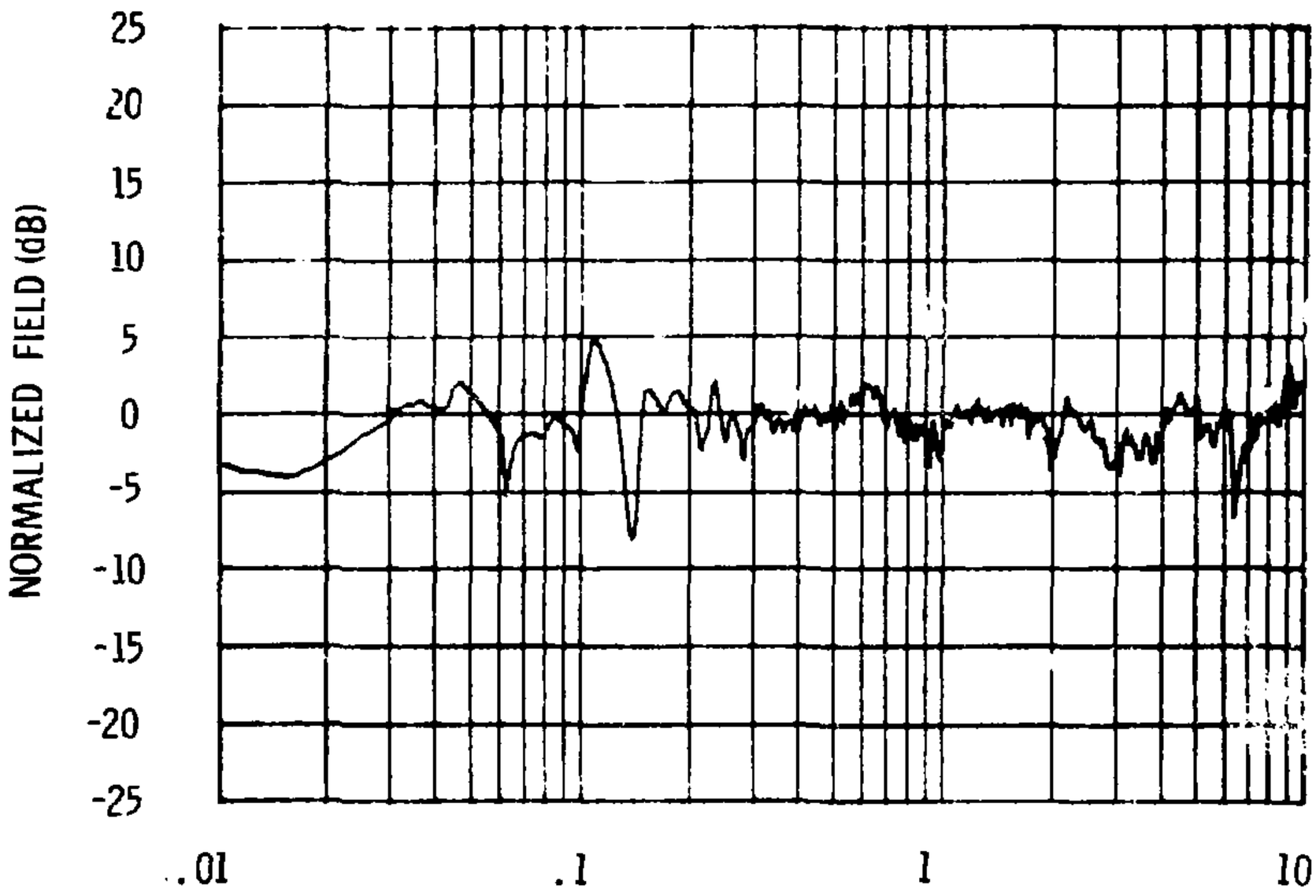

FIGURE B-13: NORMALIZED ELECTRIC FIELD STRENGTH AT THE CENTER FRONT EDGE OF THE WORKING VOLUME FOR THE TAPERED WIDTH MODEL WITH ABSORBER

data are quite similar to those for the constant width model with absorber except that the magnitudes of the resonances at 140 MHz and 6 to 7 GHz are smaller. VSWR data, shown in Figure B-14, indicate slightly higher values than were obtained for the constant width model. In Figure B-15 the normalized load power is plotted.* These data are almost identical to the results obtained for the constant width model (Figure B-12). It is apparent that with absorbing material in the output transition, tapering the side walls does not seriously degrade the performance of the facility.

Truncated Model: The normalized vertical electric field at the center front edge of the working volume of the truncated model is plotted in Figure B-16. The effect of the absorber on the field level at low frequencies (below 90 MHz) is again apparent. The resonance at 140 MHz is present in this configuration as in the earlier ones although it seems to be less pronounced.** The field level is within a range of approximately ±6 dB at all frequencies examined. The VSWR is plotted in Figure B-17 and indicates slightly larger low frequency reflections than observed in the other configurations. This is probably due to the fact that the total capacitance is slightly higher in the truncated model than in the tapered models because of the proximity of the back wall to the absorber. Also the distributed load was not as precise a termination as was the coaxial load. The increased capacitance effect is reduced by separating the absorber from the back wall as far as is possible.

---

*For this configuration, load power measurements were made only over the lower portion of the frequency range because of equipment failure.

**The quality factors (Q's) for the resonances exhibited by the models are extremely high (greater than one-thousand in some cases). It is therefore very difficult to assure that the peak or null value has been recorded with precision. Apparent differences of several dB in field level at peaks or nulls could be due to small differences in the frequencies at which measurements were made.

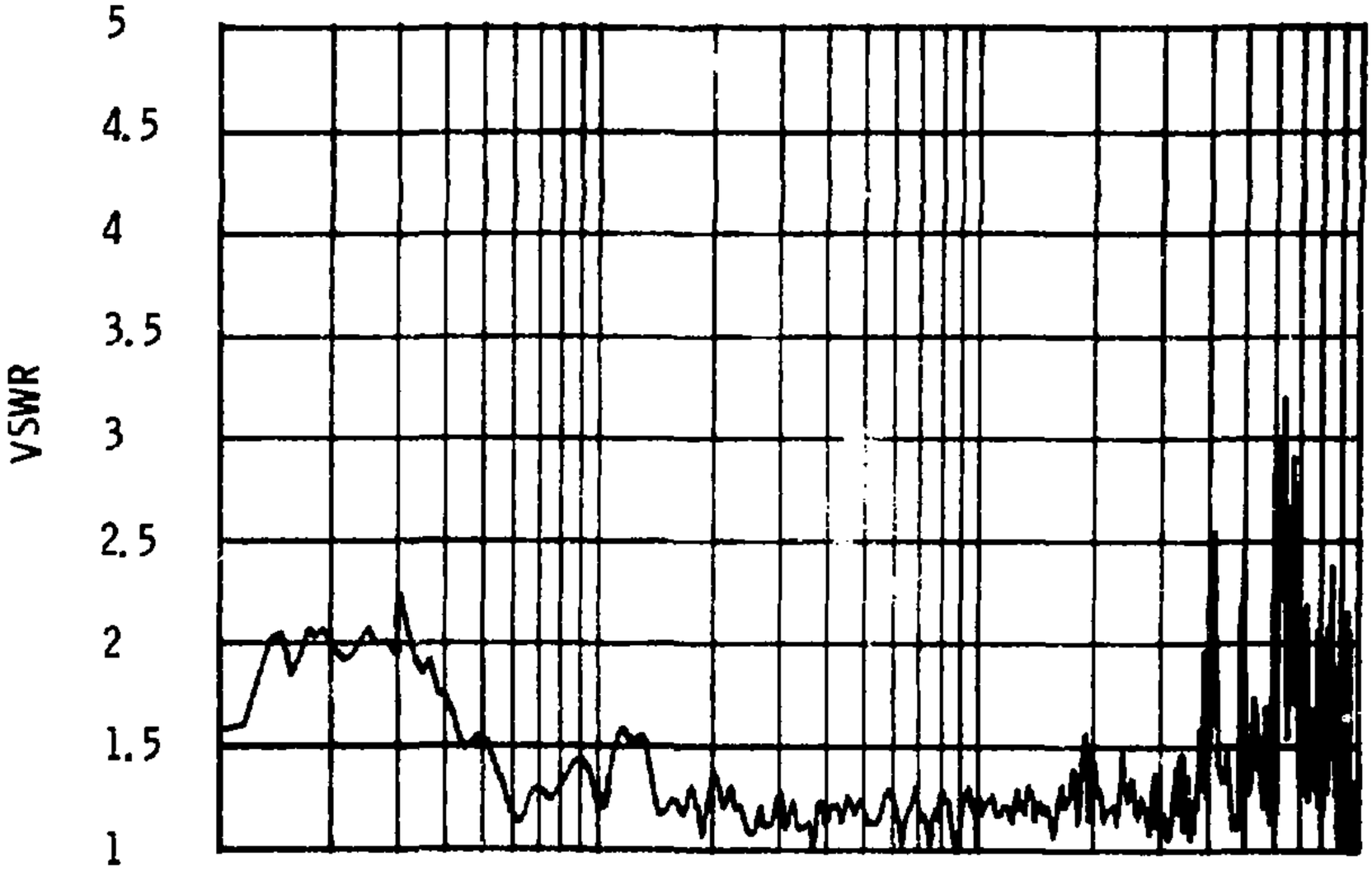

FIGURE B-14: VSWR FOR THE TAPERED WIDTH MODEL WITH ABSORBER

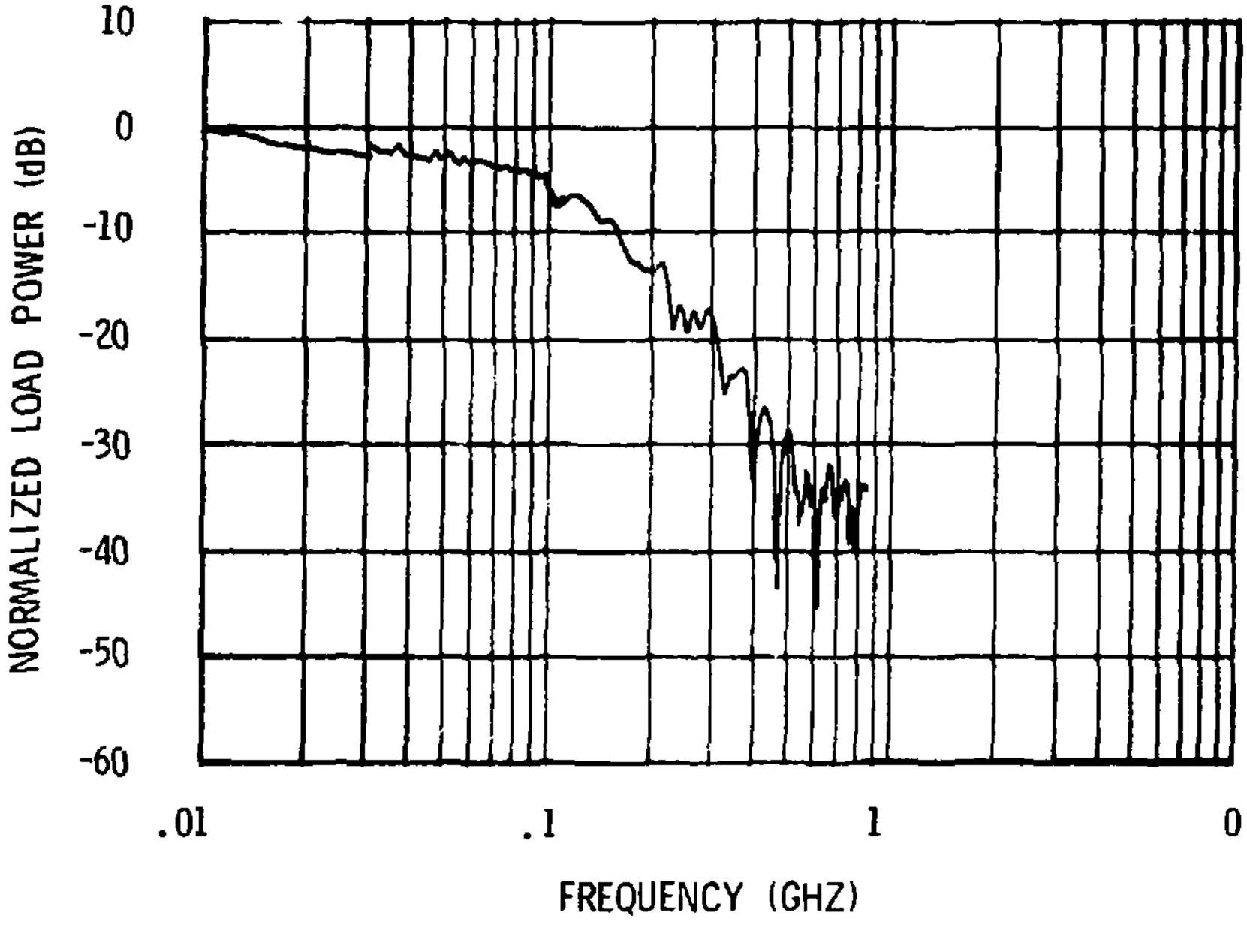

FIGURE B-15: NORMALIZED LOAD POWER FOR THE TAPERED WIDTH MODEL WITH ABSORBER

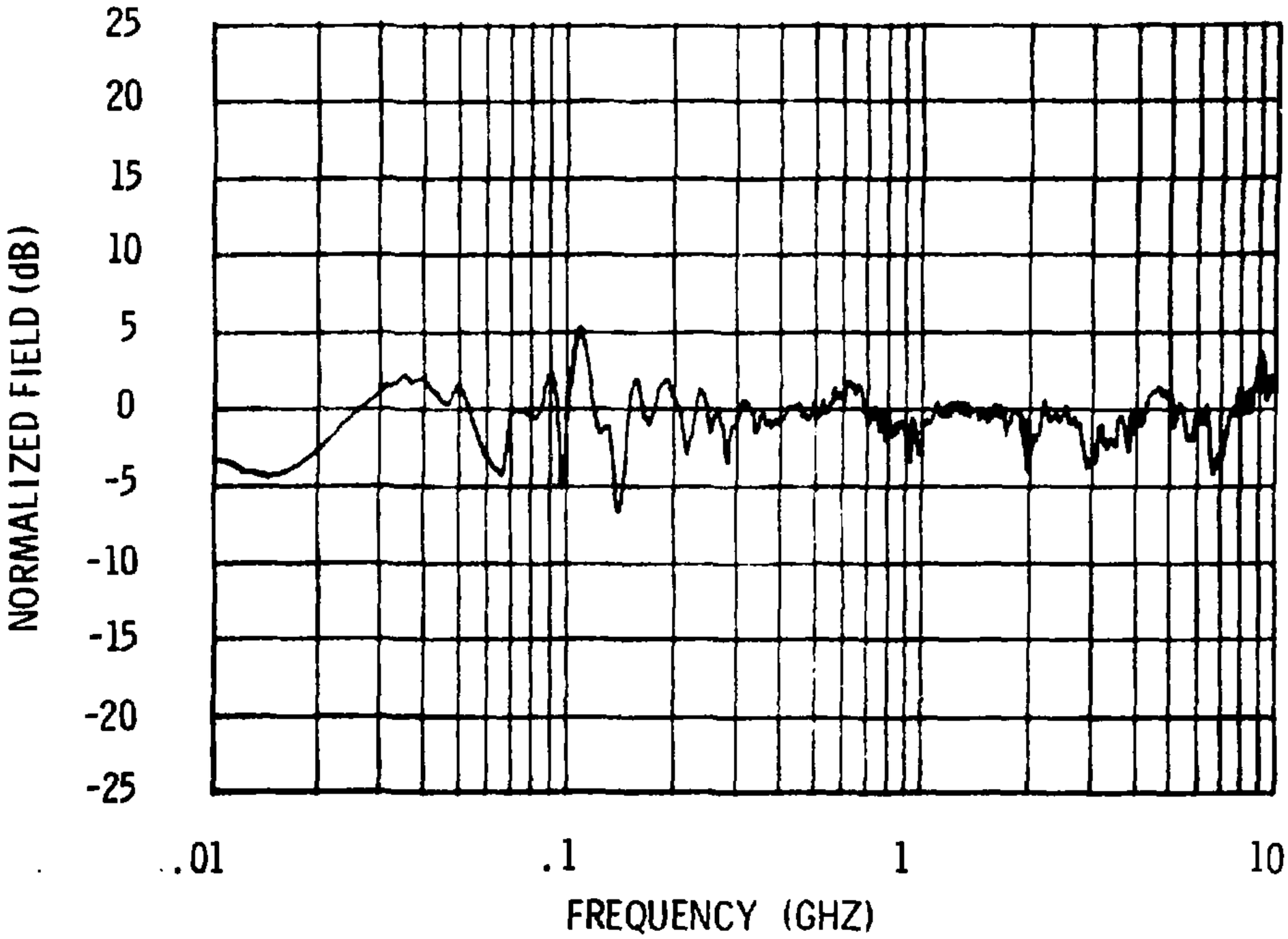

FIGURE B-16: NORMALIZED ELECTRIC FIELD STRENGTH FOR THE TRUNCATED MODEL WITH ABSORBER

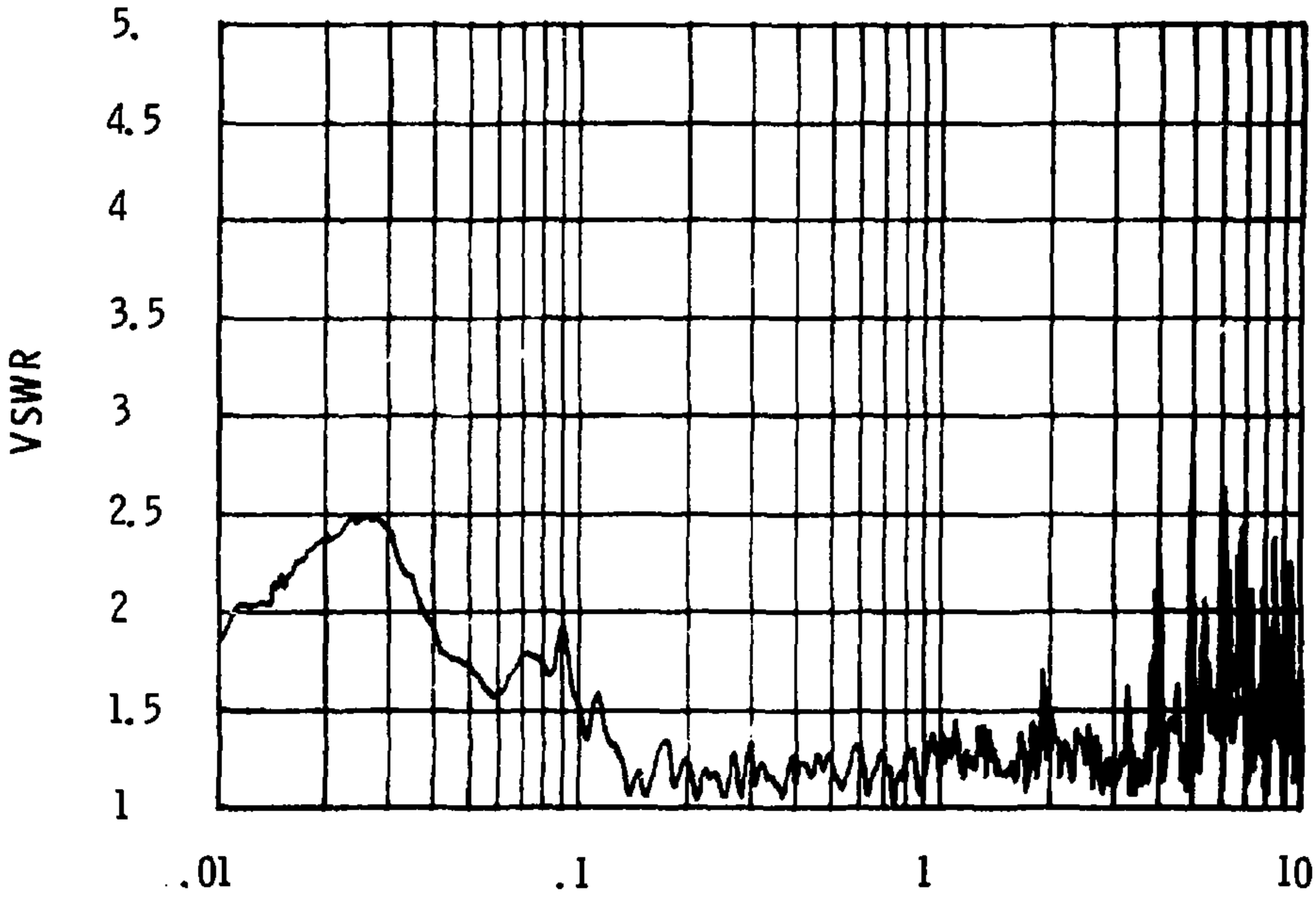

FIGURE B-17: VSWR FOR THE TRUNCATED MODEL WITH ABSORBER

Data for other probes in the working volume and for other probe polarizations (horizontal and axial) were consistent with the results for the other model configurations. It appears that truncating the facility behind the wall of absorber does not introduce any severe additional disturbances to the field pattern or the input characteristics of the line.

The shielding effectiveness of the truncated model was checked by placing a probe at several points around the outside the facility while exciting the facility with a 10 GHz signal. No readings above noise level were obtained outside the facility. Because of the limited sensitivity of the instrumentation used, it was possible only to specify that the shielding effectiveness is greater than about 30 dB for the single layer screen wire construction used in FEMES. The actual value is probably in the range of 50 to 60 dB.[30] The second layer of screen to be used in EMES will add approximately 6 dB to the shielding effectiveness of the facility.

Eccentric Model: Data for the normalized vertical electric field at the center front edge of the working volume of the eccentric model are plotted in Figure B-18. The variations are noticeably larger for this configuration with the prominant low frequency null occurring at approximately 68 MHz. This null (and therefore the one at 140 MHz for Configurations 1, 2, and 3) is obviously not due to a reflection of the TEM wave from the absorber because the relative position of the probe and the absorber are the same as for the other configurations. In fact, the resonance must be due to the excitation of a different mode altogether. Otherwise, the resonance would have moved higher in frequency when the dimensions of the facility were reduced. The null is undoubtedly due to an asymmetric mode which, due to geometrical symmetry was not excited in the other configurations at all. The mode which caused the null at 140 MHz in

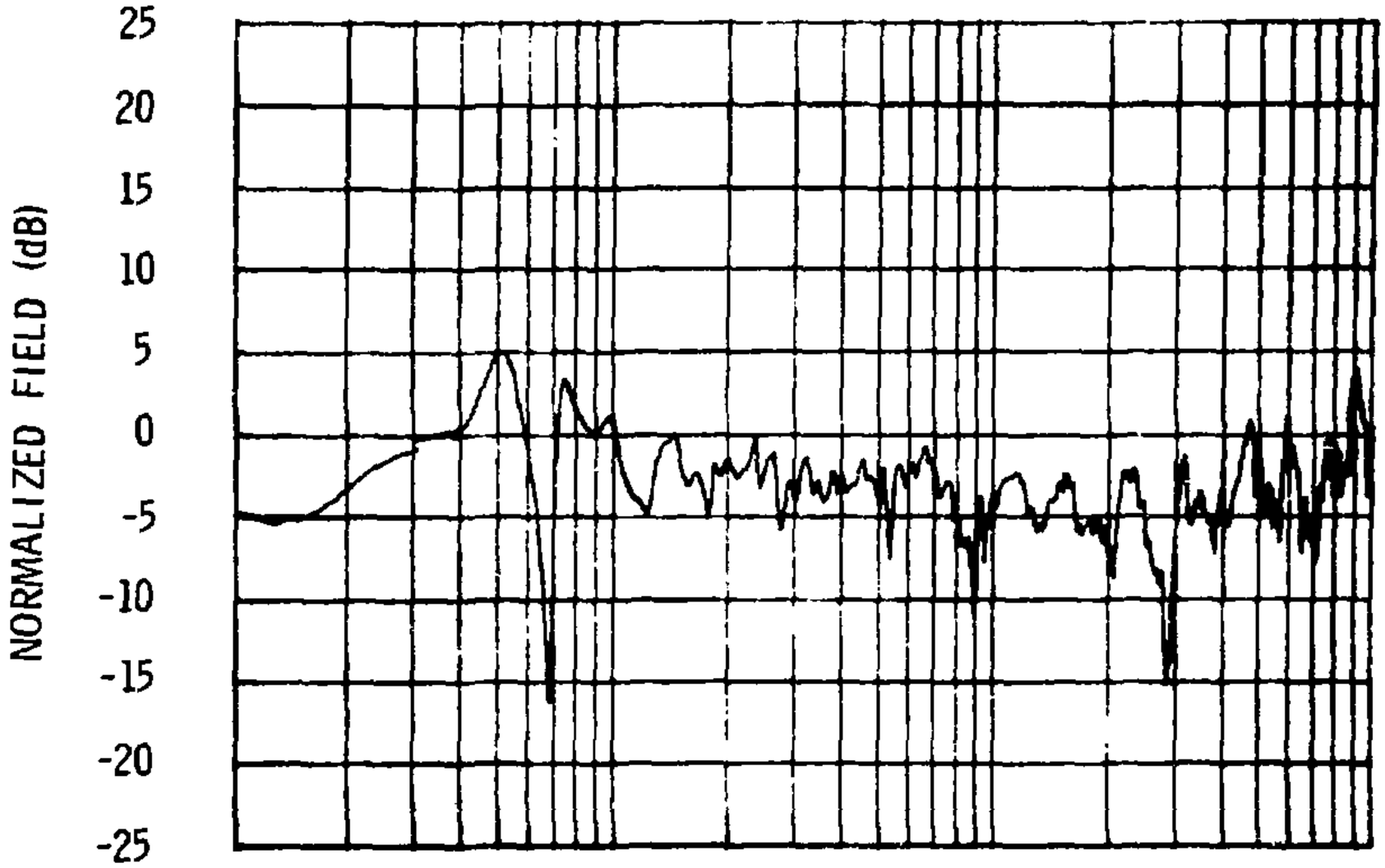

FIGURE B-18: NORMALIZED ELECTRIC FIELD STRENGTH AT THE CENTER FRONT EDGE OF THE WORKING VOLUME OF THE ECCENTRIC MODEL WITH ABSORBER.

the other configurations would produce a resonance at some higher frequency in the eccentric model because of the smaller line dimensions and was apparently absorbed more effectively.

The high frequency variations are due in part to the feed used for this model. It was not possible to fabricate a new feed with the proper geometry for the eccentric model in the time available. A feed from the balanced line design was therefore modified to provide the adaption from circular to rectangular coax, giving less than ideal matching. It is impossible to separate with confidence the effects of the changed facility geometry from the effects of the compromised feed configuration at high frequencies.

The narrower plate width of the eccentric model resulted in a narrower region of uniform field when compared with the other configurations. The effective size of the working volume for the eccentric model is about 35% smaller than that of the other configurations. This reduction of working volume is not acceptable if the facility is to accommodate the large systems scheduled for evaluation in the near future. The VSWR was essentially the same for the eccentric model as for the truncated model.

TWEMES Model: The primary purpose of the TWEMES model was to give an indication of whether truncation of the facility was feasible before it was attempted on FEMES. The initial data indicated that a truncated facility could be made to perform satisfactorily and work on the truncation of FEMES was initiated. TWEMES was also used to evaluate different types of distributed loads, determine the optimum position for the load, evaluate the effects of absorber placement on low frequency performance, and evaluate the effect of narrowing the center plate in the output transition region.*

*The purpose of narrowing the center plate was to increase the inductance of the transmission line and thereby offset the increased capacitance caused by the absorber.

APPENDIX C

ELECTROMAGNETIC ABSORBER CHARACTERISTICS

APPENDIX C

ELECTROMAGNETIC ABSORBER CHARACTERISTICS

Electromagnetic absorbers are used to prevent the reflection of energy from the metal boundaries of an enclosure. Ideally, all the electromagnetic energy striking the surface of the absorber is dissipated, and none is reflected back into the enclosure. If no reflections occur at the boundaries, the field distribution within the enclosure remains unchanged and the energy appears to be radiating into free space. The absorption is, of course, never complete, and the free space condition can only be approximated in practice.

When an electromagnetic wave encounters a boundary between two different media, part of the wave is reflected back into first medium, and part is transmitted across the boundary into the second medium. Some of the energy transmitted across the boundary will propagate all the way through the second medium and will be radiated from the other side. (At the far boundary of the second medium, reflection and transmission occur so that there is a reflected wave traveling in the second medium which produces reflection and transmission at the first boundary, and so on until the energy is, for practical purposes, dissipated in or radiated from the second medium.) For absorbing materials, it is desirable to have minimum reflection at the first boundary and maximum dissipation of the transmitted wave within the absorber.

To achieve minimum reflection at the boundary between the two media, the properties (density, conductivity, dielectric constant, etc.) of the media should be essentially the same, and the wave should strike the boundary at normal incidence. Absorbers are often made in pyramidal or conical shapes so that the volume occupied by the absorber gradually increases as a wave travels into the material. Thus, a gradual transition in the properties of the transmission

medium occurs instead of a sharp change at a plane boundary. The sloping edges of the material also serve to dispersively scatter the reflected energy so that the reflected wave encounters several absorber boundaries before it can reenter the first medium. At each boundary, more energy is transmitted into the absorber with the net effect that much less energy is reflected from the surface of pyramidal absorbers than from a flat sheet of the same material.[38]

One common type of absorbing material consists of pyramidal polyurethane foam blocks impregnated with a mixture of carbon black and neoprene. The polyurethane base provides a low density, low dielectric constant material which aids in matching the absorber characteristics to those of air. The carbon is the dissipative component of the mixture. Because carbon's properties do not depend significantly on frequency, the absorber can be used over a wide frequency range.

Absorber performance is usually specified in terms of the reflection attenuation; that is, the ratio in dB of the power incident on the absorber to the power reflected from the absorber. The reflection attenuation measurement is made with the absorber mounted on a conducting surface. The reflected component therefore consists of the power reflected from the front surfaces of the absorber, plus that which passes through the absorber and is reflected by the conducting surface. Because the shape of the absorber tends to reduce reflections from its surface, much of the reflected power is contained in a wave that has made two passes through the absorber.

Reflection attenuation varies with frequency, angle of incidence, the composition of the absorbing material, and the thickness of the absorber. The approximate characteristics of a carbon loaded polyurethane material for normal wave incidence are plotted in Figure C-1. The lowest frequency at which appreciable absorption

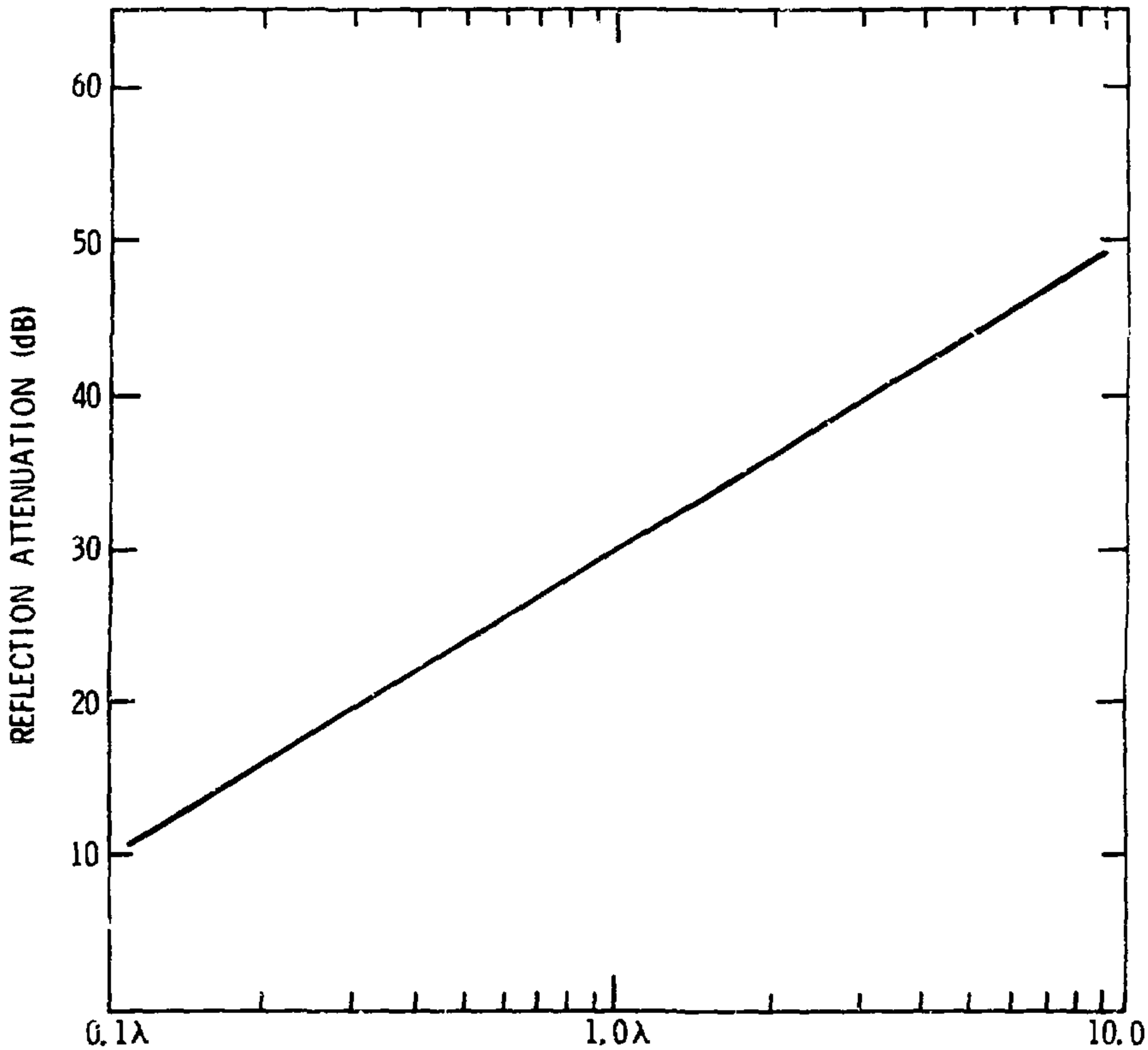

FIGURE C-1: REFLECTION ATTENUATION FOR A PYRAMIDAL CARBON LOADED POLYURETHANE ABSORBER

takes place is approximately that frequency for which the absorber is one-quarter wavelength thick (where the reflection attenuation is approximately 20 dB). At higher frequencies, most of the energy striking the absorber never returns to the first medium, and essentially the same conditions exist as if the energy were being radiated into free space.

The dielectric properties of the absorber are frequency dependent. Measurements made by Sandia's Standards Laboratory indicate that the magnitude of the relative permittivity decreases with frequency, as illustrated in Figure C-2.[39] At low frequencies (frequencies below the frequency at which the absorption is significant), the absorber tends to increase the capacitance in the volume it occupies. At high frequencies, the permittivity of the absorber is very close to that of air.

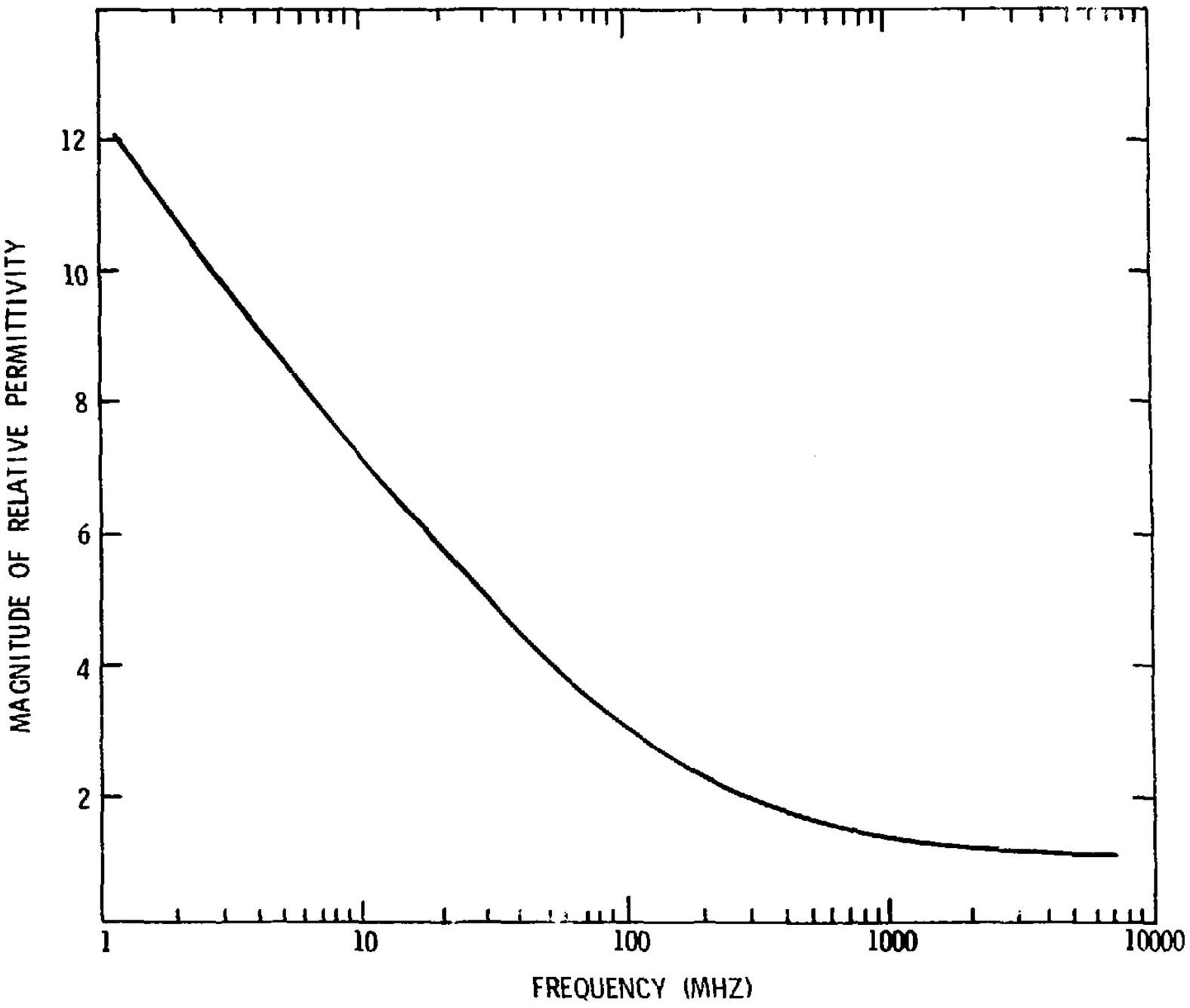

FIGURE C-2: APPROXIMATE MAGNITUDE OF THE PERMITTIVITY OF A TYPICAL CARBON LOADED POLYURETHANE ABSORBER